

Extremely high-intensity laser interactions with fundamental quantum systems

A. Di Piazza, C. Müller, K. Z. Hatsagortsyan, and C. H. Keitel

*Max-Planck-Institut für Kernphysik,
Saupfercheckweg 1,
69117 Heidelberg,
Germany*

(Dated: April 2, 2019)

The field of laser-matter interaction traditionally deals with the response of atoms, molecules and plasmas to an external light wave. However, the recent sustained technological progress is opening the possibility of employing intense laser radiation to prompt or substantially influence physical processes beyond atomic-physics energy scales. Available optical laser intensities exceeding 10^{22} W/cm² can push the fundamental light-electron interaction to the extreme limit where radiation-reaction effects dominate the electron dynamics, can shed light on the structure of the quantum vacuum and can prime the creation of particles like electrons, muons and pions and the corresponding antiparticles. Also, novel sources of intense coherent high-energy photons and laser-based particle colliders can pave the way to nuclear quantum optics and can even allow for potential discovery of new particles beyond the Standard Model. These are the main topics of the present article, which is devoted to a review of recent investigations on high-energy processes within the realm of relativistic quantum dynamics, quantum electrodynamics, nuclear and particle physics, occurring in extremely intense laser fields.

CONTENTS

I. Introduction	1	VIII. QED cascades	29
II. Novel radiation sources	3	IX. Muon-antimuon and pion-antipion pair production	32
A. Strong optical laser sources	3	A. Muon-antimuon and pion-antipion pair production in laser-driven collisions in plasmas	32
1. Next-generation 10 PW optical laser systems	4	B. Muon-antimuon and pion-antipion pair production in high-energy XFEL-nucleus collisions	33
2. Multi-Petawatt and Exawatt optical laser systems	4	X. Nuclear physics	34
B. Brilliant x-ray laser sources	4	A. Direct laser-nucleus interaction	34
III. Relativistic atomic dynamics in strong laser fields	5	1. Resonant laser-nucleus coupling	34
A. Ionization	5	2. Nonresonant laser-nucleus interactions	36
B. Recollisions and high-order harmonic generation	8	B. Nuclear signatures in laser-driven atomic and molecular dynamics	36
IV. High-intensity Thomson and Compton scattering	10	XI. Laser colliders	37
A. Thomson- and Compton-based sources of high-energy photon beams	12	A. Laser acceleration	37
V. Radiation reaction	13	B. Laser-plasma linear collider	38
A. The classical radiation dominated regime	16	C. Laser micro-collider	39
B. Quantum radiation reaction	16	XII. Particle physics within and beyond the Standard Model	41
VI. Vacuum polarization effects	18	A. Electroweak sector of the Standard Model	41
A. Low-energy vacuum-polarization effects	19	B. Particle physics beyond the Standard Model	41
1. Experimental suggestions for direct detection of photon-photon scattering	19	XIII. Conclusion and outlook	42
2. Polarimetry-based experimental suggestions	21	Acknowledgments	43
3. Low-energy vacuum-polarization effects in a plasma	22	List of frequently-used symbols	43
B. High-energy vacuum-polarization effects	22	References	44
VII. Electron-positron pair production	23	I. INTRODUCTION	
A. Pair production in photon-laser and electron-laser collisions	24	The invention of the laser in 1960 is one of the most important technological breakthroughs ever. Nowadays lasers are indispensable tools for investigating physical processes in the realm of different areas spanning from	
B. Pair production in nucleus-laser collisions	25		
C. Pair production in a standing laser wave	27		
D. Spin effects and other fundamental aspects of laser-induced pair creation	28		

atomic and plasma physics to nuclear and high-energy physics. This has been possible mainly due to the continuous progress along two specific directions: decrease of the laser pulse duration and increase of the laser peak intensity. On the one hand, multiterawatt laser systems with a pulse duration in the femtosecond time scale are readily available nowadays and different laboratories have succeeded in the generation of a single attosecond pulse. The physics at the attosecond time scale is the subject of the recent review Krausz and Ivanov, 2009. In this review it has been also pointed out how the availability of pulses in the attosecond domain has been allowing for the detailed investigation of the electron motion in atoms and during molecular reactions. The production of ultrashort pulses is strongly connected with the increase of the laser peak intensity: not only because temporal compression evidently implies an increase in intensity at a given laser energy, but also because higher and higher intensities allow in general for controlling physical processes occurring at shorter and shorter time scales, which in turn can be exploited for generating accordingly shorter light pulses (Mourou *et al.*, 2006).

Not long after the invention of the laser, available intensities were already sufficiently high to trigger nonlinear optical effects like second harmonic generation. It is, however, only after the experimental implementation of the Chirped Pulse Amplification (CPA) technique (Strickland and Mourou, 1985) that it has been possible to reach the intensity threshold of 10^{14} - 10^{15} W/cm² corresponding to electric field amplitudes of the same order of the Coulomb field in atoms. At such intensities the interplay between the laser and the atomic field significantly alters the electron's dynamics in atoms and molecules and this can be exploited, for example, for generating high-frequency radiation in the extreme-ultraviolet (XUV) and soft-x-ray regions (high-order harmonic generation or HHG) (Protopapas *et al.*, 1997). HHG as well as atomic processes in intense laser fields have been recently reviewed in Fennel *et al.*, 2010; Teubner and Gibbon, 2009; and Winterfeldt *et al.*, 2008, with specific emphasis on the control of high-harmonic spectra by spatio-temporal shaping of the driving pulse (Winterfeldt *et al.*, 2008), on harmonic generation in laser-plasma interaction (Teubner and Gibbon, 2009) and on the dynamics of clusters in strong laser fields (Fennel *et al.*, 2010).

By increasing the optical laser intensity by three to four orders of magnitude, i.e. at laser intensities of the order of 10^{17} - 10^{18} W/cm², another physically important regime in laser-matter interaction is entered: the relativistic regime. In such an intense electromagnetic field an electron reaches relativistic velocities already within one laser period, the magnetic component of the Lorentz force becomes of the same order of the electric one and the electron's motion becomes highly nonlinear as a function of the laser's electromagnetic field. Although the

increasing influence of the magnetic force causes a suppression of atomic HHG in the relativistic domain, the highly nonlinear motion of the electrons in such strong laser fields is at the origin of numerous new effects as relativistic self-focusing in plasma and laser wakefield acceleration (Mulser and Bauer, 2010). In the recent reviews Ehlötzky *et al.*, 2009; Mourou *et al.*, 2006; and Salamin *et al.*, 2006, different processes occurring at relativistic laser intensities are discussed. In particular, in Ehlötzky *et al.*, 2009, QED processes like Compton, Mott and Møller scattering in a strong laser field are covered, in Mourou *et al.*, 2006, technical aspects and new possibilities of the CPA techniques are reviewed together with relativistic effects in laser-plasma interaction as, for example, self-induced transparency and wakefield generation, while in Salamin *et al.*, 2006, spin-effects as well as relativistic multiphoton and tunneling recollision dynamics in laser-atom interaction are reviewed. Also in the same year another review has been published on nonlinear collective photon interactions, including vacuum-polarization effects in a plasma (Marklund and Shukla, 2006). Finally, the physics of laser-driven electron accelerators based on wakefield acceleration is the main subject covered in Esarey *et al.*, 2009, with a special focus on the different phases involved in a laser-based accelerator (electron trapping and injection, and pulse propagation) and on the role of plasma instabilities in the acceleration process.

In the present article we address physical processes mainly occurring at optical laser intensities mostly larger than 10^{21} W/cm², i.e. well exceeding the relativistic threshold. After reporting on the latest technological progresses in optical and x-ray laser technology (Sec. II), we bridge to lower-intensity physics by reviewing more recent achievements in relativistic ionization and HHG in atomic gases (Sec. III). Then we pass to the main subject of the review, i.e. the response of fundamental systems like electrons, photons and even the vacuum to ultra-intense radiation fields (Secs. IV-VI). As we will see, such high laser intensities will represent a unique tool to investigate fundamental processes like multiphoton Compton scattering (Sec. IV), to clarify conceptual issues like radiation reaction in classical and quantum electrodynamics (Sec. V) and to investigate the structure of the quantum vacuum (Sec. VI). Also, other fundamental quantum-relativistic phenomena like the transformation of pure light into massive particles as electrons, muons and pions (and the corresponding antiparticles) can become feasible and can even limit the attainability of arbitrarily high laser intensities (Secs. VII-IX). Finally, we will also review recent suggestions on employing novel high-frequency lasers and laser-accelerated particle beams to directly prime nuclear and high-energy processes (Secs. X-XII). The main conclusions of the article are presented in Sec. XIII.

Units with $\hbar = c = 1$ and the space-time metric $\eta^{\mu\nu} =$

diag(+1, -1, -1, -1) are employed through this review.

II. NOVEL RADIATION SOURCES

In this section we review the latest technical and experimental progress in laser technology. We will discuss separately optical and x-ray laser systems.

A. Strong optical laser sources

As we have mentioned in the Introduction, since the invention of the CPA technique (Strickland and Mourou, 1985) laser peak intensities have been boosted to higher and higher values by several orders of magnitude. Another amplification technique called Optical Parametric Chirped Pulse Amplification (OPCPA), based on the nonlinear interaction among laser beams in crystals, was suggested almost at the same time as the CPA and proved to be promising as well (Piskarskas *et al.*, 1986). As a result of increasing available laser intensities, exciting perspectives have been envisaged in different fields of physics spanning from atomic to plasma and even nuclear and high-energy physics (Feder, 2010; Gerstner, 2007; Mourou, 2010; Tajima *et al.*, 2010).

The group of G. Mourou at the University of Michigan (Michigan, USA) holds the record so far of the highest laser intensity ever achieved of 2×10^{22} W/cm² (Yanovsky *et al.*, 2008). The record intensity has been reached at the HERCULES laser, which is a 300 TW Ti:Sa system, amplified via CPA and capable of a repetition rate of 0.1 Hz. The 4-grating compressor allowed for a pulse duration of about 30 fs and adaptive optics together with a $f/1$ parabola enabled to focus the beam down to a diameter of about 1.3 μ m. This experimental achievement on the laser intensity almost took the capabilities of a multiterawatt laser to the limit. However, already in other laboratories the 1-PW threshold has been reached and/or even exceeded. For example, the Texas Petawatt Laser (TPL) at the University of Texas at Austin (Texas, USA) even exceeds the Petawatt threshold thanks to the OPCPA technique, by focusing an energy of 186 J in a pulse lasting only 167 fs (TPL, 2011). The TPL has been employed for investigating laser-plasma interaction at extreme conditions in particular relevant for astrophysics. Also, the two laser systems Vulcan (Vulcan, 2011) and Astra Gemini (Astra Gemini, 2011) at the Central Laser Facility (CLF) in the United Kingdom provide powers of the order of 1 PW. The Vulcan facility can deliver an energy of 500 J in a pulse lasting 500 fs. It is a Nd:YAG laser system amplified via CPA and it can provide intensities up to 10^{21} W/cm². Instead, the Astra Gemini laser consists of two Ti:Sa laser beams of 0.5 PW each (energy of 15 J for a pulse duration of 30 fs), with a maximum focused intensity of 10^{22} W/cm². The particular layout

of the Astra Gemini laser renders this system especially versatile for unique applications in strong-field physics, where two ultrastrong beams are required. Two laser systems are likely to be updated to the Petawatt level in Germany. The first one is the Petawatt High-Energy Laser for heavy Ion eXperiments (PHELIX) Nd:YAG laser at the Gesellschaft für Schwerionenforschung (GSI) in Darmstadt capable at the moment to deliver an energy of 120 J in about 500 fs (PHELIX, 2011). The 1-PW threshold should be reached by increasing the pulse energy to 500 J. The possibility of combining the PHELIX laser pulses with the highly-charged ion beams at GSI renders the PHELIX facility attractive for experimental investigations in strong-field quantum electrodynamics (QED). The second system to be updated to 1 PW is the Petawatt Optical Laser Amplifier for Radiation Intensive Experiments (POLARIS) laser in Jena (Hein *et al.*, 2010). At the moment, a power of about 100 TW (energy of 10 J for a pulse duration of 100 fs) has been reached and the goal power of 1 PW should be achieved by compressing 120 J in about 120 fs. The 1-PW threshold has been also exceeded in Ti:Sa laser systems like those described in Sung *et al.*, 2010 (energy of 34 J for a pulse duration of 30 fs) and in Wang *et al.*, 2011 (energy of 32.3 J for a pulse duration of 27.9 fs). All the above systems require laser energies larger than 10 J and this limits the repetition rate of such lasers in the best situation to about 0.1 Hz (Sung *et al.*, 2010). The Ti:Sa Petawatt Field Synthesizer (PFS) system under development in Garching (Germany) aims to be the first high-repetition rate petawatt laser system with an envisaged repetition rate of 10 Hz (PFS, 2011). By adopting the OPCPA technique the PFS should reach the petawatt level by compressing an energy of about 5 J in 5 fs (Major *et al.*, 2010). For a recent review on petawatt-class laser systems, see Korzhimanov *et al.*, 2011.

Finally, we also want to mention other high-power lasers, which are however mainly devoted to fast ignition and which are characterized by relatively long pulses of the order of 1 ps-1 ns. Among others we mention the OMEGA EP system at Rochester (New York, USA) (energy of 1 kJ for a pulse duration of 1 ps) (OMEGA EP, 2011) and the National Ignition Facility (NIF) at the Lawrence Livermore National Laboratory (LLNL) at Livermore (California, USA) (energy of 2 MJ distributed in 192 beams with a pulse duration of about 3 ps) (NIF, 2011). Another example is the Laser Megajoule under construction in Bordeaux (France) with a total energy of 1.8 MJ distributed in a series of 240 laser beamlines, collected into eight groups of 30 beams with a pulse duration of 0.2-25 ns (LMJ, 2011).

1. Next-generation 10 PW optical laser systems

In various laboratories the possibility of building a 10 PW laser system is under consideration. At the CLF in United Kingdom the 10 PW upgrade of the Vulcan laser has already started (Vulcan 10PW, 2011). The new laser will provide beams with an energy of 300 J in only 30 fs via the OPCPA. A 10 PW laser system is in principle capable of unprecedented intensities larger than 10^{23} W/cm² if the beam is focused to about 1 μ m. The front-end stage of the Vulcan 10 PW is already completed and it delivers pulses with about 1 J of energy at a central wavelength of 0.9 μ m.

Another 10 PW laser project is the ILE APOLLON to be realized at the Institut de Lumière Extreme (ILE) in France (Chambaret *et al.*, 2009). The laser pulses are expected to deliver an energy of 150 J in 15 fs at the last stage of amplification after the front end (energy of 100 mJ in less than 10 fs), with a repetition rate of one shot per minute. Laser intensities of the order of 10^{24} W/cm² are envisaged for the ILE APOLLON system, entering the so-called ultrarelativistic regime, where also ions (rest energy of the order of 1 GeV) become relativistic within one laser period of such an intense laser field.

We mention here also the PETawatt pARametric Laser (PEARL-10) project at the Institute of Applied Physics of the Russian Academy of Sciences in Nizhny Novgorod (Russia), which is an upgrade of the present 0.56-PW laser employing the OPCPA technique, to 10 PW (200 J of energy compressed in 20 fs) (Korzhimanov *et al.*, 2011).

2. Multi-Petawatt and Exawatt optical laser systems

The Extreme Light Infrastructure (ELI) (ELI, 2011) (see Fig. 1) and the High Power laser Energy Research (HiPER) facility at the CLF in United Kingdom (HiPER, 2011) are two envisaged laser systems with a power exceeding the 100 PW level. ELI is a large-scale laser facility consisting of four “pillars” (see Fig. 1): one devoted to nuclear physics, one to attosecond physics, one to secondary beams (photon beams, ultrarelativistic electron and ion beams) and one to high-intensity physics. This last one is of relevance here and it is supposed to comprise ten beams each with a power of 10-20 PW that, when combined in phase, should deliver a single beam of about 100-200 PW at a repetition rate of one shot per minute. The relatively high repetition rate is obtained by compressing in each beam “only” 0.3-0.4 kJ of energy in a short pulse of 15 fs. We mention that one of the aims of the ILE APOLLON system is to provide a prototype of the 10-20 PW beams, that will be then employed at ELI. In the high-field pillar of ELI ultrahigh intensities exceeding 10^{25} W/cm² are envisaged, which are well

Lasers planned for the Extreme Light Infrastructure*					
Country	Facility focus	Power (PW)	Pulse energy (J)	Pulse width (fs)	Rep rate (Hz)
Romania	Nuclear physics	10 (x2)	200	20	0.1
Hungary	Attosecond physics	1	5	5	1000
		20	400	20	0.1
Czech Republic	Secondary beam radiation, high-energy particles	1	10	10	10
		5	50	10	10
		10 (x2)	200	20	0.1
To be determined	High intensity	10 beams of 10-20 PW each, phased and combined to create total power of 100-200 PW			

*Laser parameters still subject to change.

FIG. 1 (Color online) Summary of the four pillars of ELI. A power value of 10(x2) PW indicates the availability of two laser systems each with 10 PW power. Reprinted with permission from Feder, 2010. Copyright 2010, American Institute of Physics.

above the ultrarelativistic regime and which will allow to test different aspects of fundamental physics for the first time.

The main goal of the other large-scale facility HiPER is the first demonstration of laser-driven fusion, or fast ignition. To this end HiPER will deliver: 1) an energy of about 200 kJ distributed in 40 beams with a pulse duration of several nanoseconds and a photon energy of 3 eV in the compression side; 2) an energy of about 70 kJ distributed in 24 beams with a pulse duration of 15 ps and a photon energy of 2 eV in the ignition side. The employment of HiPER for high-intensity physics would imply a feasible reconfiguration of the ignition side to deliver 10 kJ in only 10 fs via the OPCPA technique. This would render HiPER a laser facility with Exawatt (10^{18} W) power and with a potential intensity of 10^{26} W/cm².

B. Brilliant x-ray laser sources

Strong optical laser systems are sources of coherent radiation at wavelengths of the order of 1 μ m, corresponding to photon energies of the order of 1 eV. A considerable effort has been devoted in the last years to develop coherent radiation sources at photon energies larger than 100 eV. The discovery of the Self-Amplified Spontaneous Emission (SASE) regime (Bonifacio *et al.*, 1984) has opened the possibility of employing Free Electron Lasers (FELs) to generate coherent light at such short wavelengths. In a FEL relativistic bunches of electrons pass through a region where a spatially alternating magnetic field is present (undulator) and emit high-energy photons. In the SASE regime the interaction of the electron bunch with its own electromagnetic field “structures” the bunch itself into slices (microbunches) each one emitting coherently even at wavelengths below 1 nm (FELs at such small wavelengths are indicated as X-ray Free Electron Lasers (XFELs)).

The Free-Electron Laser in Hamburg (FLASH) facil-

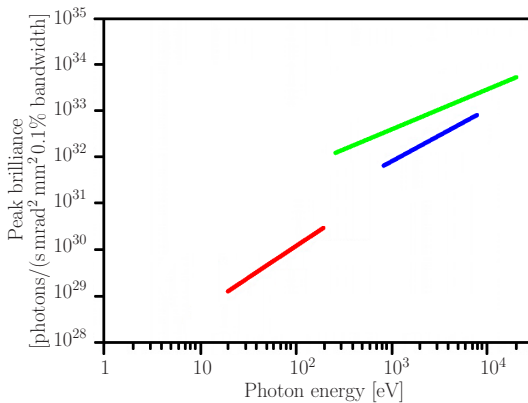


FIG. 2 Comparison among the peak brilliances of the three facilities FLASH (red line), LCLS (blue line) and European XFEL (green line) as a function of the laser photon energy. An envisaged peak brilliance of 5×10^{33} photons/(s mrad² mm² 0.1% bandwidth) at a photon energy of 12.4 keV for the SACLA facility is reported in European XFEL, 2011. See also European XFEL, 2011.

ity at the Deutsches Elektronen-Synchrotron (DESY) in Hamburg (Germany) (FLASH, 2011) is one of the most brilliant operating FEL's and it delivers short pulses (duration of about 10-100 fs) of coherent radiation in the extreme ultraviolet-soft x-ray regime (fundamental wavelength from 60 nm down to 6.5 nm corresponding to photon energies from 21 eV to 190 eV) at a repetition rate of 100 kHz. The intense electron beams available at FLASH (total charge of 0.5-1 nC at an energy of 1 GeV) allow a peak brilliance of the photon beam of about 10^{29} - 10^{30} photons/(s mrad² mm² 0.1% bandwidth) (see Fig. 2), exceeding the peak brilliance of conventional synchrotron light sources by several orders of magnitude. The Linac Coherent Light Source (LCLS) at Stanford (California, USA) uses the electron beams generated by the Stanford Linear Accelerator (SLAC) at the National Accelerator Laboratory to generate flashes of coherent x-ray radiation of unprecedented brilliance (LCLS, 2011). Since the electron beam energy can be varied from 4.5 GeV to 14.4 GeV, accordingly the wavelength of LCLS can be tuned from 1.5 nm to 0.15 nm (corresponding to photon energies from 0.8 keV to 8 keV). The peak brilliance of the LCLS is of the order of 10^{32} - 10^{33} photons/(s mrad² mm² 0.1% bandwidth) (see Fig. 2), the pulse duration is of about 200 fs and the repetition rate of 120 Hz.

Another XFEL in operation is the SPring-8 Angstrom Compact free electron LASer (SACLA) at the RIKEN Harima Institute in Japan (SACLA, 2011). The electron accelerator based on a conducting C-band high-gradient radiofrequency acceleration system and the short-period undulator allow for a relatively compact facility of around 700 m in length (compared, for example, with about 2 km for the LCLS). SACLA employs the 8 GeV electron beam

of the Super Photon Ring - 8 GeV (SPring-8) accelerator (SPring8, 2011) and it has generated x-ray beams with 0.08 nm wavelength (corresponding to a photon energy of 15.5 keV) at a repetition rate of 60 Hz (see also the caption of Fig. 2).

The European XFEL is an XFEL under development at DESY in Hamburg (Germany) (European XFEL, 2011). It is expected to deliver x-ray pulses with a peak brilliance up to about 5×10^{33} photons/(s mrad² mm² 0.1% bandwidth) at an unprecedented repetition rate of 27 kHz. The electron accelerator provides an electron beam with maximal energy of 17.5 GeV able to generate laser pulses with a central wavelength of 0.05 nm, corresponding to a photon energy of 24.8 keV and with a pulse duration of 100 fs. Moreover, the European XFEL will be a versatile machine consisting of three photon beamlines: the SASE-1 and SASE-2 with linearly polarized photons with energy in the range 3.1-24.8 keV and the SASE-3 with linearly or circularly polarized photons with energy in the range 0.26-3.1 keV.

III. RELATIVISTIC ATOMIC DYNAMICS IN STRONG LASER FIELDS

When super-intense infrared laser pulses, as those described in the previous section, impinge on an atom, the latter is immediately partly or fully ionized (Becker *et al.*, 2002; Keitel, 2001; Protopapas *et al.*, 1997). The ejected electrons experience the typical “zig-zag” motion (Salamin *et al.*, 2006) of a free electron in both laser polarization and propagation directions and will, in general, not return to the ionic core. With enhanced binding force on the remaining electrons, the ionization dynamics becomes increasingly complex and may experience subtle relativistic and correlation effects. When the binding force of the ionic core and that of the applied laser field eventually become comparable, the electrons may in special cases return to the parent ion, leading, for example, to the ejection of other electrons, to the absorption of energy in a scattering process or to the emission of high-harmonic photons in case of recombination.

A. Ionization

Originally atomic or molecular ionization has been studied with laser pulses below 10^{16} W/cm² and relativistic laser-matter interaction has been reserved to the plasma community. The parameter controlling relativistic effects for a free electron in a laser field (electric field amplitude E_0 and central angular frequency ω_0) is the so-called “classical relativistic parameter” $\xi_0 = |e|E_0/m\omega_0$. From this definition it is in fact clear that an electron in a laser field with $\xi_0 \gtrsim 1$ becomes relativistic within a laser

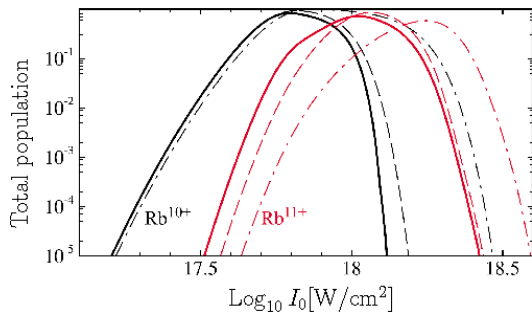


FIG. 3 (Color online) The total Rb^{10+} (black lines) and Rb^{11+} (red lines) ion populations in a gaseous target as a function of the peak intensity of a linearly-polarized laser field with a wavelength of 0.8 nm and with a pulse duration of 5 fs. The solid lines display two-electron inelastic tunneling, the dashed lines one-electron inelastic tunneling and the dashed-dotted lines the results via the PPT theory. Adapted and reprinted with permission from Kornev *et al.*, 2009. Copyright (2009) by the American Physical Society.

period T_0 . For an optical laser field ($\omega_0 \approx 1$ eV), the relativistic threshold $\xi_0 = 1$ corresponds to a laser intensity I_0 of about 10^{18} W/cm². The first pioneering experiment reported in Moore *et al.*, 1999 on the ionization behavior of atoms and ions with laser intensity of 3×10^{18} W/cm² has thus attracted considerable interest. The laser magnetic field component was shown to alter the direction of ionization characteristically while the yields displayed clear relativistic features. With highly-charged ions becoming more easily available in a wide range of charges, e.g. via super-strong laser fields or via sending the ion beams through metallic foils, relativistic laser-induced ionization has been further studied (Chowdhury *et al.*, 2001; Dammasch *et al.*, 2001; DiChiara *et al.*, 2008, 2010; Gubbini *et al.*, 2005; Palaniyappan *et al.*, 2008; Yamakawa *et al.*, 2003, 2004).

In this situation rescattering is generally suppressed and multiple ionization of atoms and ions takes place mostly via direct ionization, including especially tunneling. On the theoretical side attention was then focused on the relativistic generalization (Milosevic *et al.*, 2002; Popov *et al.*, 1997; Popov, 2004; Popov *et al.*, 2006) of the so-called Perelomov-Popov-Terent'ev (PPT) theory or Ammosov-Delone-Krainov (ADK) model (Ammosov *et al.*, 1986; Perelomov, 1967), which describes atomic ionization in the quasistatic tunneling regime. The Strong Field Approximation (SFA) (Faisal, 1973; Keldysh, 1965; Reiss, 1980), which treats in a universal way both the multiphoton and the tunneling regimes of strong-field ionization, has also been extended to the relativistic regime (Reiss, 1990a,b). Both the PPT theory and the SFA assume that the direct ionization process occurs as a single-electron phenomenon and thus neglects atomic structure effects.

When the tunneling process proceeds very fast, multi-

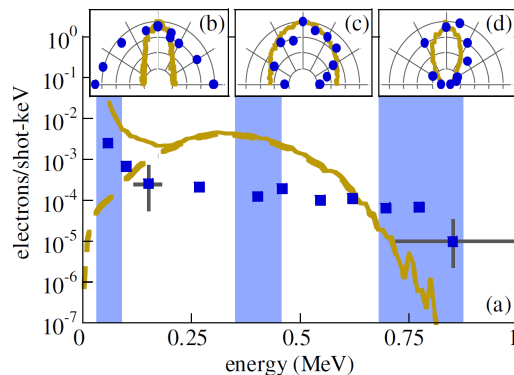


FIG. 4 (Color online) (a) Experimental photoelectron spectra for argon at $I_0 = 1.2 \times 10^{19}$ W/cm² and at an angle of 62° from the laser propagation direction. Analytical results are shown for all photoelectrons (continuous line) and for the L-shell (dashed line). The angular distributions are at an electron energy of (b) 60 keV, (c) 400 keV, and (d) 770 keV. Reprinted with permission from DiChiara *et al.*, 2008. Copyright (2008) by the American Physical Society.

electron correlation effects can occur due to so-called shake-up processes. Thus, the detachment of one electron from the atom or ion via tunneling modifies the self-consistent potential for the remaining electrons and may consequently result in the excitation of the atomic core, denoted as inelastic tunneling. A large excitation may also trigger a simultaneous escape of multiple electrons from the bound state being denoted as collective tunneling. These effects were known to occur also in the non-relativistic regime (Zon, 1999, 2000) but were concealed by competing rescattering effects. In Kornev *et al.*, 2009, it was shown that in the relativistic regime the role of inelastic and collective tunneling can significantly increase and the relativistic PPT rate has been generalized in this respect. According to the calculations in Kornev *et al.*, 2009, inelastic and collective tunneling effects have a significant contribution to the relativistic ionization dynamics at intensities larger than 10^{18} W/cm², changing the ionization probability by more than one order of magnitude (see Fig. 3).

Spin effects of bound systems in strong laser fields were shown to moderately alter the quantum dynamics and its associated radiation via spin-orbit coupling (Hu and Keitel, 1999; Walser *et al.*, 2002). More recently a non-perturbative relativistic SFA theory has been developed, describing circular dichroism and spin effects in the ionization of helium in an intense circularly polarized laser field (Bhattacharyya *et al.*, 2011). Here, two-photon ionization has been studied in the intensity range 10^{13} - 10^{15} W/cm² with a photon energy of 45 eV yielding relative spin-induced corrections of the order of 10^{-3} .

A series of experiments has been devoted to the measurement of atomic multi-electron effects in relativisti-

cally strong laser fields. In DiChiara *et al.*, 2008, the energy distribution of the ejected electrons and the angle-resolved photoelectron spectra for atomic photoionization of argon at $I_0 \sim 10^{19}$ W/cm² have been investigated experimentally. Here the isolation of the single-atom response in the multicharged environment has been achieved by measuring photoelectron yields, energies, and angular distributions as a function of the sample density. The ionization of the entire valence shell along with several inner-shell electrons was shown at $I_0 \sim 10^{17}$ - 10^{19} W/cm². A typical spectrum in the case of linear polarization is displayed in Fig. 4. An extended plateau-like structure appears in the spectrum due to the electrons originating from the L-shell and the longitudinal component of the focused laser field. A surprising feature is observed in the energy-resolved angular distribution. In contrast to the nonrelativistic case with increasing rescatterings and thus angular-distribution widths at high energies, here azimuthally isotropic angular distributions are observed at low energies (~ 60 keV in Fig. 4), which become narrower for high-energy photoelectrons. The authors attribute the anomalous broad angular distribution for low-energy electrons to electron-correlation effects. A similar experiment on the energy- and angle-resolved photoionization was later reported for xenon at a laser intensity of 10^{19} W/cm² (DiChiara *et al.*, 2010). For energies below 0.5 MeV, the yield and the angular distributions were shown not to be described by a one-electron strong-field model, but rather involve most likely multielectron and high-energy atomic excitation processes. A further experiment on relativistic ionization of the methane molecule at $I_0 \sim 10^{18}$ - 10^{19} W/cm² (Palaniyappan *et al.*, 2008) indicated that molecular mechanisms of ionization play no role and that C⁵⁺ ions are produced at these intensities mostly via the cross-shell rescattering atomic ionization mechanism. All these experimental results still require an accurate theoretical description.

On the computational side, various numerical methods have been developed to describe the laser-driven relativistic quantum dynamics in highly-charged ions. A Fast-Fourier-Transform split-operator code was implemented in Mocken and Keitel, 2008 for solving the Dirac equation in 2+1 dimensions by employing adaptive grid and parallel computing schemes. Another method has been developed in Selstø *et al.*, 2009 to solve the 3D Dirac equation by expanding the wave-function in spherical harmonics. The latter was applied to hydrogenlike ions in intense high-frequency laser pulses with emphasis on investigating the role of negative-energy states. In Bauke *et al.*, 2011, both the classical relativistic phase-space averaging method is generalized to arbitrary central potentials and enhanced time-dependent Dirac and Klein-Gordon numerical treatments are employed to investigate the relativistic ionization of highly-charged hydrogenlike ions in short intense laser pulses (for an alternative method of solving the time-dependent Dirac equation in coor-

dinate space, explicitly avoiding the fermion doubling, see Fillion-Gourdeau *et al.*, 2011). For ionization dynamics beyond the tunneling regime, quantum mechanical and classical methods give similar results for laser wavelengths from the near-infrared region to the soft x-ray regime. Furthermore a useful procedure has been developed, which employs the over-the-barrier ionization yields for highly-charged ions to determine the peak laser field strength of short ultrastrong pulses in the range $I_0 \sim 10^{18}$ - 10^{26} W/cm² (Hetzheim and Keitel, 2009). In addition, in this article the ionization angle of the ejected electrons is investigated by the full quantum mechanical solution of the Dirac equation and the laser field strength is shown to be also linked to the electron emission angle. The magnetic field-induced tilt in the lobes in the angular distributions of photoelectrons in laser-induced relativistic ionization has also been discussed in Klaiber *et al.*, 2007.

There are also several new results on the ionic quantum dynamics in strong high-frequency laser fields, i.e. in the so-called stabilization regime. An unexpected nondipole effect has been found in Førre *et al.*, 2006 via numerically solving the Schrödinger equation for a hydrogenic atom beyond the dipole approximation. For this purpose the Kramers-Henneberger transformation has been employed and the terms $\sim \xi_0^2$ have been neglected in the Hamiltonian. In Fig. 5, the resulting angular distribution of the ejected electrons in the nondipole regime of stabilization displays a third unexpected lobe anti-parallel to the laser propagation direction, together with the two expected lobes along the laser polarization direction. As a classical explanation, a drift along the laser propagation direction was identified for the bound electron wave packet in the nondipole case (see the middle panel of Fig. 5). Inside the laser field the electron has a velocity component along the positive z axis but this velocity tends to zero at the end of the pulse. Thus, the electromagnetic forces alone do not change the electron momentum along the propagation direction at the end of the pulse. The net effect of the Coulomb forces on the electron wave packet is consequently a momentum component along the negative z axis: the electron, which is most probably situated in the upper hemisphere during the pulse, undergoes a momentum kick in the negative z direction each time it passes close to the nucleus. A similar effect has been found for molecules (Førre *et al.*, 2007).

Radiative recombination, being the time-reversed process of photoionization, of a relativistic electron with a highly-charged ion in the presence of a very intense laser field has been considered in Müller *et al.*, 2009. It was shown that the strong coupling of the electron to the laser field may lead to a very broad energy spectrum of emitted recombination photons, with pronounced side wings, and to characteristic modifications of the angular photon distribution.

Specific features of nondipole quantum dynamics in

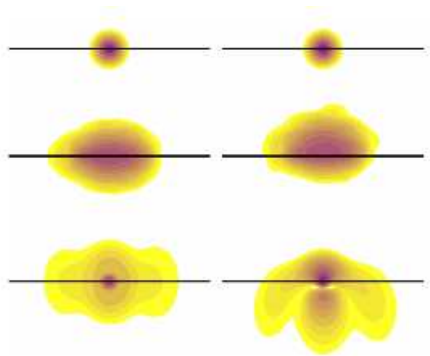


FIG. 5 (Color online) Dipole (left) and nondipole (right) probability densities of the Kramers-Henneberger wave-function in the x - z plane for a x -polarized, 10-cycle sin-like pulse propagating in the positive z direction (upward), with $E_0 = 1.5 \times 10^{11}$ V/cm and $\omega_0 = 54$ eV. The snapshots are taken at $t = 0$, $t = T_0/2$, and $t = 1.8T_0$ from top to bottom. The length of the horizontal line corresponds to about 50 Bohr radii (≈ 2.7 nm). Note that the scale is logarithmic with four contours per decade. Reprinted with permission from Førre *et al.*, 2006. Copyright (2006) by the American Physical Society.

strong and ultrashort laser pulses have also been investigated employing the so-called Magnus approximation (Dimitrovski *et al.*, 2009). The dominant nondipole effect is found to be a shift of the entire wave-function towards the propagation direction, inducing a substantial population transfer into states with similar geometry.

The recent experiment reported in Smeenk *et al.*, 2011 addresses a question how the photon momenta are shared between electron and ion during laser induced multi-photon ionization. Theoretically, this problem requires a nondipole treatment even in the nonrelativistic case to take into account explicitly the photon momentum. Energy-conservation of l -photon ionization here means that $l\omega_0 = I_p + U_p + K$, where I_p is the ionization energy of the atom, $U_p = e^2 E_0^2 / 4m\omega_0^2$ the ponderomotive energy and K the electron's kinetic energy. The experimental results in Smeenk *et al.*, 2011 then show that the fraction of the momentum, corresponding to the number of photons necessary to overcome the ionization energy I_p , is transferred to the created ion rather than to the photoelectron. The electron carries only the momentum corresponding to the kinetic energy K , while the ponderomotive energy and the corresponding portion of the momentum are transferred back to the laser field. This experiment shows that the tunneling concept for the ionization dynamics is only an approximation. In fact, the quasistatic tunneling provides no mechanism to transfer linear momentum to the ion, a conclusion in accordance with recent concerns in Reiss, 2008.

B. Recollisions and high-order harmonic generation

Tunneling in the nonrelativistic regime is generally followed by recollisions with the parent ion along with various subsequent effects (Corkum, 1993; Kuchiev, 1987; Kulander *et al.*, 1993). A characteristic feature of strong-field processes in the relativistic regime is the suppression of recollisions due to the magnetically induced relativistic drift of the ionized electron in the laser propagation direction, see e.g. Salamin *et al.*, 2006. Although relativistic effects become significant when the parameter ξ_0 exceeds unity, signatures of the drift in the laser propagation direction can be observed already in the weakly relativistic regime $\xi_0 \lesssim 1$. The drift will have a significant impact on the electron's rescattering probability if at the moment of the recollision the drift distance d_{\parallel} in the laser propagation direction is larger than the electron's wave packet size $a_{wp,\parallel}$ in that direction (Palaniyappan *et al.*, 2006). The drift distance is approximately given by $d_{\parallel} \sim \lambda_0 \xi_0^2 / 2$ (Landau and Lifshitz, 1975). Instead, the wave packet size $a_{wp,\parallel}$ can be estimated as $a_{wp,\parallel} \sim v_{\parallel} \Delta t$, where v_{\parallel} is the typical electron velocity along the laser propagation direction and Δt is the excursion time of the electron in the continuum. The velocity v_{\parallel} can be related to the tunneling time τ_{tun} via the time-energy uncertainty: $mv_{\parallel}^2 / 2 \sim 1 / \tau_{\text{tun}}$. In turn, one can estimate the tunneling time τ_{tun} as $\tau_{\text{tun}} \sim \ell_{\text{tun}} / v_b$, where $\ell_{\text{tun}} \sim I_p / |e|E_0$ is the tunneling length and $v_b \sim \sqrt{2I_p / m}$ the velocity of the bound electron. Above it was assumed that the work carried out by the laser field along the tunneling length equals I_p . Thus, at the rescattering moment $\Delta t \sim T_0$, the wave packet size $a_{wp,\parallel}$ is of the order of $\lambda_0 \sqrt{|e|E_0 / \sqrt{m^3 I_p}}$ and the role of the drift can be characterized by means of the parameter $r = (d_{\parallel} / a_{wp,\parallel})^2$ as estimated by

$$r \sim \xi_0^3 \frac{\sqrt{2mI_p}}{16\omega_0}. \quad (1)$$

The condition $r \gtrsim 1$ determines the parameter region where the signature of the drift becomes conspicuous.

As an alternative view on the relativistic drift, the ionized electron here misses the ionic core when it is ionized with zero momentum. Nevertheless, the recollision will occur if the electron is ionized with an appropriate initial momentum, $p_d \sim m\xi_0^2 / 4$, opposite to the laser propagation direction. The probability $P(p_d)$ of this process is exponentially damped though due to the nonzero momentum p_d (see, e.g., Salamin *et al.*, 2006):

$$P(p_d) \sim \exp \left[-\frac{2}{3} \frac{(2mI_p)^{3/2}}{m|e|E_0} \left(1 + \frac{p_d^2}{4mI_p} \right) \right]. \quad (2)$$

The drift term in the exponent will be important if $\sqrt{2mI_p} p_d^2 / m|e|E_0 \gtrsim 1$, which is equivalent to the condition $r \gtrsim 1$. At near-infrared wavelengths ($\omega_0 \approx 1$ eV)

and for the ionization energy $I_p = 13.6$ eV of atomic hydrogen it thus becomes relevant at laser intensities I_0 approximately above 3×10^{16} W/cm². Then, HHG and other recollision phenomena are suppressed.

The attainability of relativistic recollisions would however be very attractive for ultrahigh HHG as well as for the realization of laser controlled high-energy (Hatsagortsyan *et al.*, 2006) and nuclear processes (Chelkowski *et al.*, 2004; Milosevic *et al.*, 2004). Various methods for counteracting the relativistic drift have been proposed, such as via utilizing highly-charged ions (Hu and Keitel, 2001; Keitel and Hu, 2002) which move relativistically against the laser propagation direction (Chirilă *et al.*, 2004; Mocken and Keitel, 2004), via employing Positronium (Ps) atoms (Henrich *et al.*, 2004), or via preparing antisymmetric atomic (Fischer *et al.*, 2007) and molecular (Fischer *et al.*, 2006) orbitals. Here the impact of the drift of the ionized electron is reduced by the increase of the laser frequency in the system's center of mass, an equally strong drift via two constituents with equal mass or via appropriate initial momenta from antisymmetric orbitals, respectively. On the other hand, the laser field can also be modified to suppress the relativistic drift by employing tightly focused laser beams (Lin *et al.*, 2006), two counter-propagating laser beams with linear (Keitel *et al.*, 1993; Kylstra *et al.*, 2000; Taranukhin, 2000; Taranukhin and Shubin, 2001, 2002) or equal-handed circular polarization (Milosevic *et al.*, 2004). In the first two cases, the longitudinal component in the tightly focused laser beam may counteract the drift or the Lorentz force may be eliminated in a small area near the antinodes of the resulting standing wave, respectively. In the third case involving circularly polarized light, the relativistic drift is eliminated via equal directions of electron velocity and magnetic field. This setup is well suited for imaging attosecond dynamics of nuclear processes but not for HHG because of the phase-matching problem (Liu *et al.*, 2009). In the weakly relativistic regime the Lorentz force may also be compensated by a second weak laser beam polarized along the direction of propagation of the strong beam (Chirilă *et al.*, 2002). Furthermore the relativistic drift can be significantly reduced by means of special tailoring of the driving laser pulse, which strongly reduces the time when the electron is relativistic with respect to a sinusoidal laser pulse (Klaiber *et al.*, 2006, 2007). Two consecutive laser pulses (Verschl and Keitel, 2007a) or a single laser field assisted by a strong magnetic field can also be used to revert the drift (Verschl and Keitel, 2007b). In addition two strong Attosecond Pulse Trains (APTs) (Hatsagortsyan *et al.*, 2008) or an infrared laser pulse assisted by an APT (Klaiber *et al.*, 2008) have been employed to enhance relativistic recollisions. In fact, due to the presence of the APT the ionization can be accomplished by one XUV photon absorption and the relatively large energy ω_X of the XUV-photon with $\omega_X = I_p + p_d^2/2m$ can compensate the subsequent

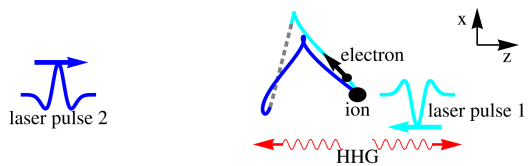


FIG. 6 (Color online) The HHG setup with two counterpropagating APTs. After ionization by the laser pulse 1, the ejected electron is driven in the same pulse (light blue), propagates freely after the pulse 1 has left (gray dashed) and is driven back to the ion by the laser pulse 2 (dark blue). From Kohler *et al.*, 2011.

momentum drift $p_d \sim m\xi_0^2/4$ in the infrared laser field.

The major motivation for the realization of relativistic recollisions is the extension of HHG towards the hard x-ray regime with obvious benefits for time-resolved high-resolution imaging. In the last decades, nonrelativistic atomic HHG (Corkum, 1993; Lewenstein *et al.*, 1994) has been developed as a reliable source of coherent XUV radiation and of attosecond pulses (Agostini and Di Mauro, 2004) opening the door for attosecond time-resolved spectroscopy (Krausz and Ivanov, 2009). Nonrelativistic HHG in an atomic gas medium allows already to generate coherent x-ray photons up to keV energies (Sansone *et al.*, 2006) and to produce XUV pulses shorter than 100 as (Goulielmakis *et al.*, 2008). The most favorable conversion efficiency for nonrelativistic keV harmonics is anticipated with mid-infrared driving laser fields (Chen *et al.*, 2010; Popmintchev *et al.*, 2009). However, progress in this field has slowed down, especially due to the above indicated usual inhibition of recollisions due to optical driving-field intensity above 3×10^{16} W/cm². This indicates the limit for the cut-off frequency ω_c of nonrelativistic HHG to $\omega_c \approx 3.17U_p \sim 10$ keV.

Another factor hindering HHG at high intensities is the less favorable phase-matching. In strong laser fields, outer-shell electrons are rapidly ionized and produce a large free electron background causing phase mismatch between the driving laser wave and the emitted x-rays. The feasibility of phase-matched relativistic HHG in a macroscopic ensemble was first investigated in Kohler *et al.*, 2011. The driving fields are here two counterpropagating APTs consisting of 100 as pulses with a peak intensity of the order of 10^{19} W/cm² (see Fig. 6). The electron is driven to the continuum by the laser pulse 1 in Fig. 6 followed by the usual relativistic drift. Thereafter, the laser pulse 2 overtakes the electron, reverts the drift and imposes the rescattering, yielding a much higher HHG signal than for a conventional laser field at the same cut-off energy. Here phase-matching can be fulfilled due to an additional intrinsic phase specific to this setup, depending on the time delay between the pulses and on the pulse intensity. The latter, being unique for this laser setup, mainly affects the electron excursion

time and varies along the propagation direction. The phase-matching is achieved by modifying the laser intensity along the propagation direction and by balancing the phase slip due to dispersion with the indicated intrinsic phase. Note, however, that HHG in the relativistic regime has been observed experimentally rather efficiently in laser plasma interaction (Dromey *et al.*, 2006).

IV. HIGH-INTENSITY THOMSON AND COMPTON SCATTERING

When an electron is accelerated by an intense laser wave, it emits electromagnetic radiation. This process occurs with absorption of energy and momentum by the electron from the laser field and it is named as multiphoton Thomson scattering or multiphoton Compton scattering, depending on whether quantum effects, like photon recoil, are negligible or not. Multiphoton Thomson and Compton scattering in a strong laser field have been studied theoretically since a long time (see Salamin and Faisal, 1998; Sarachik and Schappert, 1970; and Sengupta, 1949 for multiphoton Thomson scattering and Brown and Kibble, 1964; Goldman, 1964; and Nikishov and Ritus, 1964a for multiphoton Compton scattering). The classical calculation of the emitted spectrum is based on the analytical solution of the Lorentz equation in a plane wave and the substitution of the corresponding electron trajectory in the Liénard-Wiechert fields (Jackson, 1975; Landau and Lifshitz, 1975). Instead, the quantum calculation is performed in the Furry interaction picture (Furry, 1951) by employing the Volkov states as initial and final electron states in the photon-emission amplitude (Volkov, 1935). Volkov states are in fact a basis of the solutions of the Dirac equation in the presence of a background plane wave (see Ritus, 1985 and Zakowicz, 2005, and Boca and Florescu, 2010 for a proof of the orthogonality and of the completeness of the Volkov states, respectively) and their use allows one to take into account exactly the presence of the plane wave from the beginning (see also Par. V.B). Multiphoton Compton scattering, as well as other quantum processes involving an incoming electron (initial four-momentum p_0^μ) and a strong plane wave, are governed by the two Lorentz- and gauge-invariant parameters (Ritus, 1985) $\xi_0 = |e|E_0/m\omega_0$ and $\chi_0 = (p_{0,-}/m)(E_0/E_{cr})$. The gauge invariance of the parameter ξ_0 has to be intended with respect to gauge transformations which do not alter the dependence of the four-vector potential on $\phi = x_-$ (see Heinzl and Ilderton, 2009 for a thorough analysis of this issue). Note that $\xi_0 = 10.7\sqrt{I_0[10^{20} \text{ W/cm}^2]}/\omega_0[\text{eV}]$ and that $\chi_0 = 8.2 \times 10^{-2}\varepsilon_0[\text{GeV}]\sqrt{I_0[10^{20} \text{ W/cm}^2]}$ for an ultrarelativistic electron counterpropagating the laser field.

The parameter ξ_0 is a classical one as it does not contain \hbar and it determines the nonlinearity of the process with respect to the laser field amplitude E_0 . As we have

already mentioned in Sec. III, in fact, at $\xi_0 \gtrsim 1$ the electron becomes relativistic inside the laser field already within a single laser period. Thus, the electric and the magnetic component of the Lorentz force are of the same order and the classical trajectory of the electron depends highly nonlinearly on E_0 . Correspondingly, the parameter ξ_0 also controls the effective number n_{eff} of emitted harmonics, which for an ultrarelativistic electron can be estimated in the following way. In order to effectively emit a frequency ω , the formation length l_f of the process does not have to exceed the coherence length l_{coh} , because otherwise interference effects would hinder the emission. Since an electron with instantaneous velocity β and energy $\varepsilon = m\gamma = m/\sqrt{1-\beta^2} \gg m$ mainly emits along β within a cone with aperture $\vartheta \sim 1/\gamma \ll 1$, the formation length l_f can be estimated as $l_f \sim \varrho/\gamma$, with ϱ being the instantaneous curvature radius of the electron trajectory (Jackson, 1975). On the other hand, $l_{\text{coh}} = \pi/\omega(1-\beta\cos\vartheta) \sim \gamma^2/\omega$ (Baier *et al.*, 1994; Jackson, 1975). By requiring that $l_f \lesssim l_{\text{coh}}$, we obtain the following estimation for the largest-emitted frequency (cut-off frequency) ω_c : $\omega_c \sim \gamma^3/\varrho$. Now, in the average rest frame of the electron it is $\gamma^{(R)} \sim \xi_0$ (corresponding to the energy $\varepsilon^{(R)} \sim m\xi_0$) and $l_f^{(R)} \sim \lambda_0^{(R)}/\xi_0$, where the index (R) indicates the variable in this frame. Consequently, $\omega^{(R)} \sim \xi_0^3\omega_0^{(R)}$ and the effective number of emitted harmonics is $n_{\text{eff}} \sim \xi_0^3$ (note that n_{eff} is a Lorentz scalar). As the number of emitted harmonics corresponds quantum mechanically to the number of laser photons absorbed by the electron during the emission process, the parameter ξ_0 is also said to determine the ‘‘multiphoton’’ character of the process.

On the other hand, the so-called ‘‘nonlinear quantum parameter’’ χ_0 corresponds to the amplitude of the electric field of the laser in units of the critical field of QED in the initial rest-frame of the electron. It determines the importance of quantum effects as the recoil of the emitted photon. In fact, we can estimate classically the importance of the emitted photon recoil from the ratio ω_c/ε and our considerations above exactly indicate that $\omega_c/\varepsilon \sim \chi_0$. Thus, multiphoton Thomson scattering is characterized by the condition $\chi_0 \ll 1$, while multiphoton Compton scattering by the complementary one $\chi_0 \gtrsim 1$. As it has also been thoroughly investigated analytically and numerically in Boca and Florescu, 2011 and Seipt and Kämpfer, 2011a, in the limit $\chi_0 \rightarrow 0$ multiphoton Compton and Thomson spectra coincide, although in Seipt and Kämpfer, 2011a differences have been observed numerically in the detailed structure of the classical and quantum spectra also at $\chi_0 \ll 1$. The most important difference between classical and quantum spectra is certainly the presence of a sharp cut-off in the latter as an effect of the photon recoil: the energy of the photon emitted in a plane wave is limited by the initial energy of the electron. This does not occur classically, as there the frequency of

the emitted radiation has not the physical meaning of photon energy. The dependence of the energy cut-off on the laser intensity has been recently recognized as a possible experimental signature of multiphoton Compton scattering (Harvey *et al.*, 2009).

First calculations on multiphoton Thomson and Compton scattering have mainly focused on the easiest case of a monochromatic background plane wave either with circular or with linear polarization. The main results of these investigations, like the dressing of the electron mass and the dependence of the emitted frequencies on the laser intensities have been recently reviewed in Ehlötzky *et al.*, 2009. The complete description of multiphoton Compton scattering process with respect to the polarization properties of the incoming and the outgoing electron, and of the emitted photon in a monochromatic laser wave has been presented in Ivanov *et al.*, 2004. Recently significant attention has been devoted to the investigation of multiphoton Thomson and Compton scattering in the presence of short and even ultrashort pulses. In Boca and Florescu, 2009 multiphoton Compton scattering has been considered in the presence of a pulsed plane wave. The angular-resolved spectra are practically insensitive to the precise form of the laser pulse for $\omega_0\tau_0 \geq 20$, with τ_0 being the pulse duration. The main differences with respect to the monochromatic case are: 1) a broadening of the lines corresponding to the emitted frequencies; 2) the appearance of sub-peaks, which are due to interference effects in the emission at the beginning and at the end of the laser pulse. On the one hand, the continuous nature of the emission spectrum in a finite pulse in contrast to the discrete one in the monochromatic case has a clear mathematical counterpart. In both cases, in fact, the total transverse momenta \mathbf{P}_\perp with respect to the laser propagation direction and the total quantity P_- are conserved in the emission process. However, in the monochromatic case the following additional conservation law holds (for a linearly polarized plane wave)

$$\varepsilon_0 + p_{0,\parallel} + \frac{m^2\xi_0^2}{2p_-} + 2l\omega_0 = \omega + k_\parallel + \varepsilon' + p'_\parallel + \frac{m^2\xi_0^2}{2p'_-}, \quad (3)$$

with $p'^\mu = (\varepsilon', \mathbf{p}')$ ($k^\mu = (\omega, \mathbf{k})$) being the four-momentum of the outgoing electron (emitted photon) and with l being a positive integer, so that the resulting four-dimensional energy-momentum conservation law allows only for the emission of discrete frequencies. On the other hand, the appearance of sub-peaks has been in particular investigated in Heinzl *et al.*, 2010c, where it has been found that the number N_{s-p} of sub-peaks within the first harmonic scales linearly with the pulse duration τ_0 and with ξ_0^2 : $N_{s-p} = 0.24 \xi_0^2 \tau_0$ [fs]. In this paper the effects of spatial focusing of the driving laser pulse are also discussed. The authors investigate in particular the dependence of the deflection angle α_{out} undergone by the electron after colliding head-on with a Gaussian focused

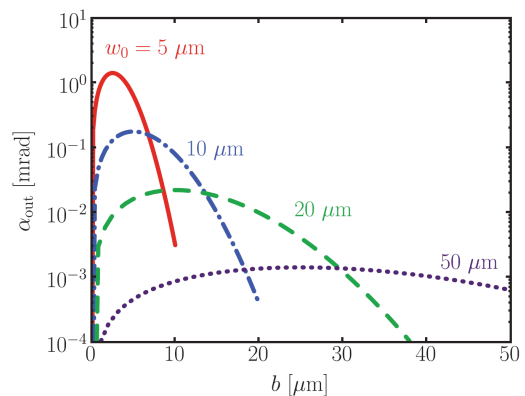


FIG. 7 (Color online) Deflection α_{out} of an electron initially counterpropagating with respect to a laser field with an energy of 3 J and a pulse duration of 20 fs, as a function of the impact parameter b for different laser waist radii w_0 . Reprinted with permission from Heinzl *et al.*, 2010c. Copyright (2010) by the American Physical Society.

beam as a function of the impact parameter b (see Fig. 7).

By further decreasing the laser pulse duration, it has been argued that effects of the relative phase between the pulse profile and the carrier wave (the so-called Carrier Envelope Phase (CEP)) should become visible in multiphoton Thomson and Compton scattering. In Boca and Florescu, 2009 the case of ultrashort pulses with $\omega_0\tau_0 \gtrsim 4$ has been discussed and effects of the CEP on the harmonic yield in specific frequency ranges have been observed. In Mackenroth *et al.*, 2010 the dependence of the angular distribution of the emitted radiation in multiphoton Thomson and Compton scattering on the CEP of few-cycles pulses has been exploited to put forward a scheme to measure the CEP of ultrarelativistic laser pulses (intensities larger than 10^{20} W/cm²). The method is essentially based on the high directionality of the photon emission by an ultrarelativistic electron, because the trajectory of the electron in turn also depends on the laser's CEP. Accuracies in the measurement of the CEP of the order of a few degrees are envisaged. Multiphoton Compton scattering in one-cycle laser pulses has been considered in Mackenroth and Di Piazza, 2011 and a substantial broadening of the emission lines with respect to the monochromatic case has been observed.

The study of multiphoton Thomson and Compton scattering in short laser pulses has also stimulated the investigations of scaling laws for the photon spectral density (Boca and Oprea, 2011; Heinzl *et al.*, 2010c; Seipt and Kämpfer, 2011a,b). For example, in Heinzl *et al.*, 2010c a scaling law has been found for backscattered radiation in the case of head-on laser-electron collisions, which simplifies the averaging over the electron-beam phase space. A more general scaling law has been determined in Seipt and Kämpfer, 2011b, which relaxes

the previous assumptions on head-on collision and on backscattered radiation employed in Heinzl *et al.*, 2010c. Moreover, in Seipt and Kämpfer, 2011a a simple relation is determined between the classical and the quantum spectral densities. Finally, in Boca and Oprea, 2011 it is found that in the ultrarelativistic case $\gamma_0 \gg 1$ the angular distribution of the emitted radiation, integrated with respect to the photon energy, only depends on the ratio ξ_0/γ_0 and not on the independent values of ξ_0 and γ_0 (see also Mackenroth *et al.*, 2010).

In the above-mentioned publications the spectral properties of the emitted radiation in the classical and in the quantum regime have been considered. In Kim *et al.*, 2009 and Zhang *et al.*, 2008, instead, the temporal properties of the emitted radiation in multiphoton Thomson scattering have been investigated. In both mentioned papers the feasibility of generating single attosecond pulses is discussed.

From an experimental point of view multiphoton effects in Thomson and Compton scattering have been already measured in various laboratories. The second-harmonic radiation was first observed in the collision of a 1 keV electron beam with a Q-switched Nd:YAG laser, although the laser intensity was such that $\xi_0 \approx 0.01$ (Englert and Rinehart, 1983), and then in the interaction of a mode-locked Nd:YAG laser ($\xi_0 = 2$) with plasma electrons (Chen *et al.*, 1998). Multiphoton Thomson scattering of laser radiation in the x-ray domain has been reported in Babzien *et al.*, 2006 (see Pogorelsky *et al.*, 2000 for a similar proof-of-principle experiment). Single-shot measurements of the angular distribution of the second harmonic (photon energy 6.5 keV) at various laser polarizations have been carried out by employing a 60 MeV electron beam and a subterawatt CO₂ laser beam with $\xi_0 = 0.35$. In the prominent SLAC experiment (Bula *et al.*, 1996) multiphoton Compton emission was detected for the first time. In this experiment an ultrarelativistic electron beam with energy of about 46.6 GeV collided with a terawatt Nd:glass laser with an intensity of 10^{18} W/cm² ($\xi_0 = 0.9$ and $\chi_0 \approx 0.4$) and four-photon Compton scattering has been observed indirectly via a nonlinear energy shift in the spectrum of the outgoing electrons.

A. Thomson- and Compton-based sources of high-energy photon beams

The single-particle theoretical analysis presented above indicates that high-energy photons can be emitted via multiphoton Thomson and Compton scattering of an ultrarelativistic electron. For example, an electron with initial energy $\varepsilon_0 \gg m$ colliding head-on with an optical laser field ($\omega_0 \approx 1$ eV) of moderate intensity ($\xi_0 \lesssim 1$) is barely deflected by the laser field ($\varrho \sim \lambda_0 \gamma_0 / \xi_0 \gg \lambda_0$) and potentially emits photons with energies ω [keV] \lesssim

$3.8 \times 10^{-3} \varepsilon_0^2$ [MeV]. This feature has boosted the idea of so-called Thomson- and Compton-based sources of high-energy photons as a valid alternative to conventional synchrotron sources, the main advantages of the former being the compactness, the wide tunability, the shortness of the photon beams in the femtosecond scale and the potential for high brightness. Unless the experiments on multiphoton Thomson and Compton scattering where laser systems with $\xi_0 \gtrsim 1$ are generally employed, Thomson- and Compton-based photon sources preferably require lasers with $\xi_0 \lesssim 1$, such that multiphoton effects are suppressed and shorter bandwidths of the photon beam are achieved. On the other hand, the electron beam quality is crucial for Thomson- and Compton-based radiation sources. In particular, the brightness of the photon beam scales inversely quadratically with the electron beam emittance, and linearly with the electron bunch current density.

The proof-of-principle of Thomson- and Compton-based photon sources has been demonstrated experimentally by crossing a high-energy laser pulse with a picosecond relativistic electron beam from a conventional linear electron accelerator (Chouffani *et al.*, 2002; Leemans *et al.*, 1996; Pogorelsky *et al.*, 2000; Sakai *et al.*, 2003; Schoenlein *et al.*, 1996; Ting *et al.*, 1995, 1996). We also mention the benchmark experiment carried out at LLNL, where photons with an energy of 78 keV have been produced with a total flux of 1.3×10^6 photons/shot, by colliding an electron beam with an energy of 57 MeV with a Ti:Sa laser beam with an intensity of about 10^{18} W/cm² ($\xi_0 \approx 0.6$) (Gibson *et al.*, 2004).

Another achievement in the development of Thomson- and Compton-based photon sources has been the experimental realization of a compact all-optical setup, where the electrons are accelerated by an intense laser. In the first experiment with an all-optical setup (Schwoerer *et al.*, 2006), x-ray photons in the range of 0.4 keV to 2 keV have been generated. In this experiment the electron beam was produced by a high-intensity Ti:Sa laser beam ($I_0 \approx 2 \times 10^{19}$ W/cm²) focused into a pulsed helium gas jet. The characteristic feature of the all-optical setup is that the electron bunches, and, consequently, the generated x-ray photon beams have an ultrashort duration (~ 100 fs) and a small size of the order of 10 μ m. Another advantage is that the electrons can be precisely synchronized with the driving laser field. In order to further improve the all-optical setup, design parameters for a proof-of-concept experiment have been analyzed in Hartemann *et al.*, 2007. It is shown that x-ray fluxes exceeding 10^{21} s⁻¹ and a peak brightness larger than 10^{19} photons/(sr mm² 0.1% bandwidth) can be achieved at photon energies approaching 1 MeV. A few years later the all-optical Compton-based photon source MonoEnergetic Gamma-ray (MEGa-ray) has been built at LLNL (Gibson *et al.*, 2010). Gamma-rays ranging from 75 keV to 0.9 MeV have been demon-

strated with a peak spectral brightness of 1.5×10^{15} photons/(s mrad² mm² 0.1% bandwidth) and with a flux of 1.6×10^5 photons/shot.

In the basic setups of Thomson- and Compton-based photon sources the electrons experience the intense laser field for a time-interval much shorter than that they need to cross the whole laser beam, the former being of the order of the laser's Rayleigh length divided by the speed of light. Thus, the request for a more intense laser pulse at a given power in order to increase the photon yield implies a tighter focusing and therefore a shorter effective interaction time, which in turn causes a broadening of the photon spectrum. In Debus *et al.*, 2010 the Traveling-Wave Thomson Scattering (TWTS) setup is put forward, which allows the electrons to stay in the focal region of the laser beam during the whole crossing time. This is achieved by employing cylindrical optics to focus the laser field only along one direction and, depending on the angle between the initial electron velocity and the laser wave-vector, by tilting the laser pulse front. As a result, an interaction length ~ 1 cm-1 m can be achieved and, correspondingly very large photon fluxes (up to 5×10^{10} photons/shot at 20 keV).

An alternative way of reaching longer effective laser-electron interaction times has been proposed in Karagodsky *et al.*, 2010, where a planar Bragg structure is employed to guide the laser pulse and realize Thomson/Compton scattering in a waveguide. In this way, the yield of x-rays can be enhanced by about two orders of magnitude with respect to the conventional free-space Gaussian-beam configuration at given electron beam and injected laser power in both configurations. However, there are two constraints specific to this setup. On the one hand, the electron beam has to have a small angular spread in order to be injected into the planar Bragg structure without causing wall damage. On the other hand, the laser field strength has to be such that $\xi_0 \lesssim 8 \times 10^{-4}$ to avoid surface damage.

Finally, in Hartemann *et al.*, 2008 a setup has been put forward to obtain bright GeV gamma-rays via Compton scattering of electrons by a thermonuclear plasma. In fact, a thermonuclear deuterium-tritium plasma produces intense blackbody radiation with a temperature ~ 20 keV and a photon density $\sim 10^{26}$ cm⁻³ (Tabak *et al.*, 1994). When a thermal photon with energy $\omega \sim 1$ keV counterpropagates with respect to a GeV electron ($\gamma_0 \sim 10^3$), a Doppler-shifted high-energy photon $\omega' \sim \gamma_0^2 \omega \sim 1$ GeV can be emitted on axis, i.e. in the same direction of the incoming electron. Since ω' has to be smaller than the initial electron energy ε_0 , a kinematical photon pileup is induced in the emitted photon spectrum at ε_0 (Zeldovich and Sunyaev, 1969) (see Fig. 8). This results in a quasimonochromatic GeV gamma-ray beam with a peak brightness $\gtrsim 10^{30}$ photons/(s mrad² mm² 0.1% bandwidth), comparable with that of the FLASH.

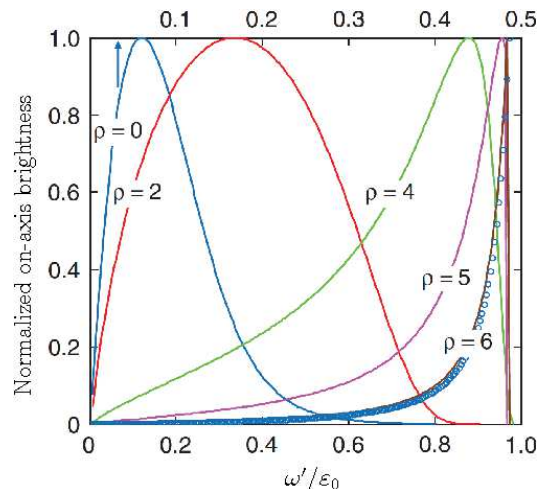


FIG. 8 (Color online) Normalized on-axis brightness for different values of the rapidity $\rho = \cosh^{-1} \gamma_0$ at a plasma temperature of 20 keV. See Hartemann *et al.*, 2008 for the meaning of the blue circles at $\rho = 6$. Adapted and reprinted with permission from Hartemann *et al.*, 2008. Copyright (2008) by the American Physical Society.

The unique features of Thomson- and Compton-based photon sources render them a powerful experimental device. For example, they can be employed for studying nuclear resonance fluorescence for *in situ* isotopes detection (Albert *et al.*, 2010). On this respect, such photon sources will represent the main experimental tool for nuclear-physics investigations at the Romanian pillar of ELI (see Fig. 1). Other possible applications at photon energies beyond the MeV threshold include the production of positrons (Omori *et al.*, 2003) as well as the investigations of high-energy processes occurring in gamma-gamma and gamma-lepton collisions (Telnov, 1990).

V. RADIATION REACTION

The problem of “radiation reaction” (RR) is one of the oldest and most fundamental problems in electrodynamics. Classically it corresponds to the determination of the equation of motion of a charged particle, an electron for definiteness, in a given electromagnetic field $F^{\mu\nu}(x)$. In fact, the Lorentz equation $mdu^\mu/ds = eF^{\mu\nu}u_\nu$, with electron four-velocity $u^\mu = dx^\mu/ds$ and proper time s , does not take into account that the electron, while being accelerated, emits electromagnetic radiation and loses in this way energy and momentum. The first attempt of taking into account the reaction of the radiation emitted by the electron on the motion of the electron itself (from here comes the expression “radiation reaction”), was accomplished by H. A. Lorentz in the nonrelativistic regime (Lorentz, 1909). Starting from the known Larmor formula $\mathcal{P}_L = (2/3)e^2\mathbf{a}^2$ for the power emitted by

an electron with instantaneous acceleration \mathbf{a} , Lorentz argued that this energy-loss corresponds to a “damping” force \mathbf{F}_R acting on the electron and is given by $\mathbf{F}_R = (2/3)e^2 d\mathbf{a}/dt$. The expression of the damping force was generalized to the relativistic case by M. Abraham in the form (Abraham, 1905)

$$F_R^\mu = \frac{2}{3}e^2 \left(\frac{d^2 u^\mu}{ds^2} + \frac{du^\nu}{ds} \frac{du_\nu}{ds} u^\mu \right). \quad (4)$$

In order to solve self-consistently the problem of a radiating electron, P. A. M. Dirac suggested in Dirac, 1938 to start from the coupled system of Maxwell and Lorentz equations

$$\begin{cases} \partial_\mu F_T^{\mu\nu} = 4\pi j^\nu \\ \partial_\lambda F_{T,\mu\nu} + \partial_\mu F_{T,\nu\lambda} + \partial_\nu F_{T,\lambda\mu} = 0 \\ m_0 \frac{du^\mu}{ds} = e F_T^{\mu\nu} u_\nu, \end{cases} \quad (5)$$

where $F_T^{\mu\nu}(x) = F^{\mu\nu}(x) + F_S^{\mu\nu}(x)$, with $F_S^{\mu\nu}(x)$ being the “self” electromagnetic field generated by the electron four-current $j^\mu(x) = e \int ds \delta(x - x(s)) u^\mu$ and where the meaning of the symbol m_0 for the electron mass will be clarified below. In order to write an “effective” equation of motion of the electron which includes RR, one “removes” the degrees of freedom of the electromagnetic field (Teitelboim, 1971). This is achieved in Landau and Lifshitz, 1975 at the level of the Lagrangian of the system electron+electromagnetic field and an interesting connection of the RR problem with the derivation of the so-called Darwin Lagrangian is indicated. By working at the level of the equations of motion (5), one first employs the Green-function method and formally determines the retarded solution $F_{T,\text{ret}}^{\mu\nu}(x)$ of the (inhomogeneous) Maxwell equations: $F_{T,\text{ret}}^{\mu\nu}(x) = F^{\mu\nu}(x) + F_{S,\text{ret}}^{\mu\nu}(x)$ (Teitelboim, 1971). The substitution of $F_{T,\text{ret}}^{\mu\nu}(x)$ in the Lorentz equation eliminates the electromagnetic field’s degrees of freedom but it is not straightforward because $F_{T,\text{ret}}^{\mu\nu}(x)$ has to be calculated at the electron’s position where the electron current diverges. This difficulty is circumvented by modeling the electron as a uniformly charged sphere with radius a tending to zero. After performing the substitution and by neglecting terms which vanish in the limit $a \rightarrow 0$, one obtains the equation $(m_0 + \delta m) du^\mu/ds = e F^{\mu\nu} u_\nu + F_R^\mu$ with $\delta m = (4/3)e^2/a$ being formally diverging. However, it is important that the only diverging term in the limit $a \rightarrow 0$ is proportional to the electron four-acceleration. At this point a sort of “classical renormalization principle” is employed, saying that what one measures experimentally as the physical electron mass m is the overall coefficient of the four-acceleration du^μ/ds . Therefore, one sets $m = m_0 + \delta m$ and obtains the so-called Lorentz-Abraham-Dirac (LAD) equation:

$$m \frac{du^\mu}{ds} = e F^{\mu\nu} u_\nu + \frac{2}{3}e^2 \left(\frac{d^2 u^\mu}{ds^2} + \frac{du^\nu}{ds} \frac{du_\nu}{ds} u^\mu \right). \quad (6)$$

We point out that renormalization in quantum field theory is based on the fact that the bare quantities, like charges and masses, appear in the Lagrangian density of the theory, which is not an observable physical quantity. On the other hand, the bare electron mass m_0 , which is formally negatively diverging for m to be finite, appears here in the system of equations (5), which should “directly” provide classical physical observables, like the electron trajectory. On the other hand, it is also known that the LAD equation is plagued by physical inconsistencies like, for example, the existence of the so-called “runaway” solutions with an exponentially-diverging electron acceleration even in the absence of an external field (see the books Hartemann, 2001 and Rohrlich, 2007 for a review on these issues).

It was first shown in Landau and Lifshitz, 1975 that in the nonrelativistic limit the RR force in Eq. (4) is much smaller than the Lorentz force if the typical wavelength λ and the typical field-amplitude F of the external electromagnetic field fulfill the two conditions

$$\lambda \gg \alpha \lambda_C, \quad F \ll \frac{F_{\text{cr}}}{\alpha}, \quad (7)$$

with $F_{\text{cr}} = m^2/|e| = 1.3 \times 10^{16}$ V/cm = 4.4×10^{14} G being the “electromagnetic” critical field of QED. This allows for the reduction of order in the LAD equation, i.e. for the substitution of the electron acceleration in the RR force via the Lorentz force divided by the electron mass. In order to be allowed to perform the analogous reduction of order in the relativistic case, the conditions (7) have to be fulfilled in the instantaneous rest-frame of the electron (Landau and Lifshitz, 1975) and the result is the so-called Landau-Lifshitz (LL) equation

$$m \frac{du^\mu}{ds} = e F^{\mu\nu} u_\nu + \frac{2}{3}e^2 \left[\frac{e}{m} (\partial_\alpha F^{\mu\nu}) u^\alpha u_\nu - \frac{e^2}{m^2} F^{\mu\nu} F_{\alpha\nu} u^\alpha + \frac{e^2}{m^2} (F^{\alpha\nu} u_\nu) (F_{\alpha\lambda} u^\lambda) u^\mu \right]. \quad (8)$$

The LL equation is not affected by the shortcomings of the LAD equation: for example, it is evident that if the external field vanishes, so does the electron acceleration. Most importantly, the conditions (7) in the instantaneous rest-frame of the electron have always to be fulfilled in the realm of classical electrodynamics, i.e. if quantum effects are neglected. In order this to be true, in fact, the two weaker conditions $\lambda \gg \lambda_C$ and $F \ll F_{\text{cr}}$ have to be fulfilled in the instantaneous rest-frame of the electron: the first guarantees that the electron’s wave function is well localized and the second that pure quantum effects, like photon recoil or spin effects are negligible (Baier *et al.*, 1994; Berestetskii *et al.*, 1982; Ritus, 1985). This observation led F. Rohrlich to state recently that the LL equation is the “physically correct” classical relativistic equation of motion of a charged particle (Rohrlich, 2008).

Rohrlich's statement is also supported by the findings in Spohn, 2000, where it is shown that the physical solutions of the LAD equation, i.e. those which are not runaway-like, are on the critical manifold of the LAD equation itself and are governed there exactly by the LL equation. On the other hand, since the LL equation is derived from the LAD equation, one can still doubt on its rigorous validity due to the application in the latter equation of the "suspicious" classical mass-renormalization procedure. This procedure is however avoided in Gralla *et al.*, 2009 by employing a more sophisticated zero-size limiting procedure, where also the charge and the mass of the particle are sent to zero but in such a way that their ratio remains constant. The authors conclude that at leading order the LL equation represents the self-consistent perturbative equation of motion for a charge without electric and magnetic moment. On this respect, in Galley *et al.*, 2010 the motion of finite-size objects in a given electromagnetic field is investigated. It is shown that high-order corrections in the particle size scale for a spherically-symmetric distribution as the "square" of the radius and not linearly, as it was previously claimed in the literature. The motion of a continuous charge distribution interacting with an external electromagnetic field is also investigated by a self-consistent model and at a more formal level in Burton *et al.*, 2007.

From the original derivation of the LL equation from the LAD one in Landau and Lifshitz, 1975, it is expected that the two equations should predict the same trajectory of the electron, possibly with differences smaller than quantum effects. This conclusion has been recently confirmed by analytical and numerical investigations in Hadad *et al.*, 2010 for an external plane-wave field with linear and circular polarization and in Bulanov *et al.*, 2011 for different time-depending external electromagnetic field configurations. An effective numerical method to calculate the trajectory of an electron via the LL equation, which explicitly maintains the relativistic covariance and the mass-shell condition $u^2 = 1$, has been put forward in Harvey *et al.*, 2011a.

We should emphasize that the LL equation is not the only equation which has been suggested to overcome the inconsistencies of the LAD equation. A list of alternative equations can be found in the recent review (Hammond, 2010). A phenomenological equation of motion including RR and quantum effects related to photon recoil has been suggested in Sokolov *et al.*, 2010a, 2009 (see also Par. V.B). The authors write the differential variation of the electron momentum as due to two contributions: one arising from the external field and one corresponding to the recoil of the emitted photon. The resulting

equation can be written as the system of equations

$$\begin{cases} m \frac{dx^\mu}{d\tau} = p^\mu + \frac{2}{3} e^2 \frac{\mathcal{I}_{\text{QED}}}{\mathcal{I}_L} \frac{eF^{\mu\nu} p_\nu}{m^2} \\ \frac{dp^\mu}{d\tau} = eF^{\mu\nu} \frac{dx_\nu}{d\tau} - \mathcal{I}_{\text{QED}} \frac{p^\mu}{m}, \end{cases} \quad (9)$$

where τ is the time in the "momentarily comoving Lorentz frame" of the electron where the spatial components of p^μ instantaneously vanish, \mathcal{I}_{QED} is the quantum radiation intensity (Ritus, 1985) and $\mathcal{I}_L = (2/3)\alpha\omega_0^2\xi_0^2$. The expression of \mathcal{I}_{QED} in the case of a plane wave is employed, which is valid for an arbitrary external field only for an ultrarelativistic electron.

It has also to be stressed that the original LAD equation is still object of extensive investigation (the first study of the LAD equation in a plane-wave field was performed in Hartemann and Kerman, 1996). In Ferris and Gratus, 2011, for example, the origin of the Schott term in the RR force, i.e. the term proportional to the derivative of the electron acceleration (see Eq. (4)), is thoroughly investigated and in Noble *et al.*, 2011 a kinetic theory of RR is proposed, based on the LAD equation and applicable to study systems of many particles including RR (this last aspect is also considered in Rohrlich, 2007). Enhancement of RR effects due to the coherent emission of radiation by a large number of charges is discussed in Smorenburg *et al.*, 2010. On this respect, we mention here that, in order to investigate strong laser-plasma interaction at intensities exceeding 10^{23} W/cm², RR effects have been also implemented in Particle-In-Cell (PIC) codes (Tamburini *et al.*, 2011, 2010; Zhidkov *et al.*, 2002) by modifying the Vlasov equation for the electron distribution function according to the LL equation. Specifically, in Zhidkov *et al.*, 2002 it is shown that in the collision of a laser beam with intensity $I_0 = 10^{23}$ W/cm² with an overdense plasma slab, about 35% of the absorbed laser energy is converted into radiation and that the effect of RR amounts to about 20%. One-dimensional (Tamburini *et al.*, 2010) and three-dimensional (Tamburini *et al.*, 2011) PIC simulations have indicated that RR effects strongly depend on the polarization of the driving field: while for circular polarization they are negligible also at $I_0 \sim 10^{23}$ W/cm², at those intensities they are important for linear polarization. The simulations also show the beneficial effects of RR in reducing the energy spread of ion beams generated via laser-plasma interaction (see also Par. XI.A). A different beneficial effect of RR on ion acceleration has been found in Chen *et al.*, 2011 for the case of a transparent plasma: RR strongly suppresses backward motion of the electrons, cools them down and increases the number of ions to be bunched and accelerated. Finally, the system in Eq. (9) has been implemented in a 3D PIC code in Sokolov *et al.*, 2009 showing that a laser pulse with intensity 10^{22} W/cm² loses about 27% of its energy in the collision with a plasma slab. The same system of equations has

been employed to study the penetration of ultra-intense laser beams into a plasma in the hole-boring regime (Nau-mova *et al.*, 2009) and to investigate the process of ponderomotive ion acceleration at ultrahigh laser intensities in overcritical bulk targets (Schlegel *et al.*, 2009).

A. The classical radiation dominated regime

As it was already observed in Landau and Lifshitz, 1975, the fact that the RR force in the LL equation has to be much smaller than the Lorentz force in the instantaneous rest-frame of the electron does not exclude that some components of the two forces can be of the same order of magnitude in the laboratory system. This occurs if the condition $\alpha\gamma^2 F/F_{\text{cr}} \sim 1$ is fulfilled at any instant, with γ being the relativistic Lorentz factor of the electron and F the amplitude of the external electromagnetic field. For an ultrarelativistic electron this condition can be fulfilled also in the realm of classical electrodynamics (quantum recoil effects are negligible if $\gamma F/F_{\text{cr}} \ll 1$) and it characterizes the so-called Classical Radiation-Dominated Regime (CRDR). The CRDR has been investigated in Shen, 1970 for a background constant and uniform magnetic field. In Koga *et al.*, 2005 an equivalent definition of the CRDR in the presence of a background laser field has been formulated, as the regime where the average energy radiated by the electron in one laser period is comparable with the initial electron energy. By estimating the radiated power \mathcal{P}_L from the relativistic Larmor formula $\mathcal{P}_L = -(2/3)e^2(du_\mu/ds)(du^\mu/ds)$ (Jackson, 1975) with $du^\mu/ds \rightarrow (e/m)F^{\mu\nu}u_\nu$, one obtains that $\mathcal{P}_L \sim \alpha\chi_0\xi_0\varepsilon_0$. Therefore, the conditions of being in the CRDR are

$$R_C = \alpha\chi_0\xi_0 \approx 1, \quad \chi_0 \ll 1, \quad (10)$$

where, as we have seen in Par. IV, the second condition ensures in particular that quantum effects like photon recoil are negligible. The same condition $R_C \approx 1$ has been obtained in Di Piazza, 2008 by solving exactly the LL equation (8) for a general plane-wave background field. The analytical solution shows in fact that for an ultrarelativistic electron the main effect of RR is due to the last term in Eq. (8). As a consequence, while the quantity $u_-(\phi)$ is constant if the equation of motion is the Lorentz one, it decreases here with respect to ϕ as $u_-(\phi) = u_{0,-}/h(\phi)$, where u_0^μ is the four-velocity at an initial ϕ_0 and

$$h(\phi) = 1 + \frac{2}{3} \frac{R_C}{\omega_0} \int_{\phi_0}^{\phi} d\varphi \psi^2(\varphi), \quad (11)$$

with $\psi(\phi)$ being the laser electric-field pulse shape. This effect has been recently suggested in Harvey *et al.*, 2011b as a possible signature to measure RR. The two conditions in Eq. (10) are in principle compatible for sufficiently large values of ξ_0 . For example, for an optical

($\omega_0 = 1$ eV) laser field with an intensity of 10^{24} W/cm² and for an electron initially counterpropagating with respect to the laser field with an energy of 20 MeV, it is $\chi_0 = 0.16$ and $R_C = 1.3$. This example shows that in general it is not experimentally easy to enter the CRDR at least with presently-available laser systems. In Di Piazza *et al.*, 2009a a different regime has been investigated, which is parametrically less demanding than the CRDR but in which the effects of RR are still large. In this regime the change in the longitudinal (with respect to the laser field propagation direction) momentum of the electron due to RR in one laser period is of the order of the electron's longitudinal momentum itself in the laser field. As a result, it is found that in the ultrarelativistic case and for a few-cycle pulse, if the conditions

$$R_C \gtrsim \frac{4\gamma_0^2 - \xi_0^2}{2\xi_0^2} > 0 \quad (12)$$

are fulfilled, then the electron is reflected in the laser field only if RR is taken into account (see also Harvey and Marklund, 2011 for a recent investigation of the electron's dynamics in the two complementary regimes $2\gamma_0 \leq \xi_0$ including RR effects). This can have measurable effects if one exploits the high directionality of the radiation emitted by an ultrarelativistic electron (see Sec. IV). The results in Di Piazza *et al.*, 2009a show in fact that the aperture of the angular distribution of the emitted radiation with and without RR effects included may differ by more than 10° already at an optical laser intensity of 5×10^{22} W/cm² ($\xi_0 \approx 150$) and at an initial electron energies of 40 MeV ($2\gamma_0 \approx 156$) for which it is $R_C \approx 0.08$. Small effects of RR on photon spectra emitted by initially bound electrons had already been predicted via numerical integration of the LL equation in Keitel *et al.*, 1998 well below the CRDR.

B. Quantum radiation reaction

The shortcomings of the classical approaches to the problem of RR suggest that this problem can be fully understood only at the quantum level. In the seminal paper Moniz and Sharp, 1977 the origin of the classical inconsistencies like the existence of runaway solutions of the LAD equation have been clarified in the nonrelativistic case. The authors first show that such inconsistencies are also absent in classical electrodynamics if one considers charge distributions with a typical radius larger than the classical electron radius r_0 . Going to the nonrelativistic quantum theory and by analyzing the Heisenberg equations of motion of the electron in an external time-dependent field, the authors conclude that the quantum theory of a pointlike particle does not show any runaway solutions, provided that the external field varies slowly along a length of the order of λ_C (this is an

obvious assumption in the realm of nonrelativistic theory, as time-dependent fields with typical wavelengths of the order of λ_C would in principle allow for electron-positron (e^+e^-) pair production). From this point of view a classical theory of RR has only physical meaning as the classical limit ($\hbar \rightarrow 0$) of the corresponding quantum theory and the authors indicate that the resulting equation of motion is the nonrelativistic LL equation with the bare mass m_0 (it is shown that the electrostatic self-energy of a point charge vanishes in nonrelativistic quantum electrodynamics). On the other hand, if one considers the quantum equations of motion of a charge distribution and performs the classical limit before the pointlike limit, then the classical equations of motion of the charge distribution are of course recovered and, once the point-like limit is then performed, runaway solutions again appear. The nonrelativistic form of the LL equation has been also recovered from quantum mechanics in Krivitskii and Tsytovich, 1991 by including radiative corrections to the time-dependent electron momentum operator in the Heisenberg representation and by calculating the time-derivative of the average momentum in a semiclassical state.

The situation in the relativistic theory is less straightforward because relativistic quantum electrodynamics, i.e. QED, is a field theory fundamentally different from classical electrodynamics. The first theory of relativistic quantum RR goes back to W. Heitler and his group (Heitler, 1984; Jauch and Rohrlich, 1976). However, the evaluations of QED amplitudes in Heitler's theory involves the solution of complicated integral equations and it has given a practical result only in the calculation of the total energy emitted by a nonrelativistic quantum oscillator with and without RR. At first sight one would say that RR effects are automatically taken into account in QED, because the electromagnetic field is treated as a collection of photons that take away energy and momentum, when they are emitted by charged particles. However, photon recoil is always proportional to \hbar and it is a pure quantum quantity with no classical counterpart. Moreover, if one calculates the spectrum of multiphoton Compton scattering in an external plane-wave field, for example, and then performs the classical limit $\chi_0 \rightarrow 0$, one obtains the corresponding multiphoton Thomson spectrum calculated via the Lorentz equation and not via the LAD or the LL equation (see also Sec. IV). Finally, we have also seen that in classical electrodynamics the effects of RR may not be a small perturbation of the Lorentz dynamics and they cannot be obtained as the result of a single limiting procedure, as otherwise they would always appear as a small correction. In order to understand what RR is in QED, it is more convenient to go back to Eq. (5) and to notice that the LAD, namely the LL, equation is equivalent to the coupled system of Maxwell and Lorentz equations. If one determines the trajectory of the electron via the LL equation

and then calculates the total electromagnetic field $F_T^{\mu\nu}(x)$ via the Liénard-Wiechert four-potential (Landau and Lifshitz, 1975), one has solved completely the classical problem of the radiating electron in the given electromagnetic field. Now, by working in the Furry interaction picture (Furry, 1951), the effects of the external electromagnetic field are taken into account exactly already from the beginning (see also Sec. IV), and the complete evolution of the system electron-positron field $\Psi(x)$ plus radiation electromagnetic field $\mathcal{F}^{\mu\nu}(x) \equiv \partial^\mu \mathcal{A}^\nu(x) - \partial^\nu \mathcal{A}^\mu(x)$ is obtained if the S -matrix

$$S = \mathcal{T} \left[\exp \left(-ie \int d^4x \bar{\Psi}^{(F)} \gamma^\mu \Psi^{(F)} \mathcal{A}_\mu \right) \right] \quad (13)$$

is determined. Here, \mathcal{T} is the chronological operator, $\bar{\Psi}(x) = \Psi^\dagger(x)\gamma^0$, γ^μ are the Dirac gamma matrices (Berestetskii *et al.*, 1982) and the index (F) indicates that the electron-positron field is quantized in the Furry interaction picture. From this point of view, solving classically the LL equation and determining the corresponding radiation field is equivalent in QED to determine completely the S -matrix and then the asymptotic state $|t \rightarrow +\infty\rangle$ for the given initial state $|t \rightarrow -\infty\rangle = |e^-\rangle$ representing a single electron. The first-order term in the perturbative expansion of the S -matrix corresponds to the process of multiphoton Compton scattering and then, classically, to the Lorentz dynamics. Instead, all high-order terms give rise to radiative corrections and to high-order coherent and incoherent (cascade) processes and determine what we call “quantum RR”. Here, by high-order coherent processes we mean processes involving more than one basic QED process (photon emission by an electron/positron or e^+e^- photoproduction) but all occurring in the same formation region. Analogously, in high-order incoherent or cascade processes each basic QED process occurs in a different formation region. Now, in the case of a background plane wave at $\xi_0 \gg 1$ and $\chi_0 \lesssim 1$ quantum effects are certainly important but radiative corrections and high-order coherent processes scale with α and can be neglected (Ritus, 1972). Also, if χ_0 does not exceed unity then the photons emitted by the electron are mainly not able, by interacting again with the laser field, to create e^+e^- pairs, as the pair production probability is exponentially suppressed (see also Secs. VII and VIII). Therefore, we conclude that at $\xi_0 \gg 1$ and $\chi_0 \lesssim 1$ RR in QED corresponds to the multiple photon recoils experienced by the electron when it emits many photons consecutively and incoherently (Di Piazza *et al.*, 2010a). In order to understand this qualitatively, we assume that $\chi_0 \ll 1$ and we estimate the average number N_γ of photons emitted by an electron in one laser period at $\xi_0 \gg 1$. Since the probability of emitting one photon in a formation length is of the order of α and since one laser period contains about ξ_0 formation lengths (Ritus, 1985) then $N_\gamma \sim \alpha\xi_0$. Also, the typical energy ω of a photon emitted by an electron

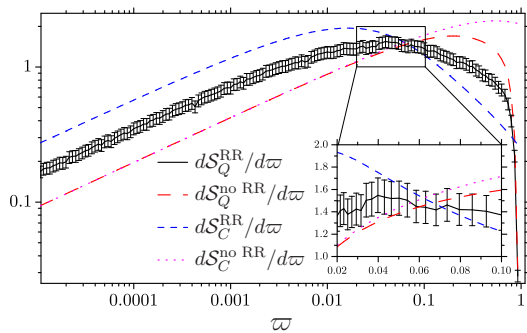


FIG. 9 (Color online) Quantum photon spectra as a function of $\varpi = k_-/p_{0,-}$ calculated with (solid, black line) and without (long dashed, red line) RR and the corresponding classical ones with (short dashed, blue line) and without (dotted, magenta line) RR. The error bars in the quantum spectrum with RR stem from numerical uncertainties in multidimensional integrations. The numerical parameters are: $\varepsilon_0 = 1$ GeV, $\omega_0 = 1.55$ eV and $I_0 = 5 \times 10^{22}$ W/cm² ($R_Q = 1.1$ and $\chi_0 = 1.8$). Reprinted with permission from Di Piazza *et al.*, 2010a. Copyright (2010) by the American Physical Society.

is of the order of $\omega \sim \chi_0 \varepsilon_0$, then the average energy \mathcal{E} emitted by the electron is $\mathcal{E} \sim \alpha \xi_0 \chi_0 \varepsilon_0 = R_C \varepsilon_0$. This estimate is in agreement with the classical result obtained from the LL equation. In other words, the classical limit of RR in this regime corresponds to the emission of a higher and higher number of photons all with an energy much smaller than the electron energy, in such a way that even though the recoil at each emission is almost negligible, the cumulative effect of all photon emissions may have a finite nonnegligible effect. Note that ω and N_γ are both pure quantum quantities and only their product \mathcal{E} has a classical analogue in the limit $\chi_0 \rightarrow 0$. These considerations have allowed for the introduction in Di Piazza *et al.*, 2010a of the Quantum Radiation-Dominated Regime (QRDR), which is characterized by multiple emission of photons already in one laser period. This regime is then characterized by the conditions

$$R_Q = \alpha \xi_0 \approx 1, \quad \chi_0 \gtrsim 1. \quad (14)$$

Quantum photon spectra have been calculated numerically in Di Piazza *et al.*, 2010a without RR, i.e. by including only the emission of one photon (four-momentum k^μ), and with RR, i.e. by including multiple-photon emissions (and by integrating with respect to all the four-momenta of the emitted photons except one indicated as k^μ). The results show that in the QRDR the effects of RR, i.e. of multiple photon emissions, are essentially three (see Fig. 9): 1) increase of the photon yield at low photon energies; 2) decrease of the photon yield at high photon energies; 3) shift of the maximum of the photon spectrum towards low photon energies. Figure 9 also shows that the classical treatment of RR (via the LL equation) would artificially overestimate the above effects, the reason being that quantum corrections decrease the average

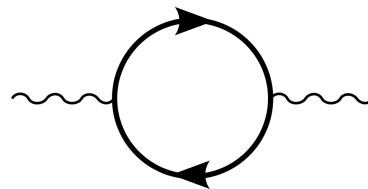


FIG. 10 Vacuum polarization diagram in an external background electromagnetic field. The “thick” electron lines indicate electron propagators calculated in the Furry picture, accounting exactly for the presence of the background field.

energy emitted by the electron with respect to the classical value. As we have mentioned in Sec. V, a semiclassical phenomenological approach to RR in the quantum regime has been proposed in Sokolov *et al.*, 2009, 2010b.

Finally, the quantum modifications induced by the electron’s self-field onto the electron states in a plane-wave field (Volkov states) have been recently investigated in Meuren and Di Piazza, 2011. It is found that the classical expression of the electron quasimomentum $p_0^\mu + m^2 \xi_0^2 n^\mu / 4p_{0,-}$ in a (linearly polarized) plane wave (Berestetskii *et al.*, 1982; Landau and Lifshitz, 1975) undergoes a correction depending on the quantum parameter χ_0 and also that self-field effects induce a peculiar dynamics of the electron spin.

VI. VACUUM POLARIZATION EFFECTS

Vacuum polarization (or diffractive QED) effects are pure quantum effects which involve the interaction among photons in vacuum. This is in contrast to classical electrodynamics where the linearity of Maxwell equations in vacuum forbids self-interaction of the electromagnetic field in the vacuum itself. The allowance of photon-photon interaction in vacuum in the framework of QED can be understood qualitatively as here a photon may locally “transform” into an e^+e^- pair and interact with other photons (see Fig. 10). This transformation in vacuum does not conserve energy-momentum if the three involved particles are real, i.e. on shell (Berestetskii *et al.*, 1982) and this is why quantum mechanically it can occur only “virtually” according to Heisenberg uncertainty principle.¹ By assuming that the background field depends only on time, the linear momentum is conserved in the transformation. Then, in general one can estimate the time duration t_f of the transformation itself, i.e. the formation time of a generic refractive QED process, from

¹ In the formalism of QED energy-momentum is conserved at any interaction vertex, but some of the interacting particles are then necessarily “off-shell” or virtual.

the time-energy uncertainty principle $t_f \sim 1/\Delta\varepsilon$, with

$$\Delta\varepsilon = \sqrt{m^2 + p_\perp^2 + p_\parallel^2} + \sqrt{m^2 + p_\perp^2 + (\omega - p_\parallel)^2} - \omega. \quad (15)$$

Here, we have indicated as ω the energy of the incoming photon and as p_\parallel (\mathbf{p}_\perp) the momentum of one of the outgoing particles along (perpendicular to) the propagation direction of the incoming photon. By estimating $p_\perp \sim m$, we obtain that if $\omega \lesssim m$ then $p_\parallel \sim m$, $\Delta\varepsilon \sim m$ and $t_f \sim \lambda_C$, while if $\omega \gg m$ then $p_\parallel \sim \omega$ implying that $\Delta\varepsilon \sim m^2/\omega$ and $t_f \sim (\omega/m^2)\lambda_C \gg \lambda_C$.

Below, we distinguish between low-energy vacuum-polarization effects if $\omega \ll m$ and high-energy ones if $\omega \gtrsim m$.

A. Low-energy vacuum-polarization effects

The scattering in vacuum of a real photon by another real photon is possibly the most fundamental vacuum-polarization process (Berestetskii *et al.*, 1982) and it has not yet been observed experimentally. The total cross section of the process depends only on the Lorentz-invariant parameter $\eta = (k_1 k_2)/m^2$, with k_1^μ and k_2^μ being the four-momenta of the colliding photons, or, which is the same, on the energy ω^* of the two colliding photons in their center-of-momentum system ($\eta = 2\omega^{*2}/m^2$). This process has been investigated in Euler, 1936 in the low-energy limit $\eta \ll 1$ and then in Akhiezer, 1937 in the high-energy limit $\eta \gg 1$. The complete expression of the cross section $\sigma_{\gamma\gamma \rightarrow \gamma\gamma}$ was calculated in Karplus and Neuman, 1950 and it can also be found in Berestetskii *et al.*, 1982. In the low-energy limit $\eta \ll 1$ the cross section $\sigma_{\gamma\gamma \rightarrow \gamma\gamma}$ is given by

$$\sigma_{\gamma\gamma \rightarrow \gamma\gamma} = \frac{973}{81000\pi} \alpha^4 \lambda_C^2 \eta^3. \quad (16)$$

By expressing $\sigma_{\gamma\gamma \rightarrow \gamma\gamma}$ in terms of the center-of-momentum energy ω^* , it results $\sigma_{\gamma\gamma \rightarrow \gamma\gamma} [\text{cm}^2] = 7.4 \times 10^{-66} (\omega^* [\text{eV}])^6$. The steep dependence of $\sigma_{\gamma\gamma \rightarrow \gamma\gamma}$ on η at $\eta \ll 1$ is the main reason why so-far real photon-photon scattering has eluded experimental verification (see the reviews Marklund and Shukla, 2006 and Salamin *et al.*, 2006 for experiments and experimental proposals until 2005 aiming to observe real photon-photon scattering in vacuum). However, various proposals have been put forward recently in order to observe this process by colliding strong laser beams containing a large number of photons. A common theoretical starting point of all these proposals is the “effective-Lagrangian” approach (Dittrich and Gies, 2000; Dittrich and Reuter, 1985), in which the interaction among photons in vacuum is described via an effective Lagrangian density of the electromagnetic field. By starting from the total Lagrangian density of the classical electromagnetic field and of the quantum electron-positron Dirac field, one integrates out

the degrees of freedom of the latter field and is left with a resulting Lagrangian density depending only on the electromagnetic field. As we have seen above, the formation region of photon-photon interaction at low energies is of the order of λ_C , therefore if the classical electromagnetic field $F^{\mu\nu}(x)$, with electric (magnetic) component $\mathbf{E}(x)$ ($\mathbf{B}(x)$) comprises only wavelengths much larger than λ_C , the interaction is approximately pointlike and the effective Lagrangian density is accordingly a local quantity. Also, since the effective Lagrangian density is a Lorentz invariant, it can depend only on the electromagnetic field invariants $\mathcal{F}(x) = F^{\mu\nu}(x)F_{\mu\nu}(x)/4 = -[E^2(x) - B^2(x)]/2$ and $\mathcal{G}(x) = F^{\mu\nu}(x)\tilde{F}_{\mu\nu}(x)/4 = -\mathbf{E}(x) \cdot \mathbf{B}(x)$, where $\tilde{F}_{\mu\nu}(x) = \epsilon_{\mu\nu\alpha\beta}F^{\alpha\beta}(x)/2$ and $\epsilon^{\mu\nu\alpha\beta}$ is the four-dimensional completely anti-symmetric tensor with $\epsilon^{0123} = +1$. The complete expression of the effective Lagrangian density has been obtained for the first time in Heisenberg and Euler, 1936 and Weisskopf, 1936 (see also Schwinger, 1951) and it is known as Euler-Heisenberg Lagrangian density. Here we are interested only in the experimentally-relevant low-intensity limit $|\mathcal{F}(x)|, |\mathcal{G}(x)| \ll F_{cr}^2$ and the leading-order Euler-Heisenberg Lagrangian density $\mathcal{L}_{EH}(x)$ reads (Dittrich and Gies, 2000; Dittrich and Reuter, 1985)

$$\mathcal{L}_{EH}(x) = -\frac{1}{4\pi}\mathcal{F}(x) + \frac{\alpha}{360\pi^2} \frac{4\mathcal{F}^2(x) + 7\mathcal{G}^2(x)}{F_{cr}^2}. \quad (17)$$

Different experimental observables have been suggested to detect low-energy vacuum-polarization effects.

1. Experimental suggestions for direct detection of photon-photon scattering

The most direct way to search for photon-photon scattering events in vacuum by means of laser fields is to let two laser beams collide and to look for scattered photons. However, by employing a third “assisting” laser beam, if one of the final photons is kinematically allowed to be emitted along this beam with the same frequency and polarization, then the number of photon-photon scattering events can be coherently enhanced (Varfolomeev, 1966). In this laser-assisted setup the “signal” of photon-photon scattering is of course the remaining outgoing photon. In Lundin *et al.*, 2007 and Lundström *et al.*, 2006 an experiment has been suggested to observe laser-assisted photon-photon scattering with the Astra-Gemini laser system (see Par. II.A). The authors found a particular “three-dimensional” setup, which turns out to be particularly favorable for the observation of the process (see Fig. 11). The number N_γ of photons scattered in one shot for an optimal choice of the geometrical factors and of the polarization angles among the incoming and the assisting beams is found to be

$$N_\gamma \approx 0.25 \frac{P_1[\text{PW}]P_2[\text{PW}]P_3[\text{PW}]}{(\lambda_4[\mu\text{m}])^3}. \quad (18)$$

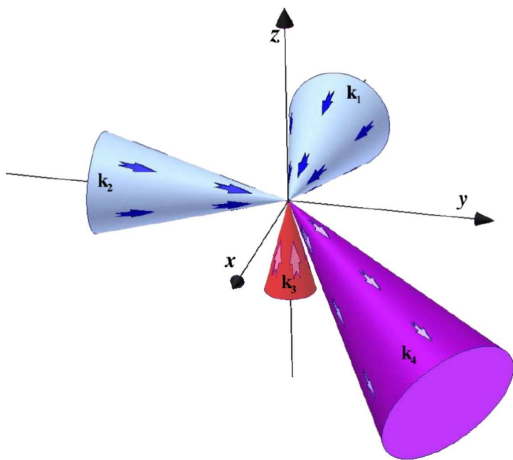


FIG. 11 (Color online) Schematic “three-dimensional” setup for laser-assisted photon-photon scattering involving two incoming beams (in blue), an assisting one (in red) and a scattered one (in violet). Reprinted with permission from Lundström *et al.*, 2006. Copyright (2006) by the American Physical Society.

Here, P_1 and P_2 are the powers of the incoming beams, P_3 is the power of the assisting beam and λ_4 is the wavelength of the scattered wave to be measured. By plugging in the feasible values for Astra-Gemini $P_1 = P_2 = 0.1$ PW and $P_3 = 0.5$ PW, one obtains $N_\gamma \approx 0.07$, i.e. roughly one photon scattered every 15 shots (for the parameters of Astra Gemini the wavelength of both the incoming beams is chosen as $0.4 \mu\text{m}$, that of the assisting beam as $0.8 \mu\text{m}$ so that the wavelength $\lambda_4 = 0.276 \mu\text{m}$ of the scattered photon is different from those of the incoming and assisting beams).

The quantum interaction among photons in vacuum has been exploited in King *et al.*, 2010a to put forward for the first time a double-slit setup comprising only of light (see also Marklund, 2010). In this setup two strong parallel beams collide head-on with a counterpropagating probe pulse. The photons of the probe have the choice to interact either with one or with the other strong beam, and, when scattered, they are predicted to build an interference pattern with alternating minima and maxima typical of double-slit experiments (see Fig. 12). Also, if one of the slits is closed, i.e. if the probe collides with only one strong beam, the interference fringes disappear. The key idea behind this setup is that the scattered beam, although propagating along the same direction of the probe, has a much wider angular distribution than the latter, offering the possibility of detecting vacuum-scattered photons outside the focus of the undiffracted probe beam. For a strong-field intensity of $I_0 \approx 5 \times 10^{24}$ W/cm² available at ELI or at HiPER and for a probe beam with wavelength $\lambda_p = 0.527 \mu\text{m}$ and intensity $I_p = 4 \times 10^{16}$ W/cm², it is predicted that about four photons per shot contribute to build up the inter-

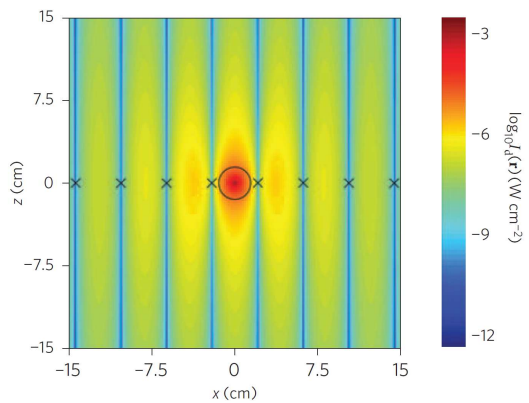


FIG. 12 (Color online) Intensity I_d of the vacuum-scattered wave for a probe beam propagating along the positive y direction and colliding with two strong beams aligned along the x axis. The crosses correspond to coordinates x_n according to the classical prediction $x_n = (n + 1/2)\lambda_p d/D$, where n is an integer number, λ_p is the wavelength of the probe field, d is the distance between the interaction region and the observation screen and D is the distance between the centers of the two strong beams. The numerical values of the parameters can be found in King *et al.*, 2010a. Adapted from King *et al.*, 2010a.

ference pattern in the observable region (it is the region outside the circle in Fig. 12, where $I_d > 100 I_p$). The diffraction of a probe beam in vacuum by a single focused strong laser pulse is also investigated in Tommasini and Michinel, 2010 in the case of almost counterpropagating beams. For optimal lasers parameters and at a strong-laser power of 100 PW the diffracted vacuum signal is predicted to be measurable in a single shot.

The concept of Bragg scattering has been exploited in Kryuchkyan and Hatsagortsyan, 2011 to observe the scattering of photons by a modulated electromagnetic-field structure in vacuum. If a probe wave passes through a series of parallel strong laser pulses and if the Bragg condition on the impinging angle is fulfilled, a large enhancement of the number of diffracted photons can be achieved. At a fixed intensity of each strong beam the enhancement factor with respect to laser-assisted photon-photon scattering is equal to the number of beams in the periodic structure. However, in experiments usually the total energy of the laser beams is fixed and an enhancement by a factor of two is predicted. By considering N_G equal Gaussian pulses propagating along the x direction, with widths $w_{y/z}$ along the y/z direction and aligned along the z direction with the centers at a distance $D > 2w_z$ from each other, the photon-photon scattering probability results proportional to the phase-matching factor \mathcal{P} , with

$$\mathcal{P} = \frac{\sin^2(\delta k_z N_G D/2)}{\sin^2(\delta k_z D/2)}, \quad (19)$$

where the vector $\delta \mathbf{k} = \mathbf{k}_2 - \mathbf{k}_1$ is the difference between

the wave vectors of reflected and incident waves. The Bragg condition is satisfied for $\delta k_z = 2\pi l/D$, with l being an integer. By employing ten optical laser beams with a wavelength of $1 \mu\text{m}$ and each with an intensity of $2.3 \times 10^{23} \text{ W/cm}^2$, about five vacuum-scattered photons are predicted per shot. Finally, an enhancement of vacuum-polarization effects in laser-laser collision has been predicted in Monden and Kodama, 2011 by employing strong laser beams with large angular aperture. For example, an enhancement of the number of vacuum-radiated photons by two orders of magnitude is predicted if the angular aperture of the colliding beams is increased from 53° to 103° .

2. Polarimetry-based experimental suggestions

The expression of the Euler-Heisenberg Lagrangian density in Eq. (17), suggests to interpret a region where only an electromagnetic field is present as a material medium characterized by a polarization $\mathbf{P}_{EH} = \partial \mathcal{L}_{EH} / \partial \mathbf{E} - \mathbf{E} / 4\pi$ and a magnetization $\mathbf{M}_{EH} = \partial \mathcal{L}_{EH} / \partial \mathbf{B} + \mathbf{B} / 4\pi$ (Jackson, 1975) given by

$$\mathbf{P}_{EH} = \frac{\alpha}{180\pi^2 F_{\text{cr}}^2} [2(E^2 - B^2)\mathbf{E} + 7(\mathbf{E} \cdot \mathbf{B})\mathbf{B}], \quad (20)$$

$$\mathbf{M}_{EH} = \frac{\alpha}{180\pi^2 F_{\text{cr}}^2} [2(B^2 - E^2)\mathbf{B} + 7(\mathbf{E} \cdot \mathbf{B})\mathbf{E}]. \quad (21)$$

In turn this implies that the presence of an electromagnetic field in the vacuum alters the vacuum's refractive index (Dittrich and Gies, 2000). The situation is even more complicated because in general the vectorial nature of the background electromagnetic field which ‘‘polarizes’’ the vacuum introduces a privileged direction in the vacuum. As a result, the vacuum's refractive index is altered in a way that it depends in general on the mutual polarizations of the probe electromagnetic field and of the background field: the polarized vacuum behaves as a birefringent medium. The birefringence of the polarized vacuum is exploited in Heinzl *et al.*, 2006 to show that if a linearly-polarized probe x-ray beam (wavelength λ_p) propagates along a strong optical standing wave, then after the interaction it results elliptically polarized with ellipticity ϵ given by

$$\epsilon = \frac{2\alpha}{15} \kappa \frac{l_{0,R}}{\lambda_p} \frac{I_0}{I_{\text{cr}}}, \quad (22)$$

where $\kappa \sim 1$ is a geometrical factor and $l_{0,R}$ is the Rayleigh length of the intense laser beam. If this beam is generated by a laser like ELI ($I_0 \sim 10^{25} \text{ W/cm}^2$), values of the ellipticities of the order of 10^{-7} are predicted at $\lambda_p = 0.1 \text{ nm}$. We mention here that recent advances on x-ray polarimetry allow for measurements of ellipticities of the order of 10^{-9} at a wavelength of 0.2 nm (Marx *et al.*, 2011). In Ferrando *et al.*, 2007 a phase-shift has been found theoretically to be induced by vacuum-polarization

effects when two laser beams cross in the vacuum, which is predicted to be measurable at laser intensities available at ELI or at HiPER.

When an electromagnetic wave with wavelength λ impinges into a material body, the features of the scattered radiation depend on the so-called diffraction parameter $\mathcal{D} = l_\perp^2 / \lambda d$ (Jackson, 1975). Here, l_\perp is the spatial dimension of the body perpendicular to the propagation direction of the impinging wave and d is the distance of the screen where the radiation is detected from the interaction region. If $\mathcal{D} \gg 1$ one is said to be in the refractive-index limit or in the near region, where the effects of the presence of the body can be described as if the wave propagates through a medium with a given refractive index. However, if $\mathcal{D} \lesssim 1$ then diffraction effects become important and the description of the interaction wave-body only in terms of a refractive index is in general not possible. This aspect has been pointed out in Di Piazza *et al.*, 2006 in the context of light-light interaction in vacuum. The tight focusing required to reach high intensities usually renders the interaction region so small that diffraction effects may become substantial at typical experimental conditions. In some cases diffractive effects reduce by an order of magnitude the values of the ellipticity calculated via the refractive-index approach and also induce a rotation of the main axis of the polarization ellipse with respect to the initial polarization direction of the probe field (Di Piazza *et al.*, 2006). The tight focusing of the strong polarizing beam required a quite detailed mathematical description employing a realistic focused Gaussian beam, while a simpler description was employed for the usually weakly-focused probe beam. This prevented the applicability of the results in the so-called far region where $\mathcal{D} \ll 1$ and where the spatial spreading of the probe field is also important. This assumption has been recently removed in King *et al.*, 2010b, where it was also pointed out that by considering the diffraction of a probe beam by two separated beams instead of that by a single standing wave, an increase in the ellipticity and in the rotation of polarization angle by a factor 1.5 is expected. A different method based on the phase-contrast Fourier imaging technique has been suggested in Homma *et al.*, 2011 to detect vacuum birefringence. This technique provides a very sensitive tool to measure the absolute phase shift of a probe beam when it crosses an intense laser field. Numerical simulations indicate the feasibility of measuring vacuum birefringence also by employing an optical probe field and a 100-PW strong laser beam.

Photon ‘‘acceleration’’ in vacuum due to vacuum polarization has been studied in Mendonça *et al.*, 2006. This effects corresponds to a shift of the photon frequency when it passes through a strong electromagnetic wave. If k_p^μ is the four-momentum of a probe photon with energy ω_p when it enters a region where a strong laser beam is present, then, due to vacuum-polarization effects, ω_p

becomes sensitive to the gradient of the intensity of the strong beam. As a result, a frequency up-shift (down-shift) is predicted at the rear (front) of the strong beam.

3. Low-energy vacuum-polarization effects in a plasma

As we have mentioned, under certain circumstances the effects of vacuum polarization amount to a modification of the vacuum refractive index from unity to $1 + \delta n_{\text{vac}}$. Although an accurate expression of the correction δn_{vac} depends on the precise form of the strong field and on the polarizations of probe and strong fields, it is roughly given by $(\alpha/45\pi)(I_0/I_{\text{cr}})$ (Dittrich and Gies, 2000). It was first realized in Di Piazza *et al.*, 2007a that this aspect can be in principle significantly improved in a plasma. For the sake of simplicity the case of a cold plasma was considered and the vacuum-polarization effects have been implemented in the inhomogeneous Maxwell equations as an additional “vacuum four-current” (Di Piazza *et al.*, 2007a). Now, unlike in the vacuum, the field invariant $\mathcal{F}(x)$ for a single monochromatic circularly polarized plane wave does not vanish in a plasma. Thus, vacuum-polarization effects in a plasma already arise in the presence of a single traveling plane wave. In Di Piazza *et al.*, 2007a the vacuum-corrected refractive index n of a two-fluid electron-ion plasma (ion mass and density given by m_i and n_i , respectively) in the presence of a circularly polarized plane wave has been found as

$$n = \sqrt{n_0^2 + \frac{2\alpha}{45\pi} \frac{I_0}{I_{\text{cr}}} (1 - n_0^2)^2}, \quad (23)$$

where

$$n_0 = \sqrt{1 - \frac{4\pi e^2 n_i}{m\omega_0^2} \left(\frac{1}{\sqrt{1 + \xi_0^2}} + \frac{Z}{\sqrt{\varrho_i^2 + Z^2 \xi_0^2}} \right)}, \quad (24)$$

with $\varrho_i = m_i/m$ is the refractive index of the plasma without vacuum-polarization effects (Mulser and Bauer, 2010). Equation (23) already indicates the possibility of enhancing the effects of vacuum polarization by working at laser frequencies ω_0 such that $n_0 \ll 1$, i.e. close to the effective plasma critical frequency. This region of parameters is in general complex to investigate, due to the arising of different instabilities. However, the idealized situation investigated in Di Piazza *et al.*, 2007a shows at least in principle the possibility of enhancing by an order of magnitude vacuum-polarization effects at a given intensity I_0 with respect, for example, to the results in Di Piazza *et al.*, 2006. The effects of the presence of an additional strong constant magnetic field have been analyzed in Lundin *et al.*, 2007. The general theory presented in this paper covers different waves propagating in a plasma as Alfvén modes, whistler modes, and large-amplitude laser modes. We also mention the recent paper

Bu and Ji, 2010, where the photon acceleration process has been investigated in a cold plasma.

B. High-energy vacuum-polarization effects

Generally speaking the treatment of vacuum-polarization effects for an incoming photon with energy ω in the presence of a background electromagnetic field with a typical angular frequency ω_b cannot be performed in an effective Lagrangian approach if $\omega\omega_b/m^2 \gtrsim 1$: the incoming photon “sees” the nonlocality of its interaction with the background electromagnetic field through its local “transformation” into an e^+e^- pair (see Fig. 10). The technical difficulty in treating vacuum-polarization effects at high energies arises from the fact that the interaction between the virtual e^+e^- pair and the background field has to be accounted for exactly. This has been accomplished for the background field of a nucleus with charge number Z such that $Z\alpha \sim 1$ and Delbrück scattering and photon splitting in such a field have also been observed experimentally (see the reviews Lee *et al.*, 2003 and Milstein and Schumacher, 1994). As we have recalled in Sec. IV, the Dirac equation in a background plane wave described by the four-vector potential $A^\mu(\phi)$ can be solved exactly and analytically. Accordingly, the exact electron (Volkov) propagator $G(x, y|A)$ in the same background field has also been determined (see, e.g., Ritus, 1985). The so-called “operator technique”, developed in Baier *et al.*, 1976a,b, turns out to be very convenient to investigate vacuum-polarization effects at high energies. In this technique a generic electron state $\Psi(x)$ in a plane-wave field and the propagator $G(x, y|A)$ are intended as the configuration representation of an abstract state $|\Psi\rangle$ and of an operator $G(A)$ such that $\Psi(x) = \langle x|\Psi\rangle$ and $G(x, y|A) = \langle x|G(A)|y\rangle$. In particular, since the propagator $G(x, y|A)$ is the solution of the equation $\{\gamma^\mu [i\partial_\mu - eA_\mu(\phi)] - m\}G(x, y|A) = \delta(x - y)$, then the abstract operator $G(A)$ is simply

$$G(A) = \frac{1}{\gamma^\mu [P_\mu - eA_\mu(\phi)] - m}, \quad (25)$$

with P^μ being the four-momentum operator. The evaluation via the operator technique of the matrix element corresponding to a generic vacuum-polarization process is then carried out by manipulating abstract operators, which results easier than by working with the corresponding quantities in the configuration space.

In Di Piazza *et al.*, 2007b the operator technique has been employed to calculate the rate of photon splitting in a strong laser field. This was the first investigation of a QED process involving three Volkov propagators. The calculated rate is valid for an arbitrary plane-wave field, provided that radiative corrections can be neglected, i.e. at $\alpha\mathcal{A}_0^{2/3} \ll 1$ in the most unfavorable regime $\xi_0, \mathcal{A}_0 \gg 1$

(Ritus, 1972). In fact, QED processes involving the collision of a photon and an intense plane wave are controlled by the two Lorentz- and gauge-invariant parameters ξ_0 and \varkappa_0 (note the analogy with QED processes involving an incoming electron and an intense plane wave discussed in Sec. IV and see also Sec. VII). In Di Piazza *et al.*, 2007b it turned out to be more convenient to perform a parametric study of the photon-splitting rate by varying the two parameters ξ_0 and $\eta_0 = \omega_0 k_- / m^2$ (note that $\varkappa_0 = \eta_0 \xi_0$). By employing the Furry theorem (Berestetskii *et al.*, 1982), it is shown that photon splitting in a laser field only occurs with absorption of an odd number of laser photons. In particular, if the strong field is circularly polarized and if it counterpropagates with respect to the incoming photon, the conservation of the total angular momentum along the propagation direction of the beams implies that at $\eta_0 \ll 1$ photon splitting can occur only via absorption of one or of three laser photons.

In Di Piazza *et al.*, 2008a a physical scenario has been put forward in which nonperturbative vacuum-polarization effects can be in principle observed (here “nonperturbative” means “high-order” in the quantum nonlinearity parameter, see below). In this scenario a high-energy proton collides head-on with a strong laser field. The quantum interaction of the Coulomb field of the proton with the laser field allows for a merging of laser photons into a single high-energy one. The use of a proton, instead for example of an electron, is required in order to suppress the background process of multiphoton Thomson/Compton scattering, where again many photons of the laser can be directly absorbed by the proton and converted into a single high-energy photon (see Sec. IV). In fact, the kinematics of the two processes, vacuum-mediated laser photon merging and multiphoton Thomson/Compton scattering is the same, except that in the treatment in Di Piazza *et al.*, 2008a only an even number of laser photons can merge in the vacuum-mediated process. The probability of n -photon Thomson/Compton scattering of a particle with charge Q and mass M depends on the parameter $\xi_{0,c} = |Q|E_0/M\omega_0$ and it scales as $\xi_{0,c}^{2n}$ at $\xi_{0,c} \ll 1$. Thus, the use of a “heavy” particle like a proton is essential to suppress this background process. Note that in order to have $\xi_{0,p} = |e|E_0/m_p\omega_0 \approx 1$ for a proton (mass m_p), a laser field with intensity of the order of 10^{24} W/cm² is required. It is found that for an optical background field such that $\xi_0 \gg 1$, the amplitude of the $(2n)$ -photon merging process depends only on the nonlinear quantum parameter

$$\chi_{0,p}^{(2n)} = \frac{E_0}{E_{\text{cr}}} \frac{2n(1+v_p)\omega_0}{m} \frac{1-\cos\vartheta}{1+v_p\cos\vartheta}, \quad (26)$$

where v_p is the proton velocity and ϑ is the angle between the direction of the emitted photon and the propagation direction of the plane wave. By colliding a proton beam with energies available at the Large Hadron Collider (LHC) of the order of 7 TeV (LHC, 2011) with

an optical laser beam of intensity of 3×10^{22} W/cm², it is demonstrated that the vacuum-mediated merging of two laser photons and the analogous two-photon Thomson/Compton scattering have comparable rates, implying that the inclusive signal should be twice the one expected without vacuum-polarization effects. By accounting for the details of the proton beams available at LHC and of the laser system PFS (see Par. II.A), about 670 two-photon merging events and about 5 four-photon merging events are expected per hour. In the discussed setup most of the photons are emitted almost in the direction of the proton’s velocity ($\vartheta \approx \pi$) and in that region $\chi_{0,p}^{(2)} \sim 1$. It is also indicated in Di Piazza *et al.*, 2008a that the use of the perturbative expression of the laser-photon merging rate at leading order in $\chi_{0,p}^{(2)} \ll 1$ would lead to an error of about 30%. Other setups for observing vacuum-polarization effects in laser-proton collisions have been discussed in Di Piazza *et al.*, 2008b, involving for example XFEL or single intense XUV pulses. Finally, the process of Delbrück scattering in a combined Coulomb and laser field has been studied in Di Piazza and Milstein, 2008. Here an incoming photon is scattered by the Coulomb field of a nucleus and by a strong laser field. While the presence of the laser field is taken into account exactly in the calculations, only leading-order effects in the nuclear parameter $Z\alpha$ are accounted for. Analogously to Di Piazza *et al.*, 2008a, it is found that high-order nonlinear corrections in the parameter \varkappa_0 on the cross section of the process already become important at $\varkappa_0 \approx 0.2$. For example, these corrections amount to about 50% at $\varkappa_0 = 0.35$.

VII. ELECTRON-POSITRON PAIR PRODUCTION

One of the most important predictions of QED has been the possibility of transforming light into matter (Dirac, 1928). If two photons with four-momenta k_1^μ and k_2^μ collide at an angle such that the parameter $\eta = (k_1 k_2) / m^2$ exceeds two, the creation of an e^+e^- pair becomes kinematically allowed (Breit-Wheeler e^+e^- pair production (Breit and Wheeler, 1934)). Shortly after the invention of the laser in 1960, theoreticians started to study possibilities for the creation of e^+e^- pairs from vacuum by very strong laser fields (Nikishov and Ritus, 1964b; Reiss, 1962; Yakovlev, 1965). Because of constraints from energy-momentum conservation, a single plane-wave laser field cannot create pairs from vacuum, no matter how intense it is. For a single plane wave, in fact, all the photons propagate along the same direction and the parameter η vanishes identically. An additional source of energy is therefore required to trigger the process. There are essentially three different possibilities:

- (i) pair production by a high-energy photon propagating in a strong laser field (intense-field Breit-

Wheeler pair production);

- (ii) pair production by a Coulomb field in the presence of a strong laser field;
- (iii) pair production by two counterpropagating strong laser beams forming a standing light wave.

These processes share the common feature to possess different interaction regimes which are mainly characterized by the value of the parameter ξ_0 . When $\xi_0 \ll 1$ the presence of the laser field can be taken into account perturbatively and this yields a pair production rate R of the form $R \sim m\xi_0^{2l}$, where l is the smallest integer number which kinematically allows the process: $l\omega_0 k_- > m^2$ for the process in (i), with k^μ being the four-momentum of the incoming photon, $l\omega_0 u_{c,-} > 2m$ for the process in (ii), with u_c^μ being the four-velocity of the charge producing the Coulomb field, and $l\omega_0 > 2m$ for the process in (iii). Due to the specific dependence of the pair production rate on ξ_0 , this regime of pair production is called multiphoton regime. In contrast, when $\xi_0 \gg 1$ the presence of the laser field has to be taken into account exactly in the calculations. As the condition $\xi_0 \gg 1$ is realized for vanishing laser frequencies at a fixed laser amplitude, this regime is called quasistatic regime and the pair-production rate here is determined by a different parameter which depends on the process at hand. For the process in (i), for example, the form of the rate depends on the physical parameter \varkappa_0 and it scales as $\sim m\varkappa_0^{3/2} \exp(-8/3\varkappa_0)$ if $\varkappa_0 \ll 1$ and as $\sim m\varkappa_0^{2/3}$ if $\varkappa_0 \gg 1$ (Nikishov and Ritus, 1964b; Reiss, 1962). For the process in (ii), we distinguish the case in which the incoming particle is an electron and that in which it is a heavier particle like a nucleus with charge number Z . In the first case the pair production rate depends on the parameter χ_0 already introduced in Sec. IV and the recoil due to the pair creation on the electron has to be taken into account (see also Par. VII.A). In the second case the motion of the nucleus is usually assumed not to be altered by the pair creation process and the nucleus itself is described as a background Coulomb field (see also Par. VII.B). The pair-production rate depends on the parameter $\chi_{0,n} = u_{n,-}(E_0/E_{\text{cr}})$, with u_n^μ being the four-velocity of the nucleus and on the nuclear parameter $Z\alpha$. Specifically, the pair-production rate scales as $m(Z\alpha)^2 \exp(-2\sqrt{3}/\chi_{0,n})$ if $\chi_{0,n} \ll 1$ and as $m(Z\alpha)^2 \chi_{0,n} \ln \chi_{0,n}$ if $\chi_{0,n} \gg 1$ (Milstein *et al.*, 2006; Yakovlev, 1965). Finally, for the process in (iii), the rate R has been derived mainly by approximating the standing wave as an oscillating electric field (see also Par. VII.C). It is found that R depends on the ratio $\Upsilon_0 = E_0/E_{\text{cr}}$, with E_0 being the amplitude of the standing wave in the (fixed) laboratory frame and that it scales as $m\Upsilon_0^2 \exp(-\pi/\Upsilon_0)$ if $\Upsilon_0 \ll 1$ and as $m\Upsilon_0^2$ if $\Upsilon_0 \gg 1$ (Brezin and Itzykson, 1970; Popov, 1971, 1972). As expected, these scalings coincide with the corresponding

ones in a constant electric field E_0 (Schwinger, 1951).

The physical meaning of the three parameters \varkappa_0 , $\chi_{0,n}$ and Υ_0 can be qualitatively understood in the following way. For the process in (i) the dressing of electrons and positrons in the plane wave (Ritus, 1985) modifies the threshold of e^+e^- pair production at $\xi_0 \gg 1$ according to $l\omega_0 k_- \gtrsim m^2 \xi_0^2$. Now, analogously to multiphoton Thomson and Compton scattering (see Sec. IV), the typical number l of laser photons absorbed in pair production via photon-laser collision is $l \sim \xi_0^3$ (Nikishov and Ritus, 1964b) and the threshold condition becomes $\varkappa_0 \gtrsim 1$. Concerning the process (ii), the appearance of the parameter $\chi_{0,n}$ in the quasistatic limit $\xi_0 \gg 1$ can be understood by noting that $E_0^* = u_{n,-}E_0$ is the amplitude of the laser field in the rest-frame of the nucleus and that a constant and uniform electric field with strength $E_0 \gtrsim E_{\text{cr}} = m^2/|e|$ supplies a e^+e^- pair with its rest energy $2m$ along the typical length scale of QED $\lambda_C = 1/m$. This last observation also clarifies the appearance of the parameter Υ_0 for the process in (iii). The typical exponential scaling of the pair production rate at $\xi_0 \gg 1$, and at $\varkappa_0 \ll 1$, $\chi_{0,n} \ll 1$ and $\Upsilon_0 \ll 1$ for the processes in (i), (ii) and (iii), respectively, is reminiscent of a quantum tunneling process. Thus, one refers to this regime also as tunneling pair production (note, however, that the notion of ‘‘tunneling’’ in relativistic laser-induced processes should not be taken too literal, see Par. III.A and Reiss, 2008).

In all processes discussed above, the laser field is always participating directly in the pair creation step and fundamental properties of the quantum vacuum under extreme high-field conditions are probed. However, as we will see in the following three paragraphs, lying at the border of experimental feasibility, the expected pair yields are generally rather small. It is worth mentioning here that lasers can also be applied for abundant generation of e^+e^- pairs (Chen *et al.*, 2009, 2010). When a solid target is irradiated by an intense laser pulse, a plasma is formed and electrons are accelerated to high energies. They may emit bremsstrahlung radiation which efficiently converts into e^+e^- pairs through the Bethe-Heitler process. The laser field plays an indirect role in the pair production here by serving solely as a particle accelerator. The prolific amounts of antimatter generated this way may allow for interesting applications in various fields of science (Müller and Keitel, 2009).

A. Pair production in photon-laser and electron-laser collisions

Among the mentioned pair-production processes, only laser-induced pair production at $\xi_0 < 1$ has been observed experimentally. Its feasibility has been shown, in fact, in the pioneering E-144 experiment at SLAC (Bamber *et al.*, 1999; Burke *et al.*, 1997) (see Reiss, 1971 for

a corresponding theoretical proposal). The experiment relied on collisions of the 46.6 GeV electron beam from SLAC's linear accelerator with a counterpropagating intense laser pulse with photon energy of $\omega_0 = 2.4$ eV and intensity of 1.3×10^{18} W/cm² ($\xi_0 \approx 0.4$). In the rest-frame of the electrons, the laser intensity and frequency are largely Doppler up-shifted to the required level and the pair generation probability is effectively enhanced. In principle both reactions (i) and (ii) contribute to pair production in this kind of collisions. Based on separate simulations of both production channels, reaction (i) was found to dominate. The high-energy photon originates from multiphoton Compton backscattering of a laser photon off the electron beam.

Despite the great significance of the SLAC experiment, only recently a unified description of pair creation in electron-laser collisions has been presented, which allows to treat the competing mechanisms (i) and (ii) within the same formalism (Hu *et al.*, 2010). Good agreement with the experimental results has been obtained. Moreover, it was shown that the SLAC study observed the onset of nonperturbative pair creation dynamics, which adds even further significance to this benchmarking experiment (see also Reiss, 2009). A formal consideration of the process has also been given in Ilderton, 2011, where special emphasis is put on effects stemming from the finite duration of the laser pulse.

Figure 13 shows a survey of various combinations of incoming electron energies and optical laser intensities which give rise to an observable pair yield. It covers the range from the perturbative few-photon regime ($\xi_0 \approx 0.1$ at $I_0 \approx 5 \times 10^{16}$ W/cm²) to the highly nonperturbative regime ($\xi_0 \approx 10$ at $I_0 \approx 5 \times 10^{20}$ W/cm²), where the contributions from thousands of photon absorption channels need to be included. We note that few-GeV electron beams can be produced today by compact laser-plasma accelerators (Leemans *et al.*, 2006) (see also Sec. XI). Future pair creation studies may therefore rely on all-optical setups, where a laser-generated electron beam collides with a counterpropagating laser pulse. Another all-optical setup for pair creation by a seed electron exposed to two counterpropagating laser pulses was put forward in Bell and Kirk, 2008, which will be discussed in Sec. VIII.

Pair creation studies could also be conducted as a non-standard application of the 17.5 GeV electron beam at the upcoming European XFEL beamline at DESY (European XFEL, 2011), which will normally serve to generate coherent x-ray pulses. However, in combination with a table-top 10-TW optical laser system, it would also be very suitable to probe the various regimes of pair production. In particular, the production channel (ii) could be revealed by a suitable choice of beam parameters (Hu *et al.*, 2010).

Also further aspects of pair creation by a high-energy photon and a strong laser field have been investigated

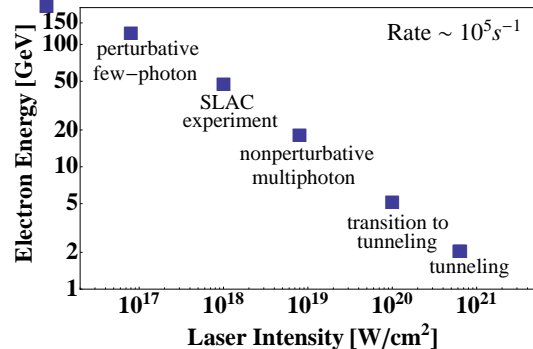


FIG. 13 (Color online) Transition from the perturbative to the fully nonperturbative regimes of e^+e^- pair creation in electron-laser collisions. The laser photon energy is 2.4 eV. Adapted and reprinted with permission from Hu *et al.*, 2010. Copyright (2010) by the American Physical Society.

in recent years. In Heinzl *et al.*, 2010a, reaction (i) was considered in the case where the laser pulse has a finite duration. It was found that the finite pulse duration is imprinted on the spectra of created particles. Pair production by a high-energy photon and an ultrashort laser pulse was also considered in Tuchin, 2010. Quantum interference effects can arise in photon-induced pair creation in a two-mode laser field of commensurate frequencies (Narozhny and Fofanov, 2000).

In addition, the fundamental process (i) may allow for applications as a novel tool in ultrashort pulse spectrometry. A corresponding detection scheme for the characterization of short gamma-ray pulses of GeV photons down to the zeptosecond (zs) scale, called Streaking at High Energies with Electrons and Positrons (SHEEP), has been proposed in Ipp *et al.*, 2011. The basic concept of SHEEP is based on e^+e^- pair production in vacuum by a photon of the test pulse, assisted by an auxiliary counter-propagating intense laser pulse. In contrast to conventional streak imaging, two particles with opposite charges, electron and positron, are created in the same relative phase within the third streaking pulse that co-propagates with the test pulse. By measuring simultaneously the energy and the momentum of the electrons and the positrons originating from different positions within the test pulse, its length and, in principle, even its shape can be reconstructed. The time resolution of SHEEP for different classes of test, streaking and strong pulses can range from fs to zs duration.

B. Pair production in nucleus-laser collisions

While in electron-laser collisions the contribution of reaction (ii) to the pair production is in general small, it becomes accessible to experimental observation when the projectile electrons are replaced by heavier particles such as protons or other nuclei. The two-step production

process via multiphoton Compton scattering is strongly suppressed by the large projectile mass then. The recent commissioning of the LHC at CERN has stimulated substantial activities on pair production in combined laser and nuclear Coulomb fields, which may be viewed as a generalization of the well-known Bethe-Heitler process to strong fields (high-intensity Bethe-Heitler pair production). The large Lorentz factors γ_n of the ultrarelativistic nuclear beams lead to an efficient enhancement of the laser parameters in the projectile rest-frame.

Indeed, when a proton beam with Lorentz factor $\gamma_p \approx 3000$, as presently available at LHC, collides head-on with a superintense laser beam of intensity $I_0 \approx 10^{22}$ W/cm², the Lorentz boosted laser field strength approaches the critical value E_{cr} . This circumstance motivated the first calculations of nonperturbative pair production in collisions of a relativistic nucleus with a superintense near-optical laser beam (Müller *et al.*, 2003a,b). Smaller projectile Lorentz factors may be sufficient, when ultrastrong XFEL pulses are employed (Avetissian *et al.*, 2003). The calculations were based on an S-matrix treatment and assumed laser fields of circular polarization. Later on, also the case of linear field polarization was studied (Kamiński *et al.*, 2006; Krajewska *et al.*, 2006; Müller *et al.*, 2004; Sieczka *et al.*, 2006) which is rendered more involved due to the appearance of generalized Bessel functions, which are of very high order when $\xi_0 \gg 1$. The underlying S-matrix element is generally of the form

$$S_{p_+p_-} = -ie \int dt \langle \Psi_{p_+}^{(+)} | V_n | \Psi_{p_-}^{(-)} \rangle. \quad (27)$$

It describes the transition of a laser-dressed (Volkov) electron from the negative-energy state $|\Psi_{p_-}^{(-)}\rangle$ to a positive-energy Volkov state $|\Psi_{p_+}^{(+)}\rangle$, which is mediated by the Coulomb potential $V_n = Z|e|/r$ of the projectile nucleus. An alternative approach to the problem based on the polarization operator in a plane electromagnetic wave has been developed in Milstein *et al.*, 2006. It allows to obtain total production rates analytically. Both approaches rely on the strong-field approximation and include the laser field exactly to all orders, whereas the nuclear field is treated at leading order in $Z\alpha$.

Since the high-intensity Bethe-Heitler process has not been observed in experiment yet, in recent years physicists have proposed scenarios which may allow to realize the various interaction regimes of the process by present-day technology. Few-photon Bethe-Heitler pair production in the perturbative domain could be realized in collisions of the LHC proton beam with an XUV pulse of angular frequency $\omega_X \approx 100$ eV and of moderate intensity $I_X \sim 10^{14}$ W/cm² (Müller, 2009). Corresponding radiation sources of table-top dimension are available nowadays in many laboratories. They are based on HHG from atomic gas jets or solid surfaces (see Par. III.B). The rate R of pair creation by two-photon absorption close to the

energetic threshold (i.e. $\omega_X^* = u_{n,-}\omega_X \gtrsim m$, for the angular frequency ω_X^* of the XUV pulse in the rest-frame of the nucleus) is given by (Milstein *et al.*, 2006)

$$R = \frac{1}{4^{3-j}} (Z\alpha)^2 \xi_0^4 \omega_X^* \left(\frac{\omega_X^*}{m} - 1 \right)^{j+2}, \quad (28)$$

with $j = 0$ for linear polarization and $j = 2$ for circular polarization.

In the quasistatic regime of the process sizable pair yields require superintense laser fields from a petawatt source in conjunction with an LHC proton beam (Müller *et al.*, 2003b; Sieczka *et al.*, 2006). Such experiments will become feasible when petawatt laser pulses are producible by high-power devices of table-top size, rather than by immobile large-scale facilities as they exist at present. A method to enable tunneling pair production with more compact multiterawatt laser systems has been proposed in Di Piazza *et al.*, 2009b, 2010b. It relies on the application of an additional weak XUV field, which is superimposed on a powerful optical laser wave. In this two-color setup, the energy threshold for pair creation can be overcome by the absorption of one photon from the high-frequency field and several additional photons from the low-frequency field. As a result, by choosing the XUV frequency ω_X^* such that the parameter $\delta = (2m - \omega_X^*)/m$ fulfills the conditions $0 < \delta \ll 1$, the tunneling barrier can be substantially reduced and even controlled. The pair production rate in the quasistatic regime at $0 < \delta \ll 1$ depends essentially only on the parameters δ and $\chi_{0,n}$, and on the classical multiphoton parameter ξ_X of the XUV field. For a circularly polarized strong laser field it results (Di Piazza *et al.*, 2009b)

$$R = \frac{1}{64\sqrt{\pi}} m (Z\alpha)^2 \xi_X^2 \chi_{0,n}^2 \sqrt{\zeta_0} \exp\left(-\frac{2}{3} \frac{1}{\zeta_0}\right) \quad (29)$$

at $\zeta_0 = \chi_{0,n}/2\delta^{3/2} \ll 1$, to be compared with the usual scaling $\sim (-2\sqrt{3}/\chi_{0,n})$ in the absence of the XUV field.

A related process is laser-assisted Bethe-Heitler pair creation, where the high-frequency photon energy satisfies $\omega_X^* > 2m$. A pronounced channeling of the e^+e^- due to the forces exerted by the laser field after their creation was found (Lötstedt *et al.*, 2008, 2009). High-intensity Bethe-Heitler pair creation in a two-color laser wave was investigated in Roshchupkin, 2001.

Analytical formulas for positron energy spectra and angular distributions in the tunneling regime of the process were obtained in Kuchiev and Robinson, 2007. For pair production at $\xi_0 \sim 1$ no analytical expressions are known because of the intermediate nature of this parameter regime. However, by performing a fitting procedure to numerically obtained results, a total pair production rate scaling as $m(Z\alpha)^2 \exp(-3.49/\chi_{0,n})$ was obtained in Müller *et al.*, 2009b, which closely resembles the tunneling exponential behaviour $m(Z\alpha)^2 \exp(-2\sqrt{3}/\chi_{0,n})$.

While in Eq. (27) the influence of the projectile is described by an external Coulomb field, the projectile can also be treated as a quantum particle which allows to study nuclear recoil effects (Krajewska and Kamiński, 2010, 2011; Müller and Müller, 2009). Besides, in laser-nucleus collisions also bound-free pair creation can occur where the electron is created in a deeply bound atomic state of the nucleus. The process was studied first for circular laser polarization (Matveev *et al.*, 2005; Müller *et al.*, 2003c) and later on also for linear polarization (Deneke and Müller, 2008), including contributions from the various atomic subshells.

C. Pair production in a standing laser wave

Purely light-induced pair production can occur when two noncopropagating laser waves are superimposed. The simplest field configuration consists of two counterpropagating laser pulses of equal frequency and intensity. The resulting field is a standing wave which is inhomogeneous both in space and time, rendering a theoretical treatment of the process very challenging. In order to render the problem tractable, in the standard approach the resulting standing light wave is approximated by a purely electric field oscillating in time. This approximation is expected to be justified for a strong ($I_0 > 10^{20}$ W/cm²), optical laser field where the typical spatial scale of the field variation $\lambda_0 \sim 1$ μ m is much larger than the pair formation length $m/|e|E_0 = \lambda_C E_{cr}/E_0 \approx 0.02$ μ m/ $\sqrt{I_0 [10^{20}$ W/cm²]} (Ritus, 1985). Pair production in an oscillating electric field is a generalization of the Schwinger mechanism (Schwinger, 1951) to time-dependent fields and it has been considered by many theoreticians, starting from the seminal works Brezin and Itzykson, 1970 and Popov, 1971, 1972 (for a comprehensive list of references until 2005, see Salamin *et al.*, 2006).

While in the laser-electron and laser-nucleus collisions of the previous sections the Doppler boost of the laser parameters due to a highly relativistic Lorentz factor could be exploited, in laser-laser collisions this is not possible so that high field strengths E_0 or high frequencies ω_0 are required to exist in the laboratory frame. Theoreticians are therefore aiming to find ways for enhancement of the pair production probability in order to render the process observable in the foreseeable future.

A first possibility to facilitate the observability of pair creation in a standing optical laser wave is to superimpose an x-ray photon (or any other high-frequency component) onto the high-field region (Dunne *et al.*, 2009; Monin and Voloshin, 2010; Schützhold *et al.*, 2008). In this way, the Schwinger mechanism is catalyzed so that the usual exponential suppression $\sim \exp(-\pi/\Upsilon_0)$ is significantly lowered. For example, in the limit when the x-ray energy approaches the threshold value $2m$, the pair

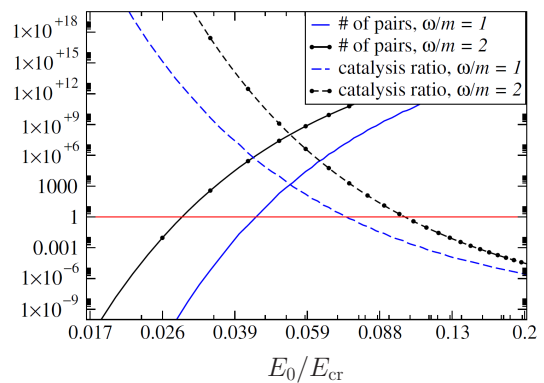


FIG. 14 (Color online) Number of pairs produced by via x-ray assisted Schwinger mechanism for two different values of the x-ray angular frequency ω_X , indicated as ω in the figure, (blue and black solid lines) and the ratio of these catalyzed pairs to those produced by the standard Schwinger mechanism (blue and black dashed lines), both as functions of the optical field strength in units of E_{cr} . Adapted and reprinted with permission from Dunne *et al.*, 2009. Copyright (2009) by the American Physical Society.

production rate R becomes

$$R \sim m \exp\left(-\frac{\pi - 2}{\Upsilon_0}\right) \quad (30)$$

assuming that the x-ray propagation direction is perpendicular to the electric field vector of the strong optical field. An overview of the pair production enhancement effect due to the x-ray assistance is shown in Fig. 14.

Another proposal to enhance the pair yield is the application of multiple colliding laser pulses instead of only two (Bulanov *et al.*, 2010a). It has been demonstrated that the threshold laser energy necessary to produce a single pair, decreases when the number of colliding pulses is increased. The results are summarized in Table I. Pair production exceeds the threshold when eight laser pulses, with a total energy of 10 kJ, are simultaneously focused on one spot. Doubling (tripling) the number of pulses leads to an enhancement by three (six) orders of magnitude. The threshold energy drops from 40 kJ for two pulses to 5.1 kJ for 24 pulses, clearly indicating that the multiple-pulse geometry is strongly favorable. Besides, it was noticed that the pre-exponential volume factor in the pair creation probability can be very large and partially compensate for the exponential suppression (Narozhny *et al.*, 2006).

Fine details of pair production in a time-dependent oscillating electric field are being studied nowadays because they might serve as characteristic signatures to discriminate the process of interest from potentially stronger background processes. For example, it was found that the momentum spectrum of the created particles is highly sensitive to a subcycle structure of the field (Hebenstreit *et al.*, 2009). This observation found an elegant mathematical explanation via the Stokes phenomenon

TABLE I Number N_{\pm} of e^+e^- pairs produced by different numbers n of laser pulses, with a total energy W of 10 kJ. The threshold value total energy W_{th} needed to produce one e^+e^- pair is shown in the third column. The precise collision geometry and pulse parameters can be found in Bulanov *et al.*, 2010a. Adapted and reprinted with permission from Bulanov *et al.*, 2010a. Copyright (2010) by the American Physical Society.

n	N_{\pm} at $W = 10$ kJ	W_{th} [kJ]
2	$< 10^{-18}$	40
4	$< 10^{-8}$	20
8	4.0	10
16	1.8×10^3	8
24	4.2×10^6	5.1

(Dumlu and Dunne, 2010). Further effects stemming from the precise shape of the external field were analyzed in Dumlu, 2010 and Dumlu and Dunne, 2011. Also, the oscillating dynamics of the e^+e^- plasma created by a uniform electric field, including backreaction effects, was investigated (Apostol, 2011; Benedetti *et al.*, 2011; Han *et al.*, 2010).

Apart from pair creation in superstrong laser pulses of low frequency, the process is also extensively discussed in connection with the upcoming XFEL facilities (see, e.g., Alkofer *et al.*, 2001 and Ringwald, 2001). Here the question arises to what extent the spatial field dependence may influence the creation process, both in terms of total probabilities and particle momentum distributions. We first mention that pair production in a time-dependent oscillating electric field occurs with conservation of the total momentum, in accordance with Noether's theorem, as well as of the total spin. The problem therefore reduces effectively to a two-level system since the field couples negative and positive-energy electron states of same momentum and spin only. The production process exhibits a resonant nature when the energy gap is an integer multiple of the laser frequency, leading to a characteristic Rabi flopping between the negative and positive-energy Dirac continua (Popov, 1971). Due to the electron dressing in the oscillating field, the resonant laser frequencies are determined by the equation $l\omega_0 = 2\langle\varepsilon\rangle$, where $\langle\varepsilon\rangle$ is the time-averaged electron energy in the time-dependent oscillating electric field. Accordingly, when the particle momentum is varied, several resonances occur corresponding to different photon numbers l . This gives rise to a characteristic ring structure in the momentum distribution (Mocken *et al.*, 2010).

Modifications of these well-established properties of the pair creation process, when the spatial field dependence and, thus, the laser magnetic-field component are accounted for, have been revealed in Ruf *et al.*, 2009. Utilizing an advanced computer code for solving the corresponding Dirac equation numerically, it was shown that

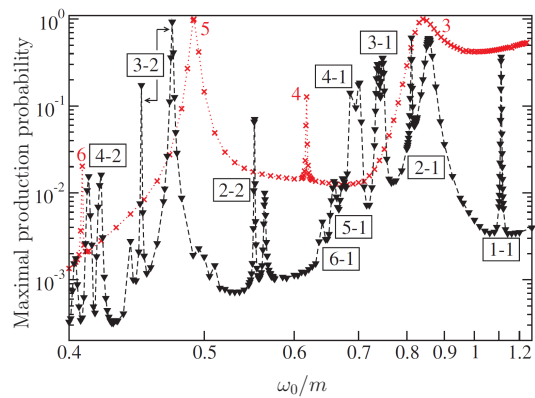


FIG. 15 (Color online) Probability spectrum of e^+e^- pair production in two counterpropagating laser pulses, with the laser magnetic field included (black triangles) and neglected (red crosses). In the first case, the labeling (l_r, l_l) signifies the number of absorbed photons from the right-left propagating wave; in the second case, the peak labels denote the total photon number l . A vanishing initial momentum (i.e. positron momentum) and $\xi_0 = 1$ have been assumed. Adapted and reprinted with permission from Ruf *et al.*, 2009. Copyright (2009) by the American Physical Society.

the positions of the resonances are shifted, several new resonances occur, and the resonance lines are split due to the influence of the spatial field dependence (see Fig. 15). The basic reason for these effects is that, in contrast to a uniform oscillating electric field, the photons in the counterpropagating laser pulses carry momentum along the beam axis. Therefore not only the total number l of absorbed laser photons matters, but also how many of them have originated from the laser pulse travelling to the right and left, respectively. For example, for the multiphoton order $l = 5$ two different resonance frequencies exist now, corresponding to $l_r = 3, l_l = 2$ on the one hand, and to $l_r = 4, l_l = 1$ on the other hand. Due to the photon momentum, the former two-level scheme is broken besides into a V -type three-level scheme. This causes a splitting of the resonance lines, in analogy with the Autler-Townes effect as known from atomic physics.

For another numerical approach to space-time dependent problem in quantum field theory, we refer to the review Cheng *et al.*, 2010. Moreover, Schwinger pair production in a space-time dependent electric field pulse has been treated very recently within the Wigner formalism (Hebenstreit *et al.*, 2011). A self-bunching effect of the created particles in phase space was found which is due to the spatiotemporal structure of the pulse.

D. Spin effects and other fundamental aspects of laser-induced pair creation

A particularly interesting aspect of tunneling pair creation is the electron and positron spin-polarization. In general, pronounced spin signatures in a field-induced

process may be expected when the background field strength approaches the critical value E_{cr} (Kirsebom *et al.*, 2001; Walser *et al.*, 2002). This indeed coincides with the condition for a sizable yield of tunneling pair production. With respect to pair production by a high-energy photon and a strong laser field, corresponding studies of spin effects were performed in Tsai, 1993 and Ivanov *et al.*, 2005, based on considerations of helicity amplitudes and the spin-polarization vector, respectively. Characteristic differences between fermionic and bosonic particles have been revealed with respect to pair creation in an oscillating electric field (Popov, 1972) and in recent studies of the Klein paradox (Cheng *et al.*, 2009b; Krekora *et al.*, 2004; Wagner *et al.*, 2010a). In the latter case it was shown that the existence of a fermionic (bosonic) particle in the initial state leads to suppression (enhancement) of the pair production probability due to the different quantum statistics. The enhancement in the bosonic case may be even exponential due to an avalanche process (Wagner *et al.*, 2010b). Concerning tunneling pair creation in combined laser and nuclear Coulomb fields, it has been shown that the internal spin-polarization vector is proportional in magnitude to $\chi_{0,n}$ and, to leading order, directed along the transverse momentum component of the electron (Di Piazza *et al.*, 2010c). A helicity analysis of pair production in laser-proton collision revealed that: 1) right-handed leptons are emitted in the laboratory frame under slightly smaller angles with respect to the proton beam than left-handed leptons; 2) the rate of spin-1/2 particles pair creation exceeds by almost one order of magnitude the corresponding quantity for spin-0 particles (Müller and Müller, 2011).

Other fundamental aspects of laser-induced pair creation have been recently investigated as well. They comprise various kinds of e^+e^- correlations (Fedorov *et al.*, 2006; Krajewska and Kamiński, 2008; Krekora *et al.*, 2005), multiple pair creation (Cheng *et al.*, 2009a), questions of locality (Cheng *et al.*, 2008) and vacuum decay times (Labun and Rafelski, 2009), and consistency restrictions on the maximum laser field strength to guarantee the validity of the external-field approximation (Gavrilov and Gitman, 2008).

VIII. QED CASCADES

As it was discussed in the previous section, the E-144 experiment at SLAC is the only experiment so far, where laser-driven multiphoton e^+e^- pair production has been observed. Considering that about 100 positrons have been detected in 22000 shots, each comprising the collision of about 10^7 electrons with the laser beam, the process results to be rather inefficient. One could ascribe this to the relatively low intensity I_0 of the laser system of about 10^{18} W/cm² ($\xi_0 \approx 0.4$ as the laser photon

energy was $\omega_0 = 2.4$ eV). However, the extremely high energy ε_0 of the electron beam of about 46.6 GeV ensured that the nonlinear quantum parameter χ_0 was about unity ($\chi_0 \approx 0.3$). A recent investigation (Sokolov *et al.*, 2010a) has pointed out in general that in the mentioned setup, i.e. an electron beam colliding with a strong laser pulse, RR effects prevent the development of a cascade or avalanche process with an efficient, prolific production of e^+e^- pairs even at much larger laser intensities such that $\xi_0 \gg 1$. With avalanche or cascade process we mean here a process where the incoming electrons emit high-energy photons in the laser field, which can interact with the field itself generating e^+e^- pairs, which in turn emit again photons and so on (of course a cascade process may also be initiated by a photon beam instead of an electron beam). The above result has been obtained by numerically integrating the kinetic equations, which describe the evolution of the electron, the positron and the photon distributions in a plane-wave background field from a given initial electron distribution, by accounting for the two basic processes that couple these distributions, i.e. multiphoton Compton scattering and multiphoton Breit-Wheeler pair production. The physical reason why an avalanche process cannot develop in a single plane-wave field can be understood in the following way. In the ultrarelativistic case $\xi_0 \gg 1$, the mentioned basic processes in a plane-wave field are essentially controlled by the parameters χ_0 and \varkappa_0 , respectively (see also Sects. IV and VII). Now, at the j^{th} step in which an electron/positron emits a photon or a photon transforms into an e^+e^- pair, the initial quantity $p_{0,-}^{(j)}$ or $k_{0,-}^{(j)}$ is conserved and it is distributed to the two final particles (an electron/positron and a photon in multiphoton Compton scattering and an e^+e^- pair in multiphoton Breit-Wheeler pair production). Thus, both resulting particles at each step will have a value of their own parameter $\chi_0^{(j)} = (p_{0,-}^{(j)}/m)(E_0/E_{\text{cr}})$ or $\varkappa_0^{(j)} = (k_{0,-}^{(j)}/m)(E_0/E_{\text{cr}})$ smaller than that of the incoming particle. Moreover, due to the special symmetry of the plane-wave field, the quantities $p_{0,-}^{(j)}$ or $k_{0,-}^{(j)}$ are also rigorously conserved between two steps. Then, the avalanche ends when the parameters $\chi_{0,i}^{(k)}$ and $\varkappa_{0,i}^{(k)}$ at a certain step k are smaller than unity for $i \in [1, \dots, N_k]$, with N_k being the number of particles at that step.

The question arises if other field configurations exist, where an avalanche process can be efficiently primed. A positive answer to this question has first been given in Bell and Kirk, 2008: even the presence of a single electron initially at rest in a standing wave generated by two equal counterpropagating circularly polarized laser fields can prime an avalanche process already at field intensities of the order of 10^{24} W/cm². We note that in the presence of a single plane wave the same process would require an intensity of the order of I_{cr} , because for an electron initially at rest it is $\chi_0 = E_0/E_{\text{cr}}$. From this

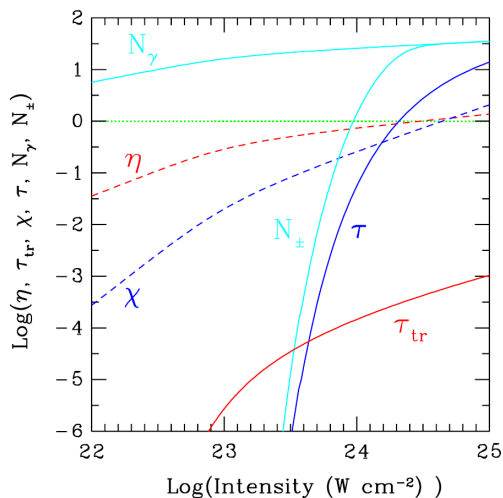


FIG. 16 (Color online) The number of e^+e^- pairs (N_{\pm}) and the number of photons (N_{γ}) created by an initial single electron in a rotating electric field as a function of the field intensity. The other plotted quantities are described in Bell and Kirk, 2008. Reprinted with permission from Bell and Kirk, 2008. Copyright (2008) by the American Physical Society.

point of view, the authors of Bell and Kirk, 2008 explain qualitatively the advantage of employing two counter-propagating laser beams by means of an analogy taken from accelerator physics: a collision between two particles in their center-of-momenta is much more efficient than if one of the particles is initially at rest, because much more of the initial energy can be transferred, for example, to create new particles. Since the production process in the standing wave mainly occurs where the electric field is larger than the magnetic one, in order to simplify the analysis, the authors considered regions close to the nodes of the magnetic field and approximated the standing wave by a rotating electric field. In such a field and for an ultrarelativistic electron the controlling parameter is $\tilde{\chi}_0 = (p_{\perp}/m)(E_0/E_{\text{cr}})$, where p_{\perp} is the component of the electron momentum perpendicular to the electric field. By estimating $p_{\perp} \sim m\xi_0$, one obtains $\tilde{\chi}_0 \approx 2I_0[10^{24} \text{ W/cm}^2]/\omega_0[\text{eV}]$ (here ω_0 , E_0 and I_0 are the standing-wave's angular frequency, electric field amplitude and intensity). The investigation in Bell and Kirk, 2008 is based on the analysis of the trajectory of the electron in the rotating electric field including RR effects via the LL equation. Since the momentum of the electron oscillates around a value of the order of $m\xi_0$, the electron emits efficiently high-energy photons that can in turn prime the cascade (see Fig. 16). The model employed in Bell and Kirk, 2008 was improved in Kirk *et al.*, 2009 by considering colliding pulsed fields with finite time duration and a realistic form of the synchrotron spectrum emitted by a relativistic electron. The results in Bell and Kirk, 2008 were essentially confirmed and nu-

merical simulations with linearly polarized beams have shown a general insensitivity of the cascade development to the polarization of the beams itself. Another interesting finding in Kirk *et al.*, 2009 is that the electrons in the standing wave tend to migrate to regions where the electric field vanishes and then they do not contribute to the pair-production process anymore. In both papers Bell and Kirk, 2008 and Kirk *et al.*, 2009 the emission of radiation by the electron was treated classically, i.e. the electron was supposed to loose continuously energy and momentum (although in Kirk *et al.*, 2009 the damping force-term in the LL equation was evaluated by employing the total emitted power calculated quantum mechanically). The stochastic nature of the emission of a photon has been taken into account in Ducloux *et al.*, 2011. Analogously, the energy of the emitted photon is chosen randomly following the synchrotron spectrum distribution and the momentum of the photon is always chosen to be parallel to that of the emitting electron. Instead, concerning the pair production process by a photon, since the photon is not deflected by the laser field it is assumed that after it has propagated one wavelength in the field, then it decays into an e^+e^- pair. The main result in Ducloux *et al.*, 2011 is that at relatively low intensities of the order of 10^{23} W/cm^2 the pair production rate is increased if the quantum nature of the photon emission is taken into account. The reason is that, due to the stochastic nature of the emission process, the electron can propagate for an unusually large distance before emitting. In this way it may gain an unusually large energy and emit consequently a high-energy photon, that can be more easily converted into an e^+e^- pair. Moreover, the discontinuous nature of the (curvature of the) electron trajectory is shown to slow down the tendency of the electrons to migrate to regions where the electric field vanishes.

The intensity threshold of the avalanche process in a rotating electric field has also been investigated in Fedotov *et al.*, 2010. By indicating as t_{acc} the time an electron needs to reach an energy corresponding to $\chi_0 = 1$ starting from rest in the given field, as t_e (t_{γ}) the electron (photon) lifetime under photon emission (e^+e^- pair production) and as t_{esc} the time after which the electron escapes from the laser field, the authors give the following condition for occurrence of the avalanche process $t_{\text{acc}} \lesssim t_e, t_{\gamma} \ll t_{\text{esc}}$. Estimates based on the classical electron trajectory without including RR effects, lead to the simple condition $E_0 \gtrsim \alpha E_{\text{cr}}$ for the avalanche to be primed in an optical field. The above estimate corresponds to an intensity of about $2.5 \times 10^{25} \text{ W/cm}^2$, i.e. one order of magnitude larger than what was found in Bell and Kirk, 2008. However, the main result of Fedotov *et al.*, 2010 was on the limitation brought about to the maximal laser intensity that can be produced in the discussed field configuration by the starting of the avalanche process. In fact, the energy to accelerate the electrons

and the positrons participating in the cascade has to come from the background electromagnetic field. By assuming an exponential increase of the number of electrons and positrons, it is found that already at laser intensities of the order of 10^{26} W/cm² the created electrons and positrons have an energy which exceeds the initial total energy of the laser beams. This hints to the fact that at such intensities the colliding laser beams are completely depleted due to the avalanche process. The results obtained from qualitative estimates in Fedotov *et al.*, 2010 have been scrutinized in Elkina *et al.*, 2011 by means of more realistic numerical methods based on kinetic or cascade equations. In general, if $f_{\mp}(\mathbf{r}, \mathbf{p}, t)$ ($f_{\gamma}(\mathbf{r}, \mathbf{k}, t)$) is the electron/positron (photon) distribution function in the phase-space (\mathbf{r}, \mathbf{p}) ((\mathbf{r}, \mathbf{k})) and $\varepsilon = \sqrt{m^2 + \mathbf{p}^2}$ ($\omega = |\mathbf{k}|$), their evolution in the presence of a given classical electromagnetic field $(\mathbf{E}(\mathbf{r}, t), \mathbf{B}(\mathbf{r}, t))$ is described by the kinetic equations

$$\begin{aligned} & \left[\frac{\partial}{\partial t} + \frac{\mathbf{p}}{\varepsilon} \cdot \frac{\partial}{\partial \mathbf{r}} \pm \mathbf{F}_L(\mathbf{r}, \mathbf{p}, t) \cdot \frac{\partial}{\partial \mathbf{p}} \right] f_{\mp}(\mathbf{r}, \mathbf{p}, t) \\ &= \int d\mathbf{k} w_{\text{rad}}(\mathbf{r}, \mathbf{p} + \mathbf{k} \rightarrow \mathbf{k}, t) f_{\mp}(\mathbf{r}, \mathbf{p} + \mathbf{k}, t) \\ & \quad - f_{\mp}(\mathbf{r}, \mathbf{p}, t) \int d\mathbf{k} w_{\text{rad}}(\mathbf{r}, \mathbf{p} \rightarrow \mathbf{k}, t) \\ & \quad + \int d\mathbf{k} w_{\text{cre}}(\mathbf{r}, \mathbf{k} \rightarrow \mathbf{p}, t) f_{\gamma}(\mathbf{r}, \mathbf{k}, t), \\ & \left(\frac{\partial}{\partial t} + \frac{\mathbf{k}}{\omega} \cdot \frac{\partial}{\partial \mathbf{r}} \right) f_{\gamma}(\mathbf{r}, \mathbf{p}, t) \\ &= \int d\mathbf{p} w_{\text{rad}}(\mathbf{r}, \mathbf{p} \rightarrow \mathbf{k}, t) [f_{+}(\mathbf{r}, \mathbf{p}, t) + f_{-}(\mathbf{r}, \mathbf{p}, t)] \\ & \quad - f_{\gamma}(\mathbf{r}, \mathbf{k}, t) \int d\mathbf{p} w_{\text{cre}}(\mathbf{r}, \mathbf{k} \rightarrow \mathbf{p}, t), \end{aligned} \quad (31)$$

where $\mathbf{F}_L(\mathbf{r}, \mathbf{p}, t) = e[\mathbf{E}(\mathbf{r}, t) + (\mathbf{p}/\varepsilon) \times \mathbf{B}(\mathbf{r}, t)]$ and where $w_{\text{rad}}(\mathbf{r}, \mathbf{p} \rightarrow \mathbf{k}, t)$ ($w_{\text{cre}}(\mathbf{r}, \mathbf{k} \rightarrow \mathbf{p}, t)$) is the local probability per unit time and unit momentum that an electron/positron (photon) with momentum \mathbf{p} (\mathbf{k}) emits (creates) at the space-time point (t, \mathbf{r}) a photon with momentum \mathbf{k} (an e^+e^- pair with the electron/positron having a momentum \mathbf{p}).

In Elkina *et al.*, 2011 the background field is approximated as a uniform, rotating electric field $\mathbf{E}(t)$ and $f_{\pm}(\mathbf{r}, \mathbf{p}, t) \rightarrow f_{\pm}(\mathbf{p}, t)$ ($f_{\gamma}(\mathbf{r}, \mathbf{k}, t) \rightarrow f_{\gamma}(\mathbf{k}, t)$). Also, analogously as in Duclous *et al.*, 2011, it is assumed that the momentum of the photon emitted in multiphoton Compton scattering is parallel to that of the emitting electron (positron); in the same way, the momenta of the electron and positron created in multiphoton Breit-Wheeler pair production are assumed to be parallel to that of the creating photon. The evolution of the electron, positron and photon distributions has been investigated by numerically integrating the resulting cascade equations via a two-dimensional Monte Carlo method with a randomly generated instant of radiation and of pair creation. In

particular, the exponential increase of the number of e^+e^- pairs and the qualitative estimate, for example, of the typical energy of the electron at the moment of the photon emission carried out in Fedotov *et al.*, 2010 have been confirmed (apart from discrepancies within one order of magnitude).

In both papers Elkina *et al.*, 2011 and Fedotov *et al.*, 2010 only the case of a rotating electric field was considered. In Bulanov *et al.*, 2010b it is pointed out that the limitation on the maximal laser intensity reachable before the cascade is primed, is strongly dependent on the polarization of the laser beams which create the standing wave. The paradigmatic cases of a rotating electric field and of an oscillating electric field are compared. The estimations presented in Bulanov *et al.*, 2010b for the case of a rotating electric field essentially confirm that the avalanche starts at laser intensities of the order of 10^{25} W/cm². The main physical reason why the cascade process in a circularly polarized standing wave starts at such an intensity is that in a rotating electric field the electron emits photons with typical energies of the order of $0.29 \omega_0 \gamma^3$, i.e. proportional to the cube of the Lorentz factor of the emitting electron γ (Bulanov *et al.*, 2010b). Instead, in an oscillating electric field the same quantity scales as γ^2 , in such a way that in order to emit a hard photon with a given energy, a much more energetic electron is needed. Thus, the authors of Bulanov *et al.*, 2010b conclude that in an oscillating electric field RR and quantum effects do not play a fundamental role at laser intensities smaller than I_{cr} and that avalanche processes do not constitute a limitation. It is crucial however, for the conclusion in Bulanov *et al.*, 2010b that the collision of the laser beams occurs in vacuum, i.e. the seed electrons and positrons which would prime the cascade are supposed to be created in the collision itself.

The question of the occurrence of the avalanche for two colliding linearly polarized pulses has also been addressed in Nerush *et al.*, 2011b, where a detailed description of the system under investigation has been provided. In fact, previous models had assumed the background electromagnetic field as given, neglecting in this way the field generated by the electrons and the positrons. The approach followed in Nerush *et al.*, 2011b exploits the existence of two energy scales for the photons: one is that of the external laser field and of the plasma fields which is much smaller than m , and the other is that of the photons produced by the high-energy electrons which is instead much larger than m . The evolution of the low-energy photons is described by means of Maxwell equations which are solved with a PIC code, i.e. the photons are treated as a classical electromagnetic field. Instead, hard photons are treated as particles and their distribution function is coupled to those of electrons and positrons via kinetic. The production of hard photons as well as the creation of e^+e^- pairs is described as a stochastic process via a Monte Carlo method. It is sur-

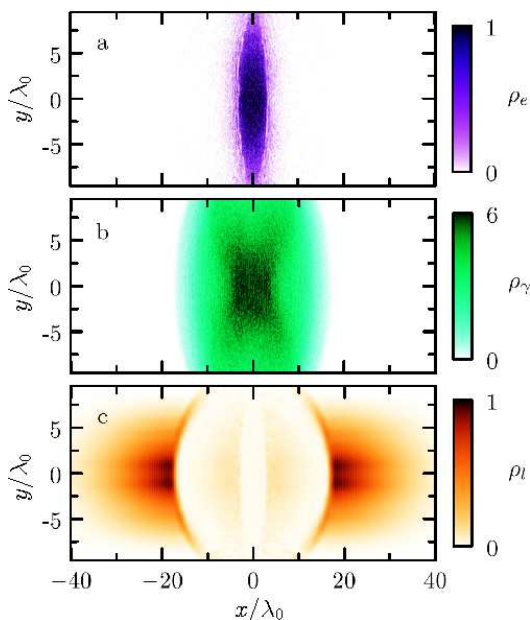


FIG. 17 (Color online) Snapshot of the normalized electron density ρ_e (part a)), of the normalized photon density ρ_γ (part b)), and of the normalized laser intensity ρ_l (part c)) 25.5 laser periods after the two laser counterpropagating beams collided. The normalized density of positrons is approximately the same as that of the electrons. Also, the intensity of each colliding beam is $I_0 = 3 \times 10^{24}$ W/cm² and the common wavelength is $\lambda_0 = 0.8$ μ m. Adapted and reprinted with permission from Nerush *et al.*, 2011b. Copyright (2011) by the American Physical Society.

prising that by considering a single seed electron initially at rest at a node of the magnetic field of a linearly polarized standing wave, an avalanche process is observed in the numerical simulation already for a laser intensity $I_0 = 3 \times 10^{24}$ W/cm² and a laser wavelength $\lambda_0 = 0.8$ μ m (see Fig. 17). The figure clearly shows the formation of an overdense e^+e^- plasma in the central region $|x| \lesssim \lambda_0$. In the same numerical simulations it is found that after about 20 laser periods almost half of the initial energy of the laser field has been transferred to the plasma. The discrepancy with the predictions in Bulanov *et al.*, 2010b is stated to be due to the formation of the avalanche in regions between the nodes of the electric and the magnetic field, where the simplified analysis of the electron motion carried out in Bulanov *et al.*, 2010b is not valid. Further analytical insight into the formation of the cascade has been obtained in Nerush *et al.*, 2011a by analyzing approximate solutions of the cascade equations in the presence of a rotating electric field.

IX. MUON-ANTIMUON AND PION-ANTIPION PAIR PRODUCTION

In Sec. VII we have discussed the production of e^+e^- pairs in strong laser fields. In view of the ongoing technical progress the question arises, whether also heavier particles such as muon-antimuon ($\mu^+-\mu^-$) or pion-antipion ($\pi^+-\pi^-$) pairs can be produced with the emerging near-future laser sources. The production of $\mu^+-\mu^-$ pairs from vacuum in the tunneling regime appears rather hopeless, though, since the required field needs to be close to $E_{cr,\mu} = \varrho_\mu^2 E_{cr} = 5.6 \times 10^{20}$ V/cm, with the ratio $\varrho_\mu = m_\mu/m \approx 207$ between the muon mass m_μ and the electron mass m . Even by boosting the effective laser fields with the Lorentz factors ($\sim 10^5$) of the most energetic available electron beams (Bamber *et al.*, 1999), the value of $E_{cr,\mu}$ seems out of reach. However, $\mu^+-\mu^-$ and $\pi^+-\pi^-$ production can occur by few-photon absorption from a high-frequency laser wave, as well as in microscopic collision processes in laser-generated or laser-driven plasmas.

A. Muon-antimuon and pion-antipion pair production in laser-driven collisions in plasmas

Energetic particle collisions in a plasma can in principle drive $\mu^+-\mu^-$ and $\pi^+-\pi^-$ production. The plasma may consist either of electrons and ions or of electrons and positrons. Both kinds of plasmas can be produced by intense laser beams interacting with a solid target. With respect to e^+e^- plasmas, this has been predicted by Liang *et al.*, 1998. As we have mentioned in Sec. VII, abundant amounts of e^+e^- pairs have been recently produced in this manner at the LLNL with pair densities of the order of 10^{16} cm⁻³ (Chen *et al.*, 2009, 2010) and much higher densities of the order of 10^{22} cm⁻³ have been also predicted (Shen and Meyer-ter-Vehn, 2001). Theoreticians have therefore started to investigate the properties and time evolution of relativistic e^+e^- plasmas (Aksenov *et al.*, 2007; Hu and Müller, 2011; Kuznetsova *et al.*, 2008; Mustafa and Kämpfer, 2009; Thoma, 2009a,b). In particular, it has been shown (Kuznetsova *et al.*, 2008; Thoma, 2009a,b) that in an e^+e^- plasma of 10 MeV temperature, $\mu^+-\mu^-$ pairs, $\pi^+-\pi^-$ pairs as well as neutral π^0 can arise from e^+e^- collisions. The required energy stems from the high-energy tails of the thermal distributions.

Also cold e^+e^- plasmas of high density can be generated nowadays due to dedicated positron accumulation and trapping techniques (Cassidy *et al.*, 2005). When such a nonrelativistic low-energy plasma interacts with a superintense laser field, $\mu^+-\mu^-$ pair production can occur as well (Müller *et al.*, 2006, 2008b). In this case, the plasma particles acquire the necessary energy by the strong coupling to the external field which drives the

electrons and positrons into violent collisions. The minimum laser intensity to ignite the reaction $e^+e^- \rightarrow \mu^+\mu^-$ amounts to a few 10^{22} W/cm² in the near-optical frequency range, corresponding to $\xi_{0,\min} = \varrho_\mu \approx 207$. The rate $R_{e^+e^- \rightarrow \mu^+\mu^-}$ of the process in the presence of a linearly polarized field reads

$$R_{e^+e^- \rightarrow \mu^+\mu^-} \approx \frac{1}{2^3\pi^2} \frac{\alpha^2}{m^2\xi_0^4} \sqrt{1 - \frac{\xi_{0,\min}^2}{\xi_0^2} \frac{N_+N_-}{V}}, \quad (33)$$

with the number N_\pm of electrons/positrons and the interaction volume V , which is determined by the laser focal spot size. Equation (33) can be equipped with an intuitive meaning by introducing the invariant cross section $\sigma_{e^+e^- \rightarrow \mu^+\mu^-}$ of $\mu^+\mu^-$ production in an e^+e^- collision in vacuum (Peskin and Schroeder, 1995):

$$\sigma_{e^+e^- \rightarrow \mu^+\mu^-} = \frac{4\pi}{3} \frac{\alpha^2}{\varepsilon'^2} \sqrt{1 - \frac{4m_\mu^2}{\varepsilon'^2}} \left(1 + \frac{2m_\mu^2}{\varepsilon'^2}\right), \quad (34)$$

where ε' is the energy of the colliding electron and positron in their ‘‘primed’’ center-of-mass system. Now, by exploiting the fact that the quantity $R_{e^+e^-}/V$ is a Lorentz invariant and that in the present physical scenario ε' can be estimated as $m\xi_0$, Eq. (33) implies the usual relation $R'_{e^+e^- \rightarrow \mu^+\mu^-}/V' \sim \sigma_{e^+e^- \rightarrow \mu^+\mu^-} n'_+ n'_-$ between the number of events per volume and time $R'_{e^+e^- \rightarrow \mu^+\mu^-}/V'$, the cross section $\sigma_{e^+e^- \rightarrow \mu^+\mu^-}$ and the densities $n'_\pm = N_\pm/V'$. The process $e^+e^- \rightarrow \mu^+\mu^-$ in the presence of an intense laser wave has also been considered in Nedoreshta *et al.*, 2009.

In laser-produced electron-ion plasmas resulting from intense laser-solid interaction, $\mu^+\mu^-$ and $\pi^+\pi^-$ pairs can be generated by the cascade mechanism via energetic bremsstrahlung, like in the case of e^+e^- pair production mentioned above. Assuming a laser-generated few-GeV electron beam, several hundreds to thousands of $\mu^+\mu^-$ pairs arise from bremsstrahlung conversion in a high- Z target material (Titov *et al.*, 2009). The production of $\pi^+\pi^-$ pairs by laser-accelerated protons was considered in Bychenkov *et al.*, 2001, where a threshold laser intensity of 10^{21} W/cm² for the process to occur was determined.

B. Muon-antimuon and pion-antipion pair production in high-energy XFEL-nucleus collisions

In this paragraph we pursue another mechanism of $\mu^+\mu^-$ pair creation by laser fields. It is based on the collision of an x-ray laser beam ($\omega_0 = 12$ keV) with an ultrarelativistic nuclear beam ($\gamma_n = 7000$). The setup is similar to the one of Par. VII.B. In the nucleus frame the photon energy amounts to $\omega_0^* \approx 2\gamma_n\omega_0 = 168$ MeV. The energy gap of $2m_\mu$ for $\mu^+\mu^-$ pair production can thus be overcome by two-photon absorption (Müller *et al.*,

2008a, 2009a). Note that because of pronounced recoil effects, the Lorentz factor which would be required for two-photon $\mu^+\mu^-$ production by a projectile electron is much larger: $\gamma \gtrsim 10^6$, corresponding to a yet unavailable electron energy in the TeV range.

At first sight, e^+e^- and $\mu^+\mu^-$ pair production in combined laser and Coulomb fields seem to be very similar processes since the electron and muon only differ by their mass (and lifetime). In this picture, the corresponding production probabilities would coincide when the laser field strength and frequency are scaled in accordance with the mass ratio ϱ_μ , i.e. $P_{\mu^+\mu^-}(E_{0,\mu}, \omega_{0,\mu}) = P_{e^+e^-}(E_0, \omega_0)$ for $E_{0,\mu} = \varrho_\mu^2 E_0$ and $\omega_{0,\mu} = \varrho_\mu \omega_0$. This simple scaling argument does not apply, however, as the large muon mass is connected with a correspondingly small Compton wavelength $\lambda_{C,\mu} = \lambda_C/\varrho_\mu \approx 1.86$ fm (1 fm = 10^{-13} cm), which is smaller than the radius of most nuclei. As a result, while the nucleus can be approximated as pointlike in e^+e^- pair production ($\lambda_C \approx 386$ fm), its finite extension must be taken into account in $\mu^+\mu^-$ pair production. Pronounced nuclear size effects have also been found for $\mu^+\mu^-$ production in relativistic heavy-ion collisions (Baur *et al.*, 2007).

Muon pair creation in XFEL-nucleus collisions can be calculated via the amplitude in Eq. (27), with the nuclear potential V_n arising from an extended nucleus. It leads to the appearance of a nuclear form factor $F(q^2)$ which depends on the recoil momentum q . For example, $F(q^2) = \exp[-(qa)^2/6]$ for a Gaussian nuclear charge distribution of root-mean-square radius a . Since the typical recoil is $q \sim m_\mu$, the form factor leads to substantial suppression of the process. The fully differential production rate $dR = dR_e + dR_i$ may be split into an elastic and inelastic part, depending on whether the nucleus remains in its ground state or gets excited during the process. They read $dR_e = dR_0 Z^2 F^2(q^2)$ and $dR_i \approx dR_0 Z[1 - F^2(q^2)]$, respectively, with dR_0 being the production rate for a pointlike proton.

Figure 18 shows $\mu^+\mu^-$ production rates for several projectiles colliding with an intense XFEL beam. For an extended nucleus, the elastic rate increases with its charge but decreases with its size. This interplay leads to the emergence of maximum elastic rates for medium-heavy ions. The total rate $R = R_e + R_i$ saturates at high Z values since R_i increases with nuclear charge. For highly-charged nuclei the main contribution stems from the inelastic channel where the protons inside the nucleus act incoherently ($R_i \propto Z$). This implies that despite the high charges, high-order Coulomb corrections in $Z\alpha$ are of minor importance. In the collision, also e^+e^- pairs are produced by single-photon absorption in the nuclear field. However, this rather strong background process does not deplete the x-ray beam.

In XFEL-proton collisions, $\pi^+\pi^-$ pairs can be generated as well. A corresponding calculation has been reported in Dadi and Müller, 2011, which includes both

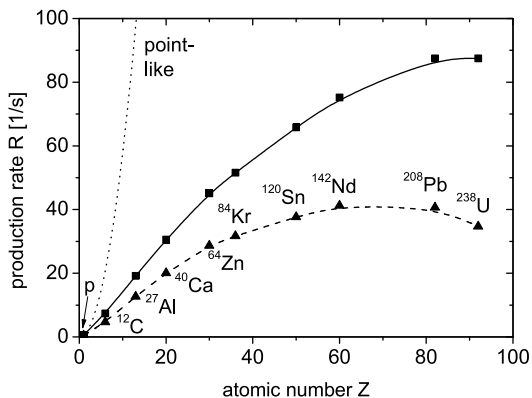


FIG. 18 Rates for $\mu^+-\mu^-$ pair creation by two-photon absorption from an intense XFEL beam ($\omega_0 = 12$ keV, $I_0 = 2.5 \times 10^{22}$ W/cm²) colliding with various ultrarelativistic nuclei ($\gamma_n = 7000$). The triangles show elastic rates, whereas the squares indicate total (“elastic + inelastic”) rates. The numerical data are connected by fit curves. The dotted line holds for a pointlike nucleus. The production rates refer to the rest-frame of the nucleus. Reprinted with permission from Müller *et al.*, 2008a. Copyright (2008) by the American Physical Society.

the electromagnetic and hadronic pion-proton interactions. The latter was described approximately by a phenomenological Yukawa potential. It was shown that, despite the larger pion mass, $\pi^+-\pi^-$ pair production by two-photon absorption from the XFEL field largely dominates over the corresponding process of $\mu^+-\mu^-$ pair production in the Doppler-boosted frequency range of $\omega_0^* \approx 150$ -210 MeV. This dominance is due to the much larger strength of the strong (hadronic) force as compared with the electromagnetic force. As a consequence, in this energy range $\mu^+-\mu^-$ pairs are predominantly produced indirectly via two-photon $\pi^+-\pi^-$ production and subsequent pion decay, $\pi^+ \rightarrow \mu^+ + \nu_\mu$ and $\pi^- \rightarrow \mu^- + \bar{\nu}_\mu$.

In relativistic laser-nucleus collisions, $\mu^+-\mu^-$ or $\pi^+-\pi^-$ pairs can also be produced indirectly within a two-step process (Kuchiev, 2007). First, upon the collision, an e^+e^- pair is created via tunneling pair production. Afterwards, the pair, being still subject to the electromagnetic forces exerted by the laser field, is driven by the field into an energetic electron-positron collision. If the collision energy is large enough, the reaction $e^+e^- \rightarrow \mu^+\mu^-$ may be triggered. This two-step mechanism thus represents a combination of the processes considered in Par. VII.B and IX.A. Besides, it may be considered as a generalization of the well-established analogy between strong-field ionization and pair production (see Sec. VII) to include also the recollision step.

X. NUCLEAR PHYSICS

Influencing atomic nuclei with laser radiation is, in general, a difficult task because of the large nuclear level spacing $\Delta\mathcal{E}$ of the order of 1 keV-1 MeV, which exceeds typical laser photon energies $\omega_0 \sim 1$ eV by orders of magnitude (Matinyan, 1998). Also the laser’s electric work performed over the tiny nuclear extension $r_n \sim 1$ -5 fm is usually too small to cause any sizable effect. In fact, the requirement $|e|E_0r_n \sim \Delta\mathcal{E}$ can only be satisfied for at least near-critical laser fields. Direct laser-nucleus interactions have therefore mostly been dismissed in the past.

Instead, starting from the late 1990s, laser-induced secondary reactions in nuclei have been explored. Via laser-heated clusters and laser-produced plasmas, various nuclear reactions have been ignited, such as fission, fusion and neutron production. In all these cases, the interaction of the laser field with the target first produces secondary particles such as photo-electrons or bremsstrahlung photons which, in a subsequent step, trigger the nuclear reaction. For a recent review on this subject we refer to Ledingham and Galster, 2010 and Ledingham *et al.*, 2003.

In recent years, however, the interest in direct laser-nucleus coupling has been revived by the ongoing technological progress towards laser sources of increasingly high intensities as well as frequencies. Indeed, when suitable nuclear isotopes are considered, intense high-frequency fields or superstrong near-optical fields may be capable of affecting the nuclear structure and dynamics.

A. Direct laser-nucleus interaction

1. Resonant laser-nucleus coupling

There are several low-lying nuclear transitions in the keV range, and even a few in the eV range. Examples for the latter are ^{229}Th ($\Delta\mathcal{E} \approx 7.6$ eV) and ^{235}U ($\Delta\mathcal{E} \approx 76$ eV) (Beck *et al.*, 2007). These isotopes can be excited by the 5th harmonic of a Ti:Sa laser and the ELI attosecond source, respectively. Even higher frequencies can be attained by laser pulse reflection from relativistic flying mirrors of electrons extracted from an underdense plasma (Bulanov *et al.*, 1994) (or possibly also from an overdense plasma (Habs *et al.*, 2008)). Otherwise keV-energy photons are generated by XFELs, which are presently emerging as large-scale facilities at SLAC (LCLS, 2011) and at DESY (European XFEL, 2011), and could be employed with focusing (Mimura *et al.*, 2010) and reflection devices (Shvyd’ko *et al.*, 2011). In addition, also XFEL facilities of table-top dimension (Grüner *et al.*, 2007; Kneip *et al.*, 2010) and even fully coherent XFEL sources are envisaged such as the future XFEL Oscillator (XFELO) (Kim *et al.*, 2008) or the Seeded XFEL (SXFEL) (Feldhaus

TABLE II The transitional energy $\Delta\mathcal{E}$, the dipole moment μ , the life-time τ_g (τ_e) of the ground (excited) state of few relevant nuclear systems and E1 transitions (Aas *et al.*, 1999; NNDC, 2011). Adapted and reprinted with permission from Bürvenich *et al.*, 2006a. Copyright (2006) by the American Physical Society.

Nucleus	Transition	$\Delta\mathcal{E}$ [keV]	μ [e fm]	τ_g	τ_e [ps]
^{153}Sm	$3/2^- \rightarrow 3/2^+$	35.8	$> 0.75^a$	47 h	< 100
^{181}Ta	$9/2^- \rightarrow 7/2^+$	6.2	0.04^a	stable	6×10^6
^{225}Ac	$3/2^+ \rightarrow 3/2^-$	40.1	0.24^a	10.0 d	720
^{223}Ra	$3/2^- \rightarrow 3/2^+$	50.1	0.12	11.435 d	730
^{227}Th	$3/2^- \rightarrow 1/2^+$	37.9	b	18.68 d	b
^{231}Th	$5/2^- \rightarrow 5/2^+$	186	0.017	25.52 h	1030

^a Estimated via the Einstein A coefficient from τ_e and $\Delta\mathcal{E}$

^b Not listed in the National Nuclear Data Center (NNDC) (NNDC, 2011)

et al., 1997; LCLS II, 2011). Brilliant gamma-ray beams with spectra peaked between 20 KeV and 150 KeV have been recently produced from resonant betatron motion of electrons in a plasma wake (Cipiccia *et al.*, 2011). A new material research center Matter-Radiation Interactions in Extremes (MaRIE) (MaRIE, 2011) is planned, allowing for both fully coherent XFEL light with photon energy up to 100 keV and accelerated ion beams. The photonuclear pillar of ELI to be set up near Bucharest in Romania is planned to simultaneously provide a compact XFEL along with an ion accelerator aiming for energies of 4-5 GeV (ELI, 2011). In addition, at this facility, also coherent gamma-rays reaching few MeV energies via electron laser interaction are envisaged (ELI, 2011; Habs *et al.*, 2009).

With these sources of coherent high-frequency pulses, driving electric dipole (E1) transitions in nuclei is becoming feasible (Bürvenich *et al.*, 2006a). Table II displays a list of nuclei with suitable E1 transitions. Along with an appropriate moderate nucleus acceleration, resonance may be induced due to the Doppler shift via the factor $(1 + v_n)\gamma_n$ in the counterpropagating setup, with v_n and γ_n being the nucleus velocity and its Lorentz factor, respectively (Bürvenich *et al.*, 2006a). For example, ^{223}Ra and an XFEL frequency of 12.4 keV a factor of $(1 + v_n)\gamma_n = 4$ would be sufficient. In general such moderate pre-accelerations of the nuclei would be of great assistance since they increase the number of possible nuclear transitions for the limited number of available light frequencies. Note that the electric field strength of the laser pulses is transforming analogously, such that the applied laser fields may be correspondingly weaker for a counterpropagating setup.

For optimal coherence properties of the envisaged high-frequency facilities, subsequent pulse applications were shown to yield notable excitation of nuclei (Bürvenich *et al.*, 2006a). In addition, many low-energy electric

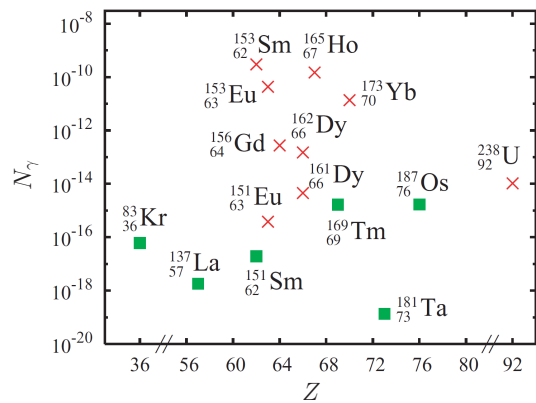


FIG. 19 (Color online) Number N_γ of signal photons per nucleus per laser pulse for several isotopes with first excited states below 12.4 keV (green squares) and above 12.4 keV (red crosses). The results are plotted versus the atomic number Z . The considered European XFEL has a pulse duration of 100 fs and an average brilliance of 1.6×10^{25} photons/(smrad² mm² 0.1% bandwidth) (European XFEL, 2011). Adapted and reprinted with permission from Pálffy *et al.*, 2008. Copyright (2008) by the American Physical Society.

quadrupole (E2) and magnetic dipole (M1) transitions are available. Here it is interesting to note that certain E2 or M1 transitions can indeed be competitive in strength with E1 transitions (Pálffy, 2008; Pálffy *et al.*, 2008). While the majority of transitions is available for high frequencies in the MeV domain (requiring substantial nucleus accelerations), Fig. 19 displays also numerous suitable nuclear transitions below 12.4 keV along with the excitation efficiencies from realistic laser pulses. While indeed experimental challenges are high, resonant direct interactions of laser radiation with nuclei is expected to pave the way to nuclear quantum optics. Especially control in exciting and deexciting certain long-living nuclear states would have dramatic implications for nuclear isomer research (Aprahamian and Sun, 2005; Pálffy *et al.*, 2007; Walker and Dracoulis, 1999). As an obvious application this would be of relevance for nuclear batteries (Aprahamian and Sun, 2005; Walker and Dracoulis, 1999), i.e. for controlled pumping and release of energy stored in long-lived nuclear states. In atomic physics, STimulated Raman Adiabatic Passage (STIRAP) has proven to be highly efficient in controlling populations robustly with high precision (Bergmann *et al.*, 1998). On the basis of currently envisaged accelerators and coherent high-frequency laser facilities it has been recently shown that such an efficient coherent population transfer shall also be feasible in nuclei (Liao *et al.*, 2011).

Serious challenges are certainly imposed by the nuclear linewidths that may either be too narrow to allow for sufficient interaction with the applied laser pulses or inhibit excitations and coherences due to large spontaneous decay. Here decades of research in atomic physics allowing

now for shaping atomic spectra via quantum interference (Evers and Keitel, 2002; Kiffner *et al.*, 2010; Postavaru *et al.*, 2011) rise hopes that such obstacles may be overcome in the near future as well.

Direct photoexcitation of giant dipole resonances with few-MeV photons via laser-electron interaction was shown to be feasible (Weidenmüller, 2011) based on envisaged experimental facilities as ELI. Finally, care has to be taken to compare the laser-induced nuclear channels with competing nuclear processes via, for example, bound electron transitions or electron captures in the atomic shells (Pálffy, 2010; Pálffy *et al.*, 2007).

2. Nonresonant laser-nucleus interactions

Already decades ago there has been a lively debate on how nuclear β -decay may be modified with the aid of strong laser pulses (Akhmedov, 1983; Becker *et al.*, 1984; Nikishov and Ritus, 1964a; Reiss, 1983). While this discussion still awaits widely accepted experimental confirmation, most recently the notion of affecting nuclear α -decay with strong laser pulses has been discussed showing that moderate changes of such nuclear reactions with the strongest envisaged laser pulses are indeed feasible (Castañeda Cortés *et al.*, 2012, 2011).

When the laser intensity is high enough ($I_0 > 10^{26}$ W/cm²) then also low-frequency laser fields are able to influence the nuclear structure without necessarily inducing nuclear reactions. In such ultrastrong fields, low-lying nuclear levels are modified by the dynamic (AC-) Stark shift (Bürvenich *et al.*, 2006b). These AC-Stark shifts are of the same order as in typical atomic quantum optical systems relative to the respective transition frequencies. At even higher, supercritical intensities ($I_0 > 10^{29}$ W/cm²) the laser field induces modifications to the proton root-mean-square radius and to the proton density distribution (Bürvenich *et al.*, 2006b).

B. Nuclear signatures in laser-driven atomic and molecular dynamics

Muonic atoms represent traditional tools for nuclear spectroscopy by employing atomic physics techniques. Due to the large muon mass $m_\mu \approx 207 m$ as compared to the electron mass and the correspondingly small Bohr radius $a_{0,\mu} = \lambda_{C,\mu}/\alpha \approx 255$ fm, the muonic wave-function has a large overlap with the nucleus. Precise measurements of x-ray transitions between stationary muonic states are therefore sensitive to nuclear-structure features such as finite size, deformation, surface thickness, or polarization.

When a muonic atom is subject to a strong laser field, the muon rather becomes a *dynamic* nuclear probe which is periodically driven across the nucleus by the field. This

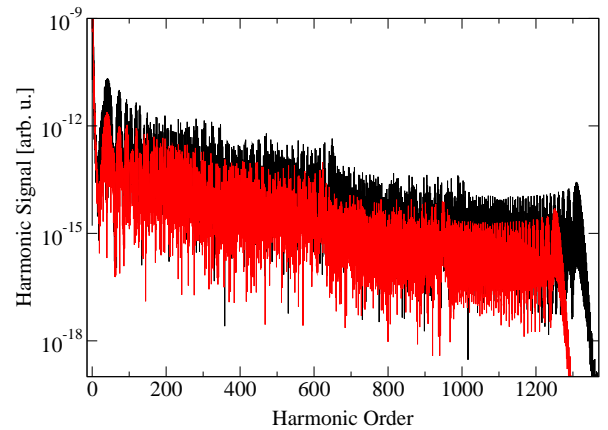


FIG. 20 (Color online) HHG spectra emitted from muonic hydrogen (black) and muonic deuterium (red) in a laser field of intensity $I_0 \approx 10^{23}$ W/cm² and photon energy $\omega_0 \approx 60$ eV. “Arb. u.” stands for “arbitrary units”. Reprinted with permission from Shahbaz *et al.*, 2007. Copyright (2007) by the American Physical Society.

can be seen, for example, in the high-harmonic radiation emitted by such systems (Shahbaz *et al.*, 2010, 2007). Figure 20 compares the HHG spectra from muonic hydrogen versus muonic deuterium subject to a very strong XUV laser field. Such fields are envisaged at the ELI attosecond source (see Fig. 1). Due to the different masses M_n of the respective nuclei ($M_n = m_p$ for an hydrogen nucleus and $M_n \approx m_p + m_n$ for a deuterium nucleus by neglecting the binding energy, with $m_{p/n}$ being the proton/neutron mass), muonic hydrogen gives rise to a significantly larger harmonic cut-off energy. The reason can be understood by inspection of the ponderomotive energy

$$U_p = \frac{e^2 E_0^2}{4\omega_0^2 M_r} = \frac{e^2 E_0^2}{4\omega_0^2} \left(\frac{1}{m_\mu} + \frac{1}{M_n} \right), \quad (35)$$

which depends in the present case on the reduced mass $M_r = m_\mu M_n / (m_\mu + M_n)$ of the muon-nucleus system. The reduced mass of muonic hydrogen (≈ 93 MeV) is smaller than that of muonic deuterium (≈ 98 MeV) and this implies a larger ponderomotive energy and an enlarged cut-off position. The influence of the nuclear mass can also be explained by the separated motions of the atomic binding partners. The muon and the nucleus are driven by the laser field into opposite directions along the laser’s polarization axis. Upon recombination their kinetic energies sum up as indicated on the right-hand side of Eq. (35). Within this picture, the larger cut-off energy for muonic hydrogen results from the fact that, due to its smaller mass, the proton is more strongly accelerated by the laser field than the deuteron.

Due to the large muon mass, very high harmonic cut-off energies can be achieved with muonic atoms with charge number Z in the nonrelativistic regime of interaction. Since the harmonic-conversion efficiency as well

as the density of muonic atom samples are rather low, it is important to maximize the radiative signal strength. A sizable HHG signal requires efficient ionization on the one hand and efficient recombination on the other. The former is guaranteed if the laser's electric field amplitude E_0 lies just below the border of over-barrier ionization,

$$E_0 \lesssim \frac{M_r^2 (Z\alpha)^3}{Q_{\text{eff}} 16}. \quad (36)$$

Here, $Q_{\text{eff}} = |e|(Z/M_n + 1/m_\mu)M_r$ represents an effective charge (Reiss, 1979; Shahbaz *et al.*, 2010). Efficient recollision is guaranteed if the magnetic drift along the laser propagation direction can be neglected. Equation (1) indicates that this is the case here if

$$\left(\frac{Q_{\text{eff}} E_0}{M_r \omega_0}\right)^3 \lesssim \frac{16\omega_0}{\sqrt{2M_r I_p}}. \quad (37)$$

The two above equations define a maximum laser intensity and a minimum laser frequency which are still in accordance with the conditions imposed. At these laser parameters, the maximum harmonic cut-off energies are attained and an efficient ionization-recollision process is guaranteed. For muonic hydrogen the corresponding lowest frequency lies in the (Vacuum Ultraviolet) VUV range ($\omega_0 \approx 27$ eV) and the maximum field intensity amounts to 1.6×10^{23} W/cm². At these values, the harmonic spectrum extends to a maximum energy of $\omega_c \approx 0.55$ MeV. For light muonic atoms with nuclear charge number $Z > 1$, the achievable cut-off energies are even higher, reaching several MeVs. This holds prospects for the production of coherent ultrashort gamma-ray pulses (see also Xiang *et al.*, 2010).

In principle, also nuclear size effects arise in the HHG signal from muonic atoms. This has been shown qualitatively in 1D numerical simulations, where a 50% enhancement of the harmonic plateau height has been obtained for muonic hydrogen as compared with muonic deuterium (Shahbaz *et al.*, 2010, 2007). This has been explained due to the enhanced final muon acceleration towards the hydrogenic core. For more precise predictions, 3D calculations are desirable.

The existing results indicate that muonic atoms in high-intensity, high-frequency laser fields can be utilized to dynamically gain structure information on nuclear ground states via their high-harmonic response. Besides, the laser-driven muonic charge cloud, causing a time-dependent Coulomb field, may lead to nuclear excitation (Shahbaz *et al.*, 2009). The excitation probabilities are quite small, however, because of the large difference between the laser photon energy and the nuclear transition energy. Nuclear excitation can also be triggered in intense laser-induced recollisions of field-ionized high-energy electrons (Kornev and Zon, 2007; Milosevic *et al.*, 2004; Mocken and Keitel, 2004).

Finally, muonic molecules are of particular interest with respect to nuclear fusion. Modifications of muon-catalyzed fusion in strongly laser-driven muonic D₂⁺ molecules have been investigated (Chelkowski *et al.*, 2004; Paramonov, 2007). It was found that applied field intensities of the order of 10^{23} W/cm² can control the molecular recollision dynamics by triggering the nuclear reaction on a femtosecond time scale. Similar theoretical studies have recently been carried out on aligned (electronic) HT molecules, i.e. involving a Tritium atom (Zhi and Sokolov, 2009).

XI. LASER COLLIDERS

The fast advancement in laser technology is opening up the possibility of employing intense laser beams to efficiently accelerate charged particles, to make them collide, and eventually even to initiate high-energy reactions.

A. Laser acceleration

Strong laser fields provide new mechanisms for particle acceleration alternative to conventional accelerator technology (Tajima and Dawson, 1979). With presently-available laser systems an enormous electron acceleration gradient ~ 1 GeV/cm can be achieved, which exceeds by three orders of magnitude that of conventional accelerators and which raises prospects for compact accelerators (Faure *et al.*, 2004; Geddes *et al.*, 2004; Mangles *et al.*, 2004). Different schemes of laser-electron acceleration are known. These include the laser wakefield accelerator, the plasma beat wave accelerator, the self-modulated laser wakefield accelerator and plasma waves driven by multiple laser pulses (see the recent review Esarey *et al.*, 2009). High-gradient plasma wakefields can also be generated with an ultrashort bunch of protons (Caldwell *et al.*, 2009), allowing electron acceleration to TeV energies in a single stage. The achievable current and emittance of the presently-available laser-accelerated electron beam is sufficient to build synchrotron radiation sources or even to aim at compact XFEL lasers (Schlenvoigt *et al.*, 2008).

Laser acceleration of ions provides quasimonoenergetic beams with energy of several MeVs per nucleon (Fuchs *et al.*, 2007; Hegelich *et al.*, 2006; Schwoerer *et al.*, 2006; Toncian *et al.*, 2006). It mostly employs the interaction of high-intensity lasers with solid targets. One of the main goals of laser-ion acceleration is to create low-cost devices for medical applications, such as for hadron cancer therapy (Combs *et al.*, 2009). Several regimes have been identified for laser-ion acceleration (see also the forthcoming review Macchi *et al.*, 2012). For laser intensities in the range 10^{18} - 10^{21} W/cm² and for solid targets with a thickness ranging from a few to tens of micrometers, the so-called target-normal-sheath accel-

ation is the main mechanism (Fuchs *et al.*, 2006). A further laser-ion interaction process is the skin-layer ponderomotive acceleration (Badziak, 2007). Instead, the radiation-pressure acceleration regime operates when the target thickness is decreased (see Esirkepov *et al.*, 2004 and Macchi *et al.*, 2009 for the so-called “laser piston” and “light sail” regimes, respectively).

A setup for direct laser acceleration of protons and bare carbon nuclei is considered in Salamin *et al.*, 2008 by employing intense laser beams tightly focused to sub-wavelength waist radii. It has been shown that laser pulses of 0.1-10 PW can accelerate the nuclei directly to energies in the ranges required for hadron therapy in this case. Simulations in Galow *et al.*, 2010 indicate that protons stemming from laser-plasma processes can be efficiently post-accelerated employing single and crossed pulsed laser beams, focused to spot radii of the order of the laser wavelength. The protons in the resulting beam have kinetic energies exceeding 200 MeV and small energy spreads of about 1%. In Galow *et al.*, 2011 a chirped ultrastrong laser pulse is applied for proton acceleration. Chirping of the laser pulse ensures optimal phase synchronization of the protons with the laser field and leads to efficient proton energy gain from the field. In this way, a dense proton beam (with about 10^7 protons per bunch) of high energy (250 MeV) and good quality (energy spread $\sim 1\%$) can be generated.

B. Laser-plasma linear collider

Laser-electron accelerators have already entered the GeV energy domain where the realm of particle physics starts. In fact, the strong interaction comes into play at distances of the order of $r \sim 1$ fm, which for relativistic processes corresponds to energies $\varepsilon \sim 1/r \sim 1$ GeV. Thus, a laser-based collider is in principle suitable for performing particle-physics experiments. However, in order to initiate high-energy reactions with sizable yield, not only GeV energies are required but also collision luminosities \mathcal{L} at least as high as 10^{26} - 10^{27} $\text{cm}^{-2}\text{s}^{-1}$. Meanwhile, for the ultimate goal of being competitive with the next International Linear Collider (ILC, 2011), energies on the order of 1 TeV and luminosities of the order of 10^{34} $\text{cm}^{-2}\text{s}^{-1}$ are required (Ellis and Wilson, 2001).

The potential of the Laser-Plasma Accelerator (LPA) scheme to develop a laser-plasma linear collider is discussed in Schroeder *et al.*, 2010. Two LPA regimes are analyzed which are distinguished by the relationship between the laser beam waist size w_0 and the plasma frequency $\omega_p = \sqrt{4\pi n_p e^2/m}$, with n_p being the plasma density: 1) the quasilinear regime at large radius of the laser beam $\omega_p^2 w_0^2 > 2\xi_0^2/\sqrt{1+\xi_0^2/2}$ ($\xi_0 \sim 1$); 2) the bubble regime, at $\omega_p w_0 \lesssim 2\sqrt{\xi_0}$ ($\xi_0 > 1$). The latter is less suitable for the collider application because the bubble cavity acts defocusing for positrons; besides, the focus-

ing forces and accelerating forces are not independently controllable here as both depend on the plasma density. Instead, in the quasilinear regime this is possible due to the existence of a second control parameter given by the laser beam waist size. In the following, we will discuss qualitatively the scaling properties of the quasilinear regime. For more accurate expressions we refer to Schroeder *et al.*, 2010.

In the standard LPA scheme, the electron plasma wave is driven by an intense laser pulse with duration τ_0 of the order of the plasma wavelength $\lambda_p = 2\pi/\omega_p$, which accelerates the electrons injected in the plasma wave due to wave breaking (Esarey *et al.*, 2009; Leemans and Esarey, 2009; Malka *et al.*, 2008). We can estimate the accelerating field E_p of the plasma wave as

$$E_p \sim \frac{m\omega_p}{|e|} \propto n_p^{1/2}. \quad (38)$$

In fact, in the plasma wave, the charge separation occurs on a length scale of the order of λ_p , producing a surface charge density $\sigma_p \sim |e|n_p\lambda_p$ and a field $E_p \sim 4\pi\sigma_p$, which corresponds to Eq. (38). The number of electrons N_e that can be accelerated in a plasma wave is given approximately by the number of charged particles required to compensate for the laser-excited wakefield, having a longitudinal component E_{\parallel} . From the relation $E_{\parallel} \sim 4\pi N_e |e|/\pi w_0^2$, it thus follows

$$N_e \sim \frac{\pi n_p}{\omega_p^3} \propto n_p^{-1/2}, \quad (39)$$

because $w_0\omega_p \sim 1$ in the quasilinear regime. The interaction length of a single LPA stage is limited by laser diffraction effects, dephasing of the electrons with respect to the accelerating field, and laser energy depletion. Laser-diffraction effects can be reduced by employing a plasma channel, and plasma density tapering can be utilized to prevent dephasing. Therefore, the LPA interaction length will be determined by the energy depletion length L_d . We can estimate the latter by equating the energy spent for accelerating the N_e electrons along L_d ($\sim N_e |e| E_p L_d$) to the energy of the laser pulse ($\sim E_0^2 \pi w_0^2 \tau_0 / 8\pi$). By reminding that $w_0\omega_p \sim 1$, this yields

$$L_d \sim \frac{\omega_0^2}{\omega_p^2} \lambda_p \propto n_p^{-3/2}. \quad (40)$$

A staging of LPA is required to achieve high current densities along with high energies. The electron energy gain $\Delta\varepsilon_s$ in a single-stage LPA is

$$\Delta\varepsilon_s \sim |e| E_p L_d \sim m \frac{\omega_0^2}{\omega_p^2} \propto n_p^{-1}. \quad (41)$$

Therefore, the number of stages N_s to achieve a total acceleration energy ε_0 is $N_s = \varepsilon_0 / \Delta\varepsilon_s \sim$

$(\varepsilon_0/m)(\omega_p/\omega_0)^2 \propto n_p$. It corresponds to a total collider length L_c of

$$L_c \sim N_s L_d \sim \frac{\varepsilon_0}{m} \lambda_p \propto n_p^{-1/2}. \quad (42)$$

When two identical beams each with N particles and with horizontal (vertical) transverse beam size σ_x (σ_y) collide with a frequency f , the luminosity \mathcal{L} is defined as $\mathcal{L} = N^2 f / 4\pi \sigma_x \sigma_y$. In LPA $N = N_e$ and f is the laser repetition rate, then

$$\mathcal{L} \sim \frac{1}{64\pi} \frac{1}{\omega_p^2 \sigma_x \sigma_y} \frac{f}{r_0^2}. \quad (43)$$

The laser energy W_s in the pulse for a single stage in the LPA collider is approximately given by $W_s \sim m(\lambda_p/r_0)(\omega_0/\omega_p)^2$ at $\xi_0 \sim 1$ and the total required power P_T amounts to $P_T \sim N_s W_s f \sim \varepsilon_0 f (\lambda_p/r_0)$.

The above estimations show that, although the number N_e of electrons in the bunch as well as the single-stage energy gain $\Delta\varepsilon_s$ increase at low plasma densities, the accelerating gradient $\Delta\varepsilon_s/L_d$ nevertheless decreases because the laser depletion length L_d and the overall collider length L_c increase as well. Limiting the total length of the each LPA in a collider to about 100 m will require a plasma density $n_p \sim 10^{17} \text{ cm}^{-3}$ to provide a center-of mass energy of $\sim 1 \text{ TeV}$ electron energy, with $\sim 10 \text{ GeV}$ energy gain per stage (Schroeder *et al.*, 2010). For a number of electrons per bunch of $N_e \sim 10^9$, a laser repetition rate of 15 kHz and a transverse beam size of about 10 nm would be required to reach the goal-value of $10^{34} \text{ cm}^{-2}\text{s}^{-1}$ for the accelerator luminosity. At the usual condition $w_0 \sim 1/\omega_p \sim 10 \text{ } \mu\text{m}$, instead, the luminosity amounts to $\mathcal{L} \sim 10^{27} \text{ cm}^{-2}\text{s}^{-1}$. In the above conditions each acceleration stage would be powered by a laser pulse with an energy of 30 J corresponding to an average power of about 0.5 MW at the required repetition rate of 15 kHz. Such high-average powers are beyond the performance of present lasers. The future hopes for high-average-power lasers are connected with diode-pumped lasers and new amplifier materials. Further challenges of LPA colliders are their complexity, as they involve plasma channels and density tapering, and, most importantly, the problem of how to accelerate positrons.

C. Laser micro-collider

We turn now to another scheme for a laser collider, which is based on quite different principles than those of the LPA scheme discussed above. In the LPA scheme, the electron is accelerated due to its synchronous motion with the propagating field. In this way the symmetry in the energy exchange process between the electron and the oscillating field is broken, as required by the Lawson-Woodward theorem (Lawson, 1979; Woodward, 1947). Another way to exploit the energy gain of the electron

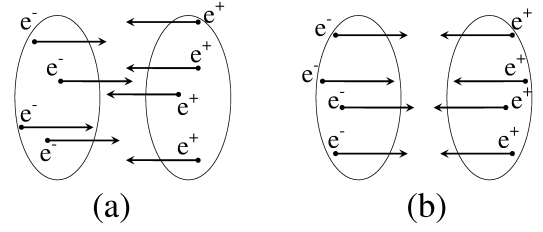


FIG. 21 (a) In conventional e^+e^- colliders bunches of accelerated electrons and positrons are focused to collide head-on-head *incoherently*, i.e., the bunches collide head-on-head but electrons and positrons in the bunch do not. (b) In the recollision-based collider, the electron and the positron originating from the same Ps atom may collide head-on-head *coherently* (Henrich *et al.*, 2004). From Hatsagortsyan *et al.*, 2006.

in the oscillating laser field is to initiate high-energy processes *in situ*, i.e. inside the laser beam (McDonald and Shmakov, 1999). In this case the temporary energy gain of the electron during a half cycle of the laser wave is used to trigger some processes during which the electron state may change (in particular, the electron may annihilate with a positron) and the desired asymmetry in the energy exchange will be achieved. In fact, this approach is widely employed in the nonrelativistic regime via laser-driven recollisions of an ionized electron with its parent ion (see Par. III.B).

The question arises whether the temporary energy gain of the electron in the laser beam can also be employed in the relativistic regime at ultrahigh energies. As pointed out in Sec. III, an extension of the established recollision scheme with normal atoms into the relativistic regime is hindered by the relativistic drift. However, the drift will not cause any problem when Ps atoms are used because its constituent particles, electron and positron, have the same absolute value of the charge-to-mass ratio.

A corresponding realization of high-energy e^+e^- recollisions in the GeV domain aiming at particle reactions has been proposed in Hatsagortsyan *et al.*, 2006. It relies on (initially nonrelativistic) Ps atoms exposed to super-intense laser pulses. After almost instantaneous ionization of Ps in the strong laser field, the free electron and positron oscillate in opposite directions along the laser electric field and experience the same ponderomotive drift motion along the laser propagation direction. In this way, the particles acquire energy from the field and are driven into periodic e^+e^- collisions (Henrich *et al.*, 2004). Provided that the applied laser intensity is large enough, elementary particle reactions like heavy lepton-pair production can be induced in these recollisions. The common center-of-mass energy ε' of the electron and the positron at the recollision time arises mainly from the transversal momentum of the particles and it scales as $\varepsilon' \sim m\xi_0$. A basic particle reaction which could be triggered in the laser-driven collider is e^+e^- annihilation

with production of a $\mu^+-\mu^-$ pair, i.e. $e^+e^- \rightarrow \mu^+\mu^-$. The energy threshold for this process is $2m_\mu \approx 210$ MeV. It can be reached with a laser field such that $\xi_0 \sim 200$, corresponding to realistic laser intensities of the order of 10^{22} W/cm².

In addition, the proposed recollision-based laser collider can yield high luminosities as compared to conventional laser accelerators. In the latter, bunches of electrons and positrons are accelerated and brought into head-on-head collision. However, the particles in the bunch are distributed randomly such that each microscopic e^+e^- collision is not head-on-head but has a mean impact parameter $b_i \sim a_b$ determined by the beam radius a_b , characterizing the collision as *incoherent* (see Fig. 21). Instead, in the recollision-based collider the electron and the positron stem from the same Ps atom with initial coordinates being confined within the range of the Bohr radius. Since they are driven coherently by the laser field, they can recollide with a mean impact parameter $b_c \sim a_{wp}$ of the order of the electron wave packet size a_{wp} (see Fig. 21). Consequently, the luminosity contains a *coherent* component (Hatsagortsyan *et al.*, 2006):

$$\mathcal{L} = \left[\frac{N_p(N_p - 1)}{b_i^2} + \frac{N_p}{b_c^2} \right] f, \quad (44)$$

where N_p is the number of particles in the bunch, and f is the bunch repetition frequency. The coherent component $(N_p/b_c^2)f$ can lead to a substantial luminosity enhancement in the case when the particle number is low and the particle's wave packet spreading is small, $N_p a_{wp}^2 < a_b^2$. We note that the reaction $\text{Ps} \rightarrow \mu^+\mu^-$ arising in a strongly laser-driven e^+e^- plasma may be considered as the coherent counterpart of the incoherent process $e^+e^- \rightarrow \mu^+\mu^-$ discussed in Par. IX.A.

Rigorous quantum-electrodynamical calculations for $\mu^+-\mu^-$ pair production in a laser field have been performed in Müller *et al.*, 2006, 2008b,c. In agreement with Eq. (44), they enabled the development of a simple-man's model in which the rate of the laser-driven process can be expressed via a convolution of the rescattering electron wave packet with the field-free cross section $\sigma_{e^+e^- \rightarrow \mu^+\mu^-}$ (see Eq. 34). The latter attains the maximal value $\sigma_{e^+e^- \rightarrow \mu^+\mu^-, M} \sim r_0^2/\varrho_\mu^2 \sim 10^{-30}$ cm² with $\varrho_\mu = m_\mu/m$, at the center-of-mass energy ε' of about 260 MeV (Peskin and Schroeder, 1995). However, when the field driving the Ps atoms is a single laser wave, the e^+e^- recollision times are long and the $\mu^+-\mu^-$ production process is substantially suppressed by extensive wave packet spreading. This obstacle can be overcome when two counterpropagating laser beams are applied.

The role of the spreading of the electron wave packet in counterpropagating focused laser beams of circular and linear polarization has been investigated in detail in Liu *et al.*, 2009. The advantage of the circular-polarization setup is the focusing of the recolliding electron wave

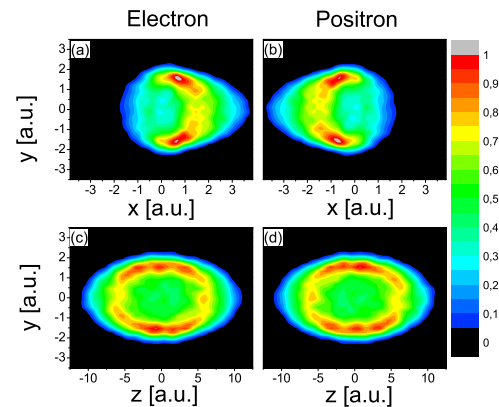


FIG. 22 (Color online) The coordinate-space distributions of the electron and the positron wave-packets at the recollision time in focused counterpropagating pulses along the z direction with $w_0 = 10 \mu\text{m}$, $\lambda_0 = 0.8 \mu\text{m}$ and with $I_0 = 4.7 \times 10^{22}$ W/cm² (parts (a) and (c)) and $I_0 = 1.4 \times 10^{23}$ W/cm² (parts (b) and (d)). The Ps atom is initially located at the origin. Spatial coordinates are given in “atomic units”, with 1 a.u. = 0.05 nm. Adapted from Liu *et al.*, 2009.

packet. However, this advantage is reduced by a spatial offset in the e^+e^- collision when the initial coordinate of the Ps atom deviates from the symmetric position between the laser pulses. The latter imposes a severe restriction on the Ps gas size along the laser propagation direction. Thus, the linear-polarization setup is preferable when the offset at the recollision is very small and the wave packet size at the recollision is within acceptable limits. Results of a Monte Carlo simulation of the e^+e^- wave-packet dynamics in counterpropagating linearly polarized laser pulses are shown in Fig. 22.

The luminosity \mathcal{L} and the number of reaction events \mathcal{N} for the recollision-based collider with counterpropagating laser pulses can be estimated as:

$$\mathcal{L} \sim N_{\text{Ps}} \frac{1}{a_{wp}^3} \tau_r f, \quad (45)$$

$$\mathcal{N} \sim \frac{\sigma_{e^+e^- \rightarrow \mu^+\mu^-}, M}{a_{wp}^3} \tau_r N_{\text{Ps}} N_L, \quad (46)$$

respectively, where N_{Ps} is the number of Ps atoms, τ_r the recollision time of the order of the lasers period, N_L the number of laser pulses, and f the laser repetition rate. By employing $N_{\text{Ps}} \approx 10^8$ (Cassidy and Mills, 2005), $f = 1$ Hz and the spatial extension of the e^+e^- from Fig. 22, one estimates a luminosity of $\mathcal{L} \sim 10^{27}$ cm⁻²s⁻¹ and about one $\mu^+-\mu^-$ pair production event every 10^3 laser shots at a laser intensity of 4.7×10^{22} W/cm².

In conclusion, the scheme of the recollision-based laser collider allows to realize high-energy and high-luminosity collisions in a microscopic setup. However, it is not easily scalable to the parameters of the ILC, namely, to TeV energies and luminosities of the order of 10^{34} cm⁻²s⁻¹.

XII. PARTICLE PHYSICS WITHIN AND BEYOND THE STANDARD MODEL

The sustained progress in laser technology towards higher and higher field intensities raises the question to what extent ultrastrong laser fields may develop into a useful tool for particle physics beyond QED. Below we review theoretical predictions regarding the influence of super-intense laser waves on electroweak processes and on their discovery potential for new physics beyond the Standard Model.

A. Electroweak sector of the Standard Model

The energy scale of weak interactions is set by the masses of the W^\pm and Z^0 exchange bosons, $m_W \approx m_Z \sim 100$ GeV. Therefore, the influence of external laser fields, even if strong on the scale of QED, is generally rather small. An overview of weak interaction processes in the presence of intense electromagnetic fields has been given in Kurilin, 1999.

Various weak decay processes in the presence of intense laser fields have been considered. They can be divided into two classes: 1) laser-assisted processes which also exist in the absence of the field but are modified due to its presence; 2) field-induced processes which can only proceed when a background field, providing an additional energy reservoir, is present. With respect to processes from the first category, $\pi \rightarrow \mu + \nu$ and $\mu^- \rightarrow e^- + \bar{\nu}_e + \nu_\mu$ have already been examined (Ritus, 1985). Laser-assisted muon decay has also been revisited recently (Dicus *et al.*, 2009; Farzinnia *et al.*, 2009; Narozhny and Fedotov, 2008). W^\pm and Z^0 boson decay into a fermion-antifermion pair was calculated in Kurilin, 2004, 2009. In all cases, the effect of the laser field was found to be small. As a general result, the presence of the laser field modifies the field-free decay rate R_0 to $R = R_0(1 + \Delta)$. The correction Δ is of the order of $\chi_{0,M}^2$ in the relevant range of parameters $\xi_{0,M} = \xi_0 m/M > 1$ and $\chi_{0,M} = \chi_0(m/M)^3 \ll 1$, where M denotes the mass of the decaying particle.

External fields can also render decay processes possible, which are energetically forbidden otherwise. In Kurilin, 1999, the field-induced lepton decay $\ell^- \rightarrow W^- + \nu_\ell$ was considered. Since the mass of the initial-state particle is smaller than the mass of the decay products, the process is clearly impossible in vacuum. The presence of the field does allow for such an exotic decay, but the probability P remains exponentially suppressed, $P \sim \exp(-1/\chi_{0,W})$, where $\chi_{0,W} = \chi_0(m/m_W)^3$.

Finally, the production of an e^+e^- pair by high-energy neutrino impact on a strong laser pulse has been calculated in Tinsley, 2005. The setup is similar to the e^+e^- pair production processes in QED discussed in Pars. VII.A and VII.B. However, as it was shown in

Tinsley, 2005, the laser-induced process $\nu \rightarrow \nu + e^+ + e^-$ is extremely unlikely. At a field intensity of about $I_0 = 3 \times 10^{18}$ W/cm², the production length is on the order of a light year, even for a neutrino energy of 1 PeV.

B. Particle physics beyond the Standard Model

In the last years a lot of attention has been devoted to the possibility of employing intense laser sources to test even aspects of physical theories which go beyond the Standard Model. In Heinzl *et al.*, 2010b, for example, it is envisaged that effects on the noncommutativity of space-time modify the kinematics of multiphoton Compton scattering by inducing a nonzero photon mass. On a different side, one of the still open problems of the Standard Model is the so-called strong CP problem (Kim and Carosi, 2010). The nontrivial structure of the vacuum as predicted by Quantum Chromodynamics (QCD) allows for the violation within QCD of the combined symmetry of charge conjugation (C) and parity (P). This implies a value for the neutron's electric dipole moment which, however, is already many orders of magnitude larger than experimental upper limits. One way of solving this problem was suggested in Peccei and Quinn, 1977 and entailed the existence of a massive pseudoscalar boson, called axion. The axion has never been observed experimentally although some of its properties can be predicted on theoretical grounds: it should be electrically neutral and its mass should not exceed 1 eV in order of magnitude. Although being electrically neutral, the axion is predicted to couple to the electromagnetic field $\mathcal{F}^{\mu\nu}(x)$ through a Lagrangian-density term

$$\mathcal{L}_{a\gamma}(x) = \frac{g}{4} a(x) \mathcal{F}^{\mu\nu}(x) \tilde{\mathcal{F}}_{\mu\nu}(x), \quad (47)$$

with g being the photon-axion coupling constant and with $a(x)$ being the axion field. This photon-axion Lagrangian density has mainly two implications: 1) the existence of axions induces a change in the polarization of a light beam passing through a background electromagnetic field; 2) a photon can transform into an axion (and viceversa) in the presence of a background electromagnetic field. The first prediction has been tested in experiments like the Brookhaven-Fermilab-Rochester-Trieste (BFRT) (Cameron *et al.*, 1993) and the Polarizzazione del Vuoto con LASer (PVLAS) (PVLAS, 2011), where a linearly polarized probe laser field crossed a region where a strong magnetic field was present (3.25 T at BFRT and 5 T at PVLAS). Testing the second prediction is the aim of the so-called ‘‘light shining through a wall’’ experiments like the Any Light Particle Search (ALPS) (ALPS, 2010), the CERN Axion Solar Telescope (CAST) (CAST, 2008) and Gamma to milli-eV particle search (GammeV) (GammeV, 2011) (see also the detailed theoretical analysis in Adler *et al.*, 2008). In the GammeV experiment,

for example, the light of a Nd:YAG laser passes through a region where a 5 T magnetic field is present. Behind that a mirror is put in order to reflect the laser light. The axions which are eventually created in the magnetic-field region pass through the mirror undisturbed and can be reconverted to photons by means of a second magnetic field activated after the mirror itself. These experiments have so far given negative results. An interesting experimental proposal has been put forward in Rabadán *et al.*, 2006, where the high-energy photon beam delivered by the XFEL facility has been suggested as a probe beam to test regions of parameters (like the axion mass m_a or the photon-axion coupling constant g) which are inaccessible via optical laser light.

The perspective of reaching ultrahigh intensities at future laser facilities has stimulated new proposals employing such fields to elicit the photon-axion interaction (Gies, 2009). In fact, an advantage of using strong uniform magnetic fields is that they can be kept strong for a macroscopic long time (of the order of hours) and on a macroscopic spatial region (of the order of 1 m). On the other hand laser beams deliver fields much stronger than those employed in the mentioned experiments (the magnetic field strength of a laser beam with available intensity of 10^{22} W/cm² amounts to about 8×10^5 T) but in a microscopic space-time region. However, it has been first realized in Mendonça, 2007 that envisaged ultrahigh intensities at future laser facilities may compensate for the tiny space-time extension of the laser spot region. In Mendonça, 2007 the coupled equations of the electromagnetic field $\mathcal{F}^{\mu\nu}(x)$ and of the axion field $a(x)$

$$\begin{cases} \partial_\mu \partial^\mu a + m_a^2 a = \frac{1}{4} g \mathcal{F}^{\mu\nu} \tilde{\mathcal{F}}_{\mu\nu} \\ \partial_\mu \mathcal{F}^{\mu\nu} = g (\partial_\mu a) \tilde{\mathcal{F}}^{\mu\nu} \end{cases} \quad (48)$$

are solved approximately. It is shown that if a probe laser field propagates through a strong plane-wave field, the axion field “grows” at the expense mainly of the probe field itself, which should be observed to lose intensity. Laser powers of the order of 1 PW have already been shown to provide larger effects of the presence of axions than magnetic-field-based experiments like the PVLAS. More realistic Gaussian laser beams are considered in Döbrich and Gies, 2010 where the starting point is also represented by Eq. (48). The suggested experimental setup assumes a probe electromagnetic beam with angular frequency $\omega_{p,\text{in}}$ passing through a strong counterpropagating Gaussian beam with angular frequency $\omega_{0,\parallel}$ and another strong Gaussian beam propagating perpendicularly and with angular frequency $\omega_{0,\perp}$. By choosing $\omega_{0,\perp} = 2\omega_{0,\parallel}$, it is found that after a photon-axion-photon double conversion, photons are generated with angular frequencies $\omega_{p,\text{out}} = \omega_{p,\text{in}} \pm \omega_{0,\parallel}$. The amplitudes of these processes are shown to be peaked at specific values of the axion mass $m_{a,\pm} =$

$2\sqrt{\omega_{p,\text{in}}\omega_{0,\parallel} + \omega_{0,\parallel}^2}(1 \pm 1)/2$. Since the values of optical photon energies are of the order of 1 eV, this setup allows for investigation of values of the axion mass in this regime. This is very important because such a region of the axion mass is inaccessible to experiments based on strong magnetic fields, which can probe regions at most in the meV range.

In addition to electrically neutral new particles such as axions, there might also be yet unobserved particles with nonzero charge. The fact that they have so far escaped from detection implies that they are either very heavy (rendering them a target for large-scale accelerator experiments), or that they are light but very weakly charged. In the latter case, these so-called minicharged particles are suitable candidates for laser-based searches (Gies, 2009). Let m_ϵ and $Q_\epsilon = \epsilon e$, with $\epsilon \ll 1$, denote the minicharged particle mass and charge, respectively. Then, the corresponding critical field scale $\sim m_\epsilon^2/|Q_\epsilon|$ can be much lower than that of QED. As a consequence, vacuum nonlinearities associated to minicharged particles may be very pronounced in an external laser field with intensity much less than $I_{\text{cr}} \sim 10^{29}$ W/cm². Even at rather moderate field strengths E_0 , the corresponding Heisenberg-Euler Lagrangian might therefore become inappropriate to describe the relevant physics since the parameter $Q_\epsilon E_0/m_\epsilon^2$ is not necessarily small. In Gies *et al.*, 2006, vacuum dichroism and birefringence effects due to the existence of minicharged particles were analyzed when a probe laser beam with $\omega_p > 2m_\epsilon$ traverses a magnetic field. It was shown that polarization measurements in this setup would provide much stronger constraints on minicharged particles in the mass range below 0.1 eV than in previous laboratory searches.

XIII. CONCLUSION AND OUTLOOK

The fast development of laser technology has been paving the way to employ laser sources for investigating relativistic, quantum electrodynamical, nuclear and high-energy processes. Starting with the lowest required intensities, relativistic atomic processes are already within the reach of available laser systems, while the proposed methods to compensate the deteriorating effects of the relativistic drift still have to be tested experimentally. Moreover, a fully consistent theoretical interpretation of recent experimental results on correlation effects in relativistic multielectron tunneling is still missing.

Concerning the interaction of free electrons with intense laser beams, we have seen that experiments have been performed in the classical regime. Only the E-144 experiment at SLAC has so far been realized on multiphoton Compton scattering, although presently available lasers and electron beams would allow for probing this regime in full detail. We have also pointed out that at laser intensities of the order of 10^{22} - 10^{23} W/cm², RR

effects come into play at electron energies of the order of a few GeV. We envisage that the quantum radiation dominated regime, where quantum and RR effects substantially alter the electron dynamics, could be one of the first extreme regimes of light-matter interaction to be probed with upcoming petawatt laser facilities. On the theoretical side most of the calculations have been performed by approximating the laser field as a plane wave, as the Dirac equation in the presence of a focused background field cannot be solved analytically. Certainly, new methods have to be developed to calculate photon spectra including quantum effects and spatio-temporal focusing of the laser field in order to be able to quantitatively interpret upcoming experimental results.

Nonlinear quantum electrodynamical effects have been shown to become observable at future multipetawatt laser facilities, as well as at ELI and at HiPER. Here the main challenges concern the measurability of tiny effects on the polarization of probe beams and on the detection of a typically very low number of signal photons out of large backgrounds. Similar challenges are envisaged to detect the presence of light and weakly-interacting hypothetical particles like axions and minicharged particles. The physical properties (mass, coupling constants etc.) of such hypothetical particles are of course unknown. In this respect intense laser fields may be employed here to set bounds on physical quantities like the axion mass and, in particular, to scan regions of physical parameters, which are inaccessible to conventional methods based, for example, on astrophysical observations.

Different schemes have been proposed to observe e^+e^- pair production at intensities below the Schwinger limit, which seems now to be feasible in the near future, at least from a theoretical point of view. Corresponding studies would complement the results of the pioneering E-144 experiment and deepen our understanding of the QED vacuum in the presence of extreme electromagnetic fields. This is also connected with the recent investigations on the development of QED cascades in laser-laser collisions. Among its intrinsic interest, the development of QED cascades is expected to set a limit on the maximal attainable laser intensity. However, the study of quantum cascades in intense laser fields has started relatively recently and it is still under vivid development. More advanced analytical and numerical methods are required in order to describe realistically and quantitatively such a complex system as an electron-positron-photon plasma in the presence of a strong driving laser field.

Nuclear quantum optics is also a new exciting and promising field. Since the energy difference among nuclear levels is usually in the multi-keV and MeV range, high-frequency laser pulses, especially in combination with accelerators, are preferable in controlling nuclear dynamics. As pointed out, especially table-top highly coherent x-ray light beams as envisaged for the future open up perspectives for exciting applications including

nuclear state preparation and nuclear batteries.

Finally, we want to point out that most of the considered processes have not yet been observed or tested experimentally. This is in our opinion one of the most challenging aspects of upcoming laser physics not only from an experimental point of view but also from the point of view of theoretical methods. Experimentally the main reason is that in order to test, for example, nonlinear quantum electrodynamics or to investigate nuclear quantum optics, high-energy particle beams (including photon beams) are required to be available in the same laboratory as the strong laser. On the one hand, the combined expertise from different experimental physical communities is required to perform such complex but fundamental experiments. On the other hand, the fast technological development of laser-plasma accelerators is very promising and exciting, as this seems the most feasible way towards the realization of stable, table-top high-energy particle accelerators. Combining such high-energy probe beams together with an ultrarelativistic laser beam in a single all-optical setup will certainly result in a unique tool for advancing our understanding of intense laser-matter interaction.

ACKNOWLEDGMENTS

We are grateful to many students, colleagues and collaborators for inspiring discussions, ideas, and suggestions, in particular in joint publications during the here most relevant last six years, to H. Bauke, T. J. Bürvenich, A. Dadi, C. Deneke, J. Evers, B. Galow, R. Grobe, Z. Harman, H. Hu, A. Ipp, U. D. Jentschura, B. King, M. Klaiber, M. Kohler, G. Yu. Kryuchkyan, W.-T. Liao, C. Liu, E. Lötstedt, A. Macchi, F. Mackenroth, S. Meuren, A. I. Milstein, G. Mocken, S. J. Müller, T.-O. Müller, A. Pálffy, F. Pegoraro, M. Ruf, Y. I. Salamin, M. Tamburini, M. Verschl and A. B. Voitkiv.

LIST OF FREQUENTLY-USED SYMBOLS

$B_{\text{cr}} = m^2/ e $	critical magnetic field ($\approx 4.4 \times 10^{13}$ G)
E_0	laser field amplitude
$E_{\text{cr}} = m^2/ e $	critical electric field ($\approx 1.3 \times 10^{16}$ V/cm)
I_0	laser peak intensity
$I_{\text{cr}} = E_{\text{cr}}^2/8\pi$	critical laser intensity ($\approx 2.3 \times 10^{29}$ W/cm ²)
Z	nuclear charge number
e	electron charge ($\approx -1/\sqrt{137} \approx -0.085$)
$k^\mu = (\omega, \mathbf{k})$	photon four-momentum
$k_0^\mu = \omega_0 n^\mu = \omega_0(1, \mathbf{n})$	laser photon four-momentum

m	electron mass (≈ 0.511 MeV)
$p_0^\mu = m\gamma_0(1, \beta_0)$	initial electron four-momentum
$r_0 = e^2/m$	classical electron radius ($\approx 2.8 \times 10^{-13}$ cm)
v_-	four-product $(nv) = n^\mu v_\mu$ for a generic four-vector v^μ
$\alpha = e^2$	fine-structure constant ($\approx 1/137 \approx 7.3 \times 10^{-3}$)
$\chi_0 = (p_{0,-}/m)(E_0/E_{cr})$	nonlinear electron quantum parameter
$\varkappa_0 = (k_{0,-}/m)(E_0/E_{cr})$	nonlinear photon quantum parameter
$\lambda_0 = T_0 = 2\pi/\omega_0$	laser wavelength and period
$\lambda_C = 1/m$	Compton wavelength ($\approx 3.9 \times 10^{-11}$ cm)
$\xi_0 = e E_0/m\omega_0$	classical relativistic parameter
ω_0	laser angular frequency

REFERENCES

- Aas, A., H. Mach, J. Kvasil, M. Borge, B. Fogelberg, I. Grant, K. Gulda, E. Hagebø, P. Hoff, W. Kurcewicz, A. Lindroth, G. Løvholden, *et al.*, 1999, Nucl. Phys. A **654**, 499.
- Abraham, M., 1905, *Theorie der Elektrizität* (Teubner, Leipzig).
- Adler, S. L., J. Gamboa, F. Méndez, and J. López-Sarrión, 2008, Ann. Phys. (N.Y.) **323**, 2851.
- Agostini, P., and L. F. Di Mauro, 2004, Rep. Prog. Phys. **67**, 813.
- Akhiezer, A. I., 1937, Phys. Z. Sowjetunion **11**, 263.
- Akhmedov, E. K., 1983, Sov. Phys. JETP **58**, 883.
- Aksenov, A. G., R. Ruffini, and G. V. Vereshchagin, 2007, Phys. Rev. Lett. **99**, 125003.
- Albert, F., S. G. Anderson, D. J. Gibson, C. A. Haggmann, M. S. Johnson, M. Messlerly, V. Semenov, M. Y. Shverdin, B. Rusnak, A. M. Tremaine, F. V. Hartemann, C. W. Siders, *et al.*, 2010, Phys. Rev. ST Accel. Beams **13**, 070704.
- Alkofer, R., M. B. Hecht, C. D. Roberts, S. M. Schmidt, and D. V. Vinnik, 2001, Phys. Rev. Lett. **87**, 193902.
- ALPS (Any Light Particle Search), 2010, URL <http://alps.desy.de/>.
- Ammosov, M. V., N. B. Delone, and V. P. Krainov, 1986, Sov. Phys. JETP **64**, 1191.
- Apostol, M., 2011, J. Mod. Opt. **58**, 611.
- Aprahamian, A., and Y. Sun, 2005, Nature Phys. **1**, 81.
- Astra Gemini, 2011, URL <http://www.clf.rl.ac.uk/Science/12258.aspx>.
- Avetissian, H. K., A. K. Avetissian, G. F. Mkrtchian, and K. V. Sedrakian, 2003, Nucl. Instr. Meth. Phys. Res. A **507**, 582.
- Babzien, M., I. Ben-Zvi, K. Kusche, I. V. Pavlishin, I. V. Pogorelsky, D. P. Siddons, V. Yakimenko, D. Cline, F. Zhou, T. Hirose, Y. Kamiya, T. Kumita, *et al.*, 2006, Phys. Rev. Lett. **96**, 054802.
- Badziak, J., 2007, Opto-Electron. Rev. **15**, 1.
- Baier, V. N., V. M. Katkov, A. I. Milstein, and V. M. Strakhovenko, 1976a, Sov. Phys. JETP **42**, 400.
- Baier, V. N., V. M. Katkov, and V. M. Strakhovenko, 1994, *Electromagnetic Processes at High Energies in Oriented Single Crystals* (World Scientific, Singapore).
- Baier, V. N., A. I. Milstein, and V. M. Strakhovenko, 1976b, Sov. Phys. JETP **42**, 961.
- Bamber, C., S. J. Boege, T. Koffas, T. Kotseroglou, A. C. Melissinos, D. D. Meyerhofer, D. A. Reis, W. Ragg, C. Bula, K. T. McDonald, E. J. Prebys, D. L. Burke, *et al.*, 1999, Phys. Rev. D **60**, 092004.
- Bauke, H., H. G. Hetzheim, G. R. Mocken, M. Ruf, and C. H. Keitel, 2011, Phys. Rev. A **83**, 063414.
- Baur, G., K. Hencken, and D. Trautmann, 2007, Phys. Rep. **453**, 1.
- Beck, B. R., J. A. Becker, P. Beiersdorfer, G. V. Brown, K. J. Moody, J. B. Wilhelmy, F. S. Porter, C. A. Kilbourne, and R. L. Kelley, 2007, Phys. Rev. Lett. **98**, 142501.
- Becker, W., F. Grasbon, R. Kopold, D. Milosevic, G. Paulus, and H. Walther, 2002, Adv. Atom. Mol. Opt. Phys. **48**, 35.
- Becker, W., R. R. Schlicher, and M. O. Scully, 1984, Nucl. Phys. A **426**, 125.
- Bell, A. R., and J. G. Kirk, 2008, Phys. Rev. Lett. **101**, 200403.
- Benedetti, A., W.-B. Han, R. Ruffini, and G. Vereshchagin, 2011, Phys. Lett. B **698**, 75.
- Berestetskii, V., E. M. Lifshitz, and L. P. Pitaevskii, 1982, *Quantum electrodynamics* (Elsevier Butterworth-Heinemann, Oxford).
- Bergmann, K., H. Theuer, and B. W. Shore, 1998, Rev. Mod. Phys. **70**, 1003.
- Bhattacharyya, S., M. Mazumder, J. Chakrabarti, and F. H. M. Faisal, 2011, Phys. Rev. A **83**, 043407.
- Boca, M., and V. Florescu, 2009, Phys. Rev. A **80**, 053403.
- Boca, M., and V. Florescu, 2010, Rom. J. Phys. **55**, 511.
- Boca, M., and V. Florescu, 2011, Eur. Phys. J. D **61**, 449.
- Boca, M., and A. Oprea, 2011, Phys. Scr. **83**, 055404.
- Bonifacio, R., C. Pellegrini, and L. Narducci, 1984, Opt. Commun. **50**, 373.
- Breit, G., and J. A. Wheeler, 1934, Phys. Rev. **46**, 1087.
- Brezin, E., and C. Itzykson, 1970, Phys. Rev. D **2**, 1191.
- Brown, L. S., and T. W. B. Kibble, 1964, Phys. Rev. **133**, A705.
- Bu, Z., and P. Ji, 2010, Phys. Plasmas **17**, 073103.
- Bula, C., K. T. McDonald, E. J. Prebys, C. Bamber, S. Boege, T. Kotseroglou, A. C. Melissinos, D. D. Meyerhofer, W. Ragg, D. L. Burke, R. C. Field, G. Horton-Smith, *et al.*, 1996, Phys. Rev. Lett. **76**, 3116.
- Bulanov, S. S., V. D. Mur, N. B. Narozhny, J. Nees, and V. S. Popov, 2010a, Phys. Rev. Lett. **104**, 220404.
- Bulanov, S. S., T. Zh. Esirkepov, A. G. R. Thomas, J. K. Koga, and S. V. Bulanov, 2010b, Phys. Rev. Lett. **105**, 220407.
- Bulanov, S. V., N. M. Naumova, and F. Pegoraro, 1994, Phys. Plasmas **1**, 745.
- Bulanov, S. V., T. Zh. Esirkepov, M. Kando, J. K. Koga, and S. S. Bulanov, 2011, Phys. Rev. E (in press) eprint arXiv:1103/0613.
- Burke, D. L., R. C. Field, G. Horton-Smith, J. E. Spencer, D. Walz, S. C. Berridge, W. M. Bugg, K. Shmakov, A. W. Weidemann, C. Bula, K. T. McDonald, E. J. Prebys, *et al.*,

- 1997, Phys. Rev. Lett. **79**, 1626.
- Burton, D., J. Gratus, and R. Tucker, 2007, Ann. Phys. (N.Y.) **322**, 599.
- Bürvenich, T. J., J. Evers, and C. H. Keitel, 2006a, Phys. Rev. Lett. **96**, 142501.
- Bürvenich, T. J., J. Evers, and C. H. Keitel, 2006b, Phys. Rev. C **74**, 044601.
- Bychenkov, V., Y. Sentoku, S. Bulanov, K. Mima, G. Mourou, and S. Tolokonnikov, 2001, JETP Letters **74**, 586.
- Caldwell, A., K. Lotov, A. Pukhov, and F. Simon, 2009, Nature Phys. **5**, 563.
- Cameron, R., G. Cantatore, A. C. Melissinos, G. Ruoso, Y. Semertzidis, H. J. Halama, D. M. Lazarus, A. G. Prodell, F. Nezzrick, C. Rizzo, and E. Zavattini, 1993, Phys. Rev. D **47**, 3707.
- Cassidy, D. B., S. H. M. Deng, R. G. Greaves, T. Maruo, N. Nishiyama, J. B. Snyder, H. K. M. Tanaka, and A. P. Mills, 2005, Phys. Rev. Lett. **95**, 195006.
- Cassidy, D. B., and A. P. Mills, 2005, Nature (London) **449**, 195.
- CAST (CERN Axion Solar Telescope), 2008, URL <http://cast.web.cern.ch/CAST/>.
- Castañeda Cortés, H. M., A. Pálffy, and C. H. Keitel, 2012, to be published.
- Castañeda Cortés, H. M., S. V. Popruzhenko, D. Bauer, and A. Pálffy, 2011, New J. Phys. **13**, 063007.
- Chambaret, J. P., P. Georges, G. Chériaux, G. Rey, C. L. Blanc, P. Audebert, D. Douillet, J. L. Paillard, P. Cavillac, D. Fournet, F. Mathieu, and G. Mourou, 2009, in *Frontiers in Optics*, p. FMI2.
- Chelkowski, S., A. D. Bandrauk, and P. B. Corkum, 2004, Phys. Rev. Lett. **93**, 083602.
- Chen, H., S. C. Wilks, J. D. Bonlie, E. P. Liang, J. Myatt, D. F. Price, D. D. Meyerhofer, and P. Beiersdorfer, 2009, Phys. Rev. Lett. **102**, 105001.
- Chen, M., A. Pukhov, T.-P. Yu, and Z.-M. Sheng, 2011, Plasma Phys. Control. Fusion **53**, 014004.
- Chen, M.-C., P. Arpin, T. Popmintchev, M. Gerrity, B. Zhang, M. Seaberg, D. Popmintchev, M. M. Murnane, and H. C. Kapteyn, 2010, Phys. Rev. Lett. **105**, 173901.
- Chen, S.-Y., A. Maksimchuk, and D. Umstadter, 1998, Nature (London) **396**, 653.
- Cheng, T., S. P. Bowen, C. C. Gerry, Q. Su, and R. Grobe, 2008, Phys. Rev. A **77**, 032106.
- Cheng, T., Q. Su, and R. Grobe, 2009a, Phys. Rev. A **80**, 013410.
- Cheng, T., Q. Su, and R. Grobe, 2010, Contemp. Phys. **51**, 315.
- Cheng, T., M. R. Ware, Q. Su, and R. Grobe, 2009b, Phys. Rev. A **80**, 062105.
- Chirilă, C. C., C. J. Joachain, N. J. Kylstra, and R. M. Potvliege, 2004, Phys. Rev. Lett. **93**, 243603.
- Chirilă, C. C., N. J. Kylstra, R. M. Potvliege, and C. J. Joachain, 2002, Phys. Rev. A **66**, 063411.
- Chouffani, K., D. Wells, F. Harmon, J. Jones, and G. Lancaster, 2002, Nucl. Instr. Meth. Phys. Res. A **495**, 95.
- Chowdhury, E. A., C. P. J. Barty, and B. C. Walker, 2001, Phys. Rev. A **63**, 042712.
- Cipiccia, S., M. R. Islam, B. Ersfeld, R. P. Shanks, E. Brunetti, G. Vieux, X. Yang, R. C. Issac, S. M. Wiggins, G. H. Welsh, M.-P. Anania, D. Maneuski, *et al.*, 2011, Nature Phys. **7**, 867.
- Combs, S. E., A. Nikoghosyan, O. Jaekel, C. P. Karger, T. Haberer, M. W. Münter, P. E. Huber, J. Debus, and D. Schulz-Ertner, 2009, Cancer **115**, 1348.
- Corkum, P. B., 1993, Phys. Rev. Lett. **71**, 1994.
- Dadi, A., and C. Müller, 2011, Phys. Lett. B **697**, 142.
- Dammasch, M., M. Dörr, U. Eichmann, E. Lenz, and W. Sandner, 2001, Phys. Rev. A **64**, 061402.
- Debus, A., M. Bussmann, M. Siebold, A. Jochmann, U. Schramm, T. Cowan, and R. Sauerbrey, 2010, Appl. Phys. B **100**, 61.
- Deneke, C., and C. Müller, 2008, Phys. Rev. A **78**, 033431.
- Di Piazza, A., 2008, Lett. Math. Phys. **83**, 305.
- Di Piazza, A., K. Hatsagortsyan, and C. Keitel, 2007a, Phys. Plasmas **14**, 032102.
- Di Piazza, A., K. Z. Hatsagortsyan, and C. H. Keitel, 2006, Phys. Rev. Lett. **97**, 083603.
- Di Piazza, A., K. Z. Hatsagortsyan, and C. H. Keitel, 2008a, Phys. Rev. Lett. **100**, 010403.
- Di Piazza, A., K. Z. Hatsagortsyan, and C. H. Keitel, 2008b, Phys. Rev. A **78**, 062109.
- Di Piazza, A., K. Z. Hatsagortsyan, and C. H. Keitel, 2009a, Phys. Rev. Lett. **102**, 254802.
- Di Piazza, A., K. Z. Hatsagortsyan, and C. H. Keitel, 2010a, Phys. Rev. Lett. **105**, 220403.
- Di Piazza, A., E. Lötstedt, A. I. Milstein, and C. H. Keitel, 2009b, Phys. Rev. Lett. **103**, 170403.
- Di Piazza, A., E. Lötstedt, A. I. Milstein, and C. H. Keitel, 2010b, Phys. Rev. A **81**, 062122.
- Di Piazza, A., and A. I. Milstein, 2008, Phys. Rev. A **77**, 042102.
- Di Piazza, A., A. I. Milstein, and C. H. Keitel, 2007b, Phys. Rev. A **76**, 032103.
- Di Piazza, A., A. I. Milstein, and C. Müller, 2010c, Phys. Rev. A **82**, 062110.
- DiChiara, A. D., I. Ghebregziabher, R. Sauer, J. Waesche, S. Palaniyappan, B. L. Wen, and B. C. Walker, 2008, Phys. Rev. Lett. **101**, 173002.
- DiChiara, A. D., I. Ghebregziabher, J. M. Waesche, T. Stanev, N. Ekanayake, L. R. Barclay, S. J. Wells, A. Watts, M. Videtto, C. A. Mancuso, and B. C. Walker, 2010, Phys. Rev. A **81**, 043417.
- Dicus, D. A., A. Farzinnia, W. W. Repko, and T. M. Tinsley, 2009, Phys. Rev. D **79**, 013004.
- Dimitrovski, D., M. Førre, and L. B. Madsen, 2009, Phys. Rev. A **80**, 053412.
- Dirac, P. A. M., 1928, Proc. R. Soc. London, Ser. A **117**, 610.
- Dirac, P. A. M., 1938, Proc. R. Soc. London, Ser. A **167**, 148.
- Dittrich, W., and H. Gies, 2000, *Probing the Quantum Vacuum* (Springer, Heidelberg).
- Dittrich, W., and M. Reuter, 1985, *Effective Lagrangians in Quantum Electrodynamics* (Springer, Heidelberg).
- Döbrich, B., and H. Gies, 2010, J. High Energy Phys. **10**, 022.
- Dromey, B., M. Zepf, A. Gopal, K. Lancaster, M. S. Wei, K. Krushelnick, M. Tatarakis, N. Vakakis, S. Moustazis, R. Kodama, M. Tampo, C. Stoeckl, *et al.*, 2006, Nature Phys. **2**, 456.
- Duclous, R., J. G. Kirk, and A. R. Bell, 2011, Plasma Phys. Control. Fusion **53**, 015009.
- Dumlu, C. K., 2010, Phys. Rev. D **82**, 045007.
- Dumlu, C. K., and G. V. Dunne, 2010, Phys. Rev. Lett. **104**, 250402.
- Dumlu, C. K., and G. V. Dunne, 2011, Phys. Rev. D **83**, 065028.
- Dunne, G. V., H. Gies, and R. Schützhold, 2009, Phys. Rev. D **80**, 111301(R).
- Ehlotzky, F., K. Krajewska, and J. Z. Kaminski, 2009, Rep.

- Progr. Phys. **72**, 046401.
- ELI (Extreme Light Infrastructure), 2011, URL <http://www.extreme-light-infrastructure.eu/>.
- Elkina, N. V., A. M. Fedotov, I. Yu. Kostyukov, M. V. Legkov, N. B. Narozhny, E. N. Nerush, and H. Ruhl, 2011, Phys. Rev. ST Accel. Beams **14**, 054401.
- Ellis, J., and I. Wilson, 2001, Nature (London) **409**, 431.
- Englert, T. J., and E. A. Rinehart, 1983, Phys. Rev. A **28**, 1539.
- Esarey, E., C. B. Schroeder, and W. P. Leemans, 2009, Rev. Mod. Phys. **81**, 1229.
- Esirkepov, T., M. Borghesi, S. V. Bulanov, G. Mourou, and T. Tajima, 2004, Phys. Rev. Lett. **92**, 175003.
- Euler, H., 1936, Ann. Phys. (Leipzig) **26**, 398.
- European XFEL, 2011, URL <http://xfel.eu/>.
- Evers, J., and C. H. Keitel, 2002, Phys. Rev. Lett. **89**, 163601.
- Faisal, F. H. M., 1973, J. Phys. B **6**, L89.
- Farzinnia, A., D. A. Dicus, W. W. Repko, and T. M. Tinsley, 2009, Phys. Rev. D **80**, 073004.
- Faure, J., Y. Glinec, A. Pukhov, S. Kiselev, S. Gordienko, E. Lefebvre, J.-P. Rousseau, F. Burgy, and V. Malka, 2004, Nature (London) **431**, 541.
- Feder, T., 2010, Phys. Today **63**, 20.
- Fedorov, M. V., M. A. Efremova, and P. A. Volkov, 2006, Opt. Commun. **264**, 413.
- Fedotov, A. M., N. B. Narozhny, G. Mourou, and G. Korn, 2010, Phys. Rev. Lett. **105**, 080402.
- Feldhaus, J., E. L. Saldin, J. R. Schneider, E. A. Schneidmiller, and M. V. Yurkov, 1997, Opt. Commun. **140**, 341.
- Fennel, Th., K.-H. Meiwes-Broer, J. Tiggesbäumker, P.-G. Reinhard, P. M. Dinh, and E. Suraud, 2010, Rev. Mod. Phys. **82**, 1793.
- Ferrando, A., H. Michinel, M. Seco, and D. Tommasini, 2007, Phys. Rev. Lett. **99**, 150404.
- Ferris, M. R., and J. Gratus, 2011, J. Math. Phys. **52**, 092902.
- Fillion-Gourdeau, F., E. Lorin, and A. D. Bandrauk, 2011, eprint arXiv:1107.4650v1.
- Fischer, R., M. Lein, and C. H. Keitel, 2006, Phys. Rev. Lett. **97**, 143901.
- Fischer, R., M. Lein, and C. H. Keitel, 2007, J. Phys. B **40**, F113.
- FLASH (Free-Electron Laser in Hamburg), 2011, URL http://hasylab.desy.de/facilities/flash/index_eng.html.
- Førre, M., J. P. Hansen, L. Kocbach, S. Selstø, and L. B. Madsen, 2006, Phys. Rev. Lett. **97**, 043601.
- Førre, M., S. Selstø, J. P. Hansen, T. K. Kjeldsen, and L. B. Madsen, 2007, Phys. Rev. A **76**, 033415.
- Fuchs, J., P. Antici, E. d'Humières, E. Lefebvre, M. Borghesi, E. Brambrink, C. A. Cecchetti, M. Kaluza, V. Malka, M. Manclossi, S. Meyroneinc, P. Mora, *et al.*, 2006, Nature Phys. **2**, 48.
- Fuchs, J., C. A. Cecchetti, M. Borghesi, T. Grismayer, E. d'Humières, P. Antici, S. Atzeni, P. Mora, A. Pipahl, L. Romagnani, A. Schiavi, Y. Sentoku, *et al.*, 2007, Phys. Rev. Lett. **99**, 015002.
- Furry, W. H., 1951, Phys. Rev. **81**, 115.
- Galley, C. R., A. K. Leibovich, and I. Z. Rothstein, 2010, Phys. Rev. Lett. **105**, 094802.
- Galow, B. J., Z. Harman, and C. H. Keitel, 2010, Opt. Express **18**, 25950.
- Galow, B. J., Y. I. Salamin, T. V. Liseykina, Z. Harman, and C. H. Keitel, 2011, Phys. Rev. Lett. **107**, 185002.
- GammeV (Gamma to milli-eV particle search), 2011, URL <http://gammev.fnal.gov/>.
- Gavrilov, S. P., and D. M. Gitman, 2008, Phys. Rev. Lett. **101**, 130403.
- Geddes, C. G. R., C. Toth, J. van Tilborg, E. Esarey, C. B. Schroeder, D. Bruhwiler, C. Nieter, J. Cary, and W. P. Leemans, 2004, Nature (London) **431**, 538.
- Gerstner, E., 2007, Nature (London) **446**, 17.
- Gibson, D. J., F. Albert, S. G. Anderson, S. M. Betts, M. J. Messerly, H. H. Phan, V. A. Semenov, M. Y. Shverdin, A. M. Tremaine, F. V. Hartemann, C. W. Siders, D. P. McNabb, *et al.*, 2010, Phys. Rev. ST Accel. Beams **13**, 070703.
- Gibson, D. J., S. G. Anderson, C. P. J. Barty, S. M. Betts, R. Booth, W. J. Brown, J. K. Crane, R. R. Cross, D. N. Fittinghoff, F. V. Hartemann, J. Kuba, G. P. L. Sage, *et al.*, 2004, Phys. Plasmas **11**, 2857.
- Gies, H., 2009, Eur. Phys. J. D **55**, 311.
- Gies, H., J. Jaeckel, and A. Ringwald, 2006, Phys. Rev. Lett. **97**, 140402.
- Goldman, I., 1964, Sov. Phys. JETP **46**, 1412.
- Goulielmakis, E., M. Schultze, M. Hofstetter, V. S. Yakovlev, J. Gagnon, M. Uiberacker, A. L. Aquila, E. M. Gullikson, D. T. Attwood, R. Kienberger, F. Krausz, and U. Kleineberg, 2008, Science **320**, 1614.
- Gralla, S. E., A. I. Harte, and R. M. Wald, 2009, Phys. Rev. D **80**, 024031.
- Grüner, F., S. Becker, U. Schramm, T. Eichner, M. Fuchs, R. Weingartner, D. Habs, J. Meyer-ter Vehn, M. Geissler, M. Ferrario, L. Serafini, B. van der Geer, *et al.*, 2007, Appl. Phys. B **86**, 431.
- Gubbini, E., U. Eichmann, M. Kalashnikov, and W. Sandner, 2005, Phys. Rev. Lett. **94**, 053602.
- Habs, D., M. Hegelich, J. Schreiber, M. Gross, A. Henig, D. Kiefer, and D. Jung, 2008, Appl. Phys. B **93**, 349.
- Habs, D., T. Tajima, J. Schreiber, C. P. Barty, M. Fujiwara, and P. G. Thirolf, 2009, Eur. Phys. J. D **55**, 279.
- Hadad, Y., L. Labun, J. Rafelski, N. Elkina, C. Klier, and H. Ruhl, 2010, Phys. Rev. D **82**, 096012.
- Hammond, R. T., 2010, Electron. J. Theor. Phys. **7**, 221.
- Han, W.-B., R. Ruffini, and S.-S. Xue, 2010, Phys. Lett. B **691**, 99.
- Hartemann, F. V., 2001, *High-Field Electrodynamics* (CRC Press, Boca Raton).
- Hartemann, F. V., D. J. Gibson, W. J. Brown, A. Rousse, K. T. Phuoc, V. Malka, J. Faure, and A. Pukhov, 2007, Phys. Rev. ST Accel. Beams **10**, 011301.
- Hartemann, F. V., and A. K. Kerman, 1996, Phys. Rev. Lett. **76**, 624.
- Hartemann, F. V., C. W. Siders, and C. P. J. Barty, 2008, Phys. Rev. Lett. **100**, 125001.
- Harvey, C., T. Heinzl, N. Iji, and K. Langfeld, 2011a, Phys. Rev. D **83**, 076013.
- Harvey, C., T. Heinzl, and A. Ilderton, 2009, Phys. Rev. A **79**, 063407.
- Harvey, C., T. Heinzl, and M. Marklund, 2011b, eprint arXiv:1110.0628.
- Harvey, C., and M. Marklund, 2011, eprint arXiv:1110.0996.
- Hatsagortsyan, K. Z., M. Klaiber, C. Müller, M. C. Kohler, and C. H. Keitel, 2008, J. Opt. Soc. Am. B **25**, B92.
- Hatsagortsyan, K. Z., C. Müller, and C. H. Keitel, 2006, Europhys. Lett. **76**, 29.
- Hebenstreit, F., R. Alkofer, G. V. Dunne, and H. Gies, 2009, Phys. Rev. Lett. **102**, 150404.
- Hebenstreit, F., R. Alkofer, and H. Gies, 2011, Phys. Rev.

- Lett. **107**, 180403.
- Hegelich, B. M., B. J. Albright, J. Cobble, K. Flippo, S. Letzring, M. Paffett, H. Ruhl, J. Schreiber, R. K. Schulze, and J. C. Fernández, 2006, *Nature (London)* **439**, 441.
- Hein, J., M. Hornung, R. Bödefeld, S. Podleska, A. Sävert, R. Wachs, A. Kessler, S. Keppler, M. Wolf, J. Polz, O. Jäckel, M. Nicolai, *et al.*, 2010, *AIP Conf. Proc.* **1228**, 159.
- Heinzl, T., and A. Ilderton, 2009, *Opt. Commun.* **282**, 1879.
- Heinzl, T., A. Ilderton, and M. Marklund, 2010a, *Phys. Lett. B* **692**, 250.
- Heinzl, T., A. Ilderton, and M. Marklund, 2010b, *Phys. Rev. D* **81**, 051902(R).
- Heinzl, T., B. Liesfeld, K.-U. Amthor, H. Schwöerer, R. Sauerbrey, and A. Wipf, 2006, *Opt. Commun.* **267**, 318.
- Heinzl, T., D. Seipt, and B. Kämpfer, 2010c, *Phys. Rev. A* **81**, 022125.
- Heisenberg, W., and H. Euler, 1936, *Z. Phys.* **98**, 714.
- Heitler, W., 1984, *The Quantum Theory of Radiation* (Dover Publications, New York).
- Henrich, B., K. Z. Hatsagortsyan, and C. H. Keitel, 2004, *Phys. Rev. Lett.* **93**, 013601.
- Hetzheim, H. G., and C. H. Keitel, 2009, *Phys. Rev. Lett.* **102**, 083003.
- HiPER (High Power laser Energy Research), 2011, URL <http://www.hiper-laser.org/>.
- Homma, K., D. Habs, and T. Tajima, 2011, *Appl. Phys. B* **104**, 769.
- Hu, H., and C. Müller, 2011, *Phys. Rev. Lett.* **107**, 090402.
- Hu, H., C. Müller, and C. H. Keitel, 2010, *Phys. Rev. Lett.* **105**, 080401.
- Hu, S. X., and C. H. Keitel, 1999, *Phys. Rev. Lett.* **83**, 4709.
- Hu, S. X., and C. H. Keitel, 2001, *Phys. Rev. A* **63**, 053402.
- ILC (International Linear Collider), 2011, URL <http://www.linearcollider.org/>.
- Ilderton, A., 2011, *Phys. Rev. Lett.* **106**, 020404.
- Ipp, A., J. Evers, C. H. Keitel, and K. Z. Hatsagortsyan, 2011, *Phys. Lett. B* **702**, 383.
- Ivanov, D. Y., G. L. Kotkin, and V. G. Serbo, 2005, *Eur. Phys. J. C* **40**, 27.
- Ivanov, D. Yu., G. L. Kotkin, and V. G. Serbo, 2004, *Eur. Phys. J. C* **36**, 127.
- Jackson, J. D., 1975, *Classical Electrodynamics* (Wiley, New York).
- Jauch, J. M., and F. Rohrlich, 1976, *The Theory of Photons and Electrons* (Springer, Berlin).
- Kamiński, J. Z., K. Krajewska, and F. Ehlötzky, 2006, *Phys. Rev. A* **74**, 033402.
- Karagodsky, V., D. Schieber, and L. Schächter, 2010, *Phys. Rev. Lett.* **104**, 024801.
- Karplus, R., and M. Neuman, 1950, *Phys. Rev.* **80**, 380.
- Keitel, C. H., 2001, *Contemp. Phys.* **42**, 353.
- Keitel, C. H., and S. X. Hu, 2002, *Appl. Phys. Lett.* **80**, 541.
- Keitel, C. H., P. L. Knight, and K. Burnett, 1993, *Europhys. Lett.* **24**, 539.
- Keitel, C. H., C. Szymanowski, P. L. Knight, and A. Maquet, 1998, *J. Phys. B* **31**, L75.
- Keldysh, L. V., 1965, *Sov. Phys. JETP* **20**, 1307.
- Kiffner, M., M. Macovei, J. Evers, and C. Keitel, 2010, *Prog. Opt.* **55**, 85.
- Kim, D., H. Lee, S. Chung, and K. Lee, 2009, *New J. Phys.* **11**, 063050.
- Kim, J. E., and G. Carosi, 2010, *Rev. Mod. Phys.* **82**, 557.
- Kim, K.-J., Yu. V. Shvyd'ko, and S. Reiche, 2008, *Phys. Rev. Lett.* **100**, 244802.
- King, B., A. Di Piazza, and C. H. Keitel, 2010a, *Nature Photon.* **4**, 92.
- King, B., A. Di Piazza, and C. H. Keitel, 2010b, *Phys. Rev. A* **82**, 032114.
- Kirk, J. G., A. R. Bell, and I. Arka, 2009, *Plasma Phys. Control. Fusion* **51**, 085008.
- Kirsebom, K., U. Mikkelsen, E. Uggerhøj, K. Elsener, S. Ballestrero, P. Sona, and Z. Z. Vilakazi, 2001, *Phys. Rev. Lett.* **87**, 054801.
- Klaiber, M., K. Z. Hatsagortsyan, and C. H. Keitel, 2006, *Phys. Rev. A* **74**, 051803.
- Klaiber, M., K. Z. Hatsagortsyan, and C. H. Keitel, 2007, *Phys. Rev. A* **75**, 063413.
- Klaiber, M., K. Z. Hatsagortsyan, C. Müller, and C. H. Keitel, 2008, *Opt. Lett.* **33**, 411.
- Kneip, S., C. McGuffey, J. L. Martins, S. F. Martins, C. Bellei, V. Chvykov, F. Dollar, R. Fonseca, C. Huntington, G. Kalintchenko, A. Maksimchuk, S. P. D. Mangles, *et al.*, 2010, *Nature Phys.* **6**, 980.
- Koga, J., T. Zh. Esirkepov, and S. V. Bulanov, 2005, *Phys. Plasmas* **12**, 093106.
- Kohler, M. C., M. Klaiber, K. Z. Hatsagortsyan, and C. H. Keitel, 2011, *Europhys. Lett.* **94**, 14002.
- Kornev, A. S., E. B. Tulenko, and B. A. Zon, 2009, *Phys. Rev. A* **79**, 063405.
- Kornev, A. S., and B. A. Zon, 2007, *Laser Phys. Lett.* **4**, 588.
- Korzhimanov, A. V., A. A. Gonoskov, E. A. Khazanov, and A. M. Sergeev, 2011, *Phys. Usp.* **54**, 9.
- Krajewska, K., and J. Z. Kamiński, 2008, *Laser Phys.* **18**, 185.
- Krajewska, K., and J. Z. Kamiński, 2010, *Phys. Rev. A* **82**, 013420.
- Krajewska, K., and J. Z. Kamiński, 2011, *Phys. Rev. A* **84**, 033416.
- Krajewska, K., J. Z. Kamiński, and F. Ehlötzky, 2006, *Laser Phys.* **16**, 272.
- Krausz, F., and M. Yu. Ivanov, 2009, *Rev. Mod. Phys.* **81**, 163.
- Krekora, P., Q. Su, and R. Grobe, 2004, *Phys. Rev. Lett.* **92**, 040406.
- Krekora, P., Q. Su, and R. Grobe, 2005, *J. Mod. Opt.* **52**, 489.
- Krivitskii, V. S., and V. N. Tsytovich, 1991, *Sov. Phys. Usp.* **34**, 250.
- Kryuchyan, G. Yu., and K. Z. Hatsagortsyan, 2011, *Phys. Rev. Lett.* **107**, 053604.
- Kuchiev, M. Yu., 1987, *JETP Lett.* **45**, 404.
- Kuchiev, M. Yu., 2007, *Phys. Rev. Lett.* **99**, 130404.
- Kuchiev, M. Yu., and D. J. Robinson, 2007, *Phys. Rev. A* **76**, 012107.
- Kulander, K. C., K. J. Schafer, and J. L. Krause, 1993, in *Super-Intense Laser-Atom Physics*, edited by B. Piraux, A.L'Huillier, and K.Rzazewski (Plenum), p. 95.
- Kurilin, A. V., 1999, *Nuovo Cim.* **112**, 977.
- Kurilin, A. V., 2004, *Phys. Atom. Nucl.* **67**, 2095.
- Kurilin, A. V., 2009, *Phys. Atom. Nucl.* **72**, 1034.
- Kuznetsova, I., D. Habs, and J. Rafelski, 2008, *Phys. Rev. D* **78**, 014027.
- Kylstra, N. J., R. A. Worthington, A. Patel, P. L. Knight, J. R. Vázquez de Aldana, and L. Roso, 2000, *Phys. Rev. Lett.* **85**, 1835.
- Labun, L., and J. Rafelski, 2009, *Phys. Rev. D* **79**, 057901.
- Landau, L. D., and E. M. Lifshitz, 1975, *The Classical Theory*

- of *Fields* (Elsevier, Oxford).
- Lawson, J. D., 1979, IEEE Trans. Nucl. Sci. **NS-26**, 4217.
- LCLS (Linac Coherent Laser Source), 2011, URL https://slacportal.slac.stanford.edu/sites/lcls_public/Pages/Default.aspx.
- LCLS II (Linac Coherent Light Source II), 2011, URL https://slacportal.slac.stanford.edu/sites/lcls_public/lcls_ii.
- Ledingham, K. W. D., and W. Galster, 2010, New J. Phys. **12**, 045005.
- Ledingham, K. W. D., P. McKenna, and R. P. Singhal, 2003, Science **300**, 1107.
- Lee, R. N., A. L. Maslennikov, A. I. Milstein, V. Strakhovenko, and Yu. A. Tikhonov, 2003, Phys. Rep. **373**, 213.
- Leemans, W., and E. Esarey, 2009, Phys. Today **62**, 44.
- Leemans, W. P., B. Nagler, A. J. Gonsalves, C. Tóth, C. G. R. G. K. Nakamura and, E. Esarey, C. B. Schroeder, and S. M. Hooker, 2006, Nature Phys. **2**, 696.
- Leemans, W. P., R. W. Schoenlein, P. Volfbeyn, A. H. Chin, T. E. Glover, P. Balling, M. Zolotarev, K. J. Kim, S. Chattopadhyay, and C. V. Shank, 1996, Phys. Rev. Lett. **77**, 4182.
- Lewenstein, M., P. Balcou, M. Yu. Ivanov, A. L'Huillier, and P. B. Corkum, 1994, Phys. Rev. A **49**, 2117.
- LHC, 2011, URL <http://lhc.web.cern.ch/lhc/>.
- Liang, E. P., S. C. Wilks, and M. Tabak, 1998, Phys. Rev. Lett. **81**, 4887.
- Liao, W., A. Pálffy, and C. H. Keitel, 2011, Phys. Lett. B **705**, 134.
- Lin, Q., S. Li, and W. Becker, 2006, Opt. Lett. **31**, 2163.
- Liu, C., M. Kohler, K. Z. Hatsagortsyan, C. Müller, and C. H. Keitel, 2009, New J. Phys. **11**, 105045.
- LMJ (Laser MégaJoule), 2011, (Homepage in French), URL <http://www-lmj.cea.fr/index.htm>.
- Lorentz, H. A., 1909, *The Theory of Electrons* (Teubner, Leipzig).
- Lötstedt, E., U. D. Jentschura, and C. H. Keitel, 2008, Phys. Rev. Lett. **101**, 203001.
- Lötstedt, E., U. D. Jentschura, and C. H. Keitel, 2009, New J. Phys. **11**, 013054.
- Lundin, J., L. Stenflo, G. Brodin, M. Marklund, and P. K. Shukla, 2007, **14**, 064503.
- Lundström, E., G. Brodin, J. Lundin, M. Marklund, R. Bingham, J. Collier, J. T. Mendonça, and P. Norreys, 2006, Phys. Rev. Lett. **96**, 083602.
- Macchi, A., M. Borghesi, and M. Passoni, 2012, Rev. Mod. Phys. , to be published.
- Macchi, A., S. Veghini, and F. Pegoraro, 2009, Phys. Rev. Lett. **103**, 085003.
- Mackenroth, F., and A. Di Piazza, 2011, Phys. Rev. A **83**, 032106.
- Mackenroth, F., A. Di Piazza, and C. H. Keitel, 2010, Phys. Rev. Lett. **105**, 063903.
- Major, Z., S. Klingebiel, C. Skrobol, I. Ahmad, C. Wandt, S. A. Trushin, F. Krausz, and S. Karsch, 2010, AIP Conf. Proc. **1228**, 117.
- Malka, V., J. Faure, Y. A. Gauduel, E. Lefebvre, A. Rousse, and K. T. Phuoc, 2008, Nature Phys. **4**, 447.
- Mangles, S. P. D., C. D. Murphy, Z. Najmudin, A. G. R. Thomas, J. L. Collier, A. E. Dangor, E. J. Divall, P. S. Foster, J. G. Gallacher, C. J. Hooker, D. A. Jaroszynski, A. J. Langley, *et al.*, 2004, Nature (London) **431**, 535.
- MaRIE (Matter-Radiation Interactions in Extremes Experimental), 2011, URL <http://marie.lanl.gov/>.
- Marklund, M., 2010, Nature Photon. **4**, 72.
- Marklund, M., and P. K. Shukla, 2006, Rev. Mod. Phys. **78**, 591.
- Marx, B., I. Uschmann, S. Höfer, R. Löttsch, O. Wehrhan, E. Förster, M. Kaluza, T. Stöhlker, H. Gies, C. Detlefs, T. Roth, J. Härtwig, *et al.*, 2011, Opt. Commun. **284**, 915.
- Matinyan, S., 1998, Phys. Rep. **298**, 199.
- Matveev, V. I., E. S. Gusarevich, and I. N. Pashev, 2005, J. Exp. Theor. Phys. **100**, 1043.
- McDonald, K. T., and K. Shmakov, 1999, Phys. Rev. ST Accel. Beams **2**, 121301.
- Mendonça, J., M. Marklund, P. Shukla, and G. Brodin, 2006, Phys. Lett. A **359**, 700.
- Mendonça, J. T., 2007, Europhys. Lett. **79**, 21001.
- Meuren, S., and A. Di Piazza, 2011, Phys. Rev. Lett. (in press) eprint arXiv:1107.4531.
- Milosevic, N., P. B. Corkum, and T. Brabec, 2004, Phys. Rev. Lett. **92**, 013002.
- Milosevic, N., V. P. Krainov, and T. Brabec, 2002, Phys. Rev. Lett. **89**, 193001.
- Milstein, A. I., C. Müller, K. Z. Hatsagortsyan, U. D. Jentschura, and C. H. Keitel, 2006, Phys. Rev. A **73**, 062106.
- Milstein, A. I., and M. Schumacher, 1994, Phys. Rep. **243**, 183.
- Mimura, H., S. Handa, T. Kimura, H. Yumoto, D. Yamakawa, H. Yokoyama, S. Matsuyama, K. Inagaki, K. Yamamura, Y. Sano, K. Tamasaku, Y. Nishino, *et al.*, 2010, Nature Phys. **6**, 122.
- Mocken, G., and C. H. Keitel, 2008, Comp. Phys. Commun. **178**, 868.
- Mocken, G. R., and C. H. Keitel, 2004, J. Phys. B **37**, L275.
- Mocken, G. R., M. Ruf, C. Müller, and C. H. Keitel, 2010, Phys. Rev. A **81**, 022122.
- Monden, Y., and R. Kodama, 2011, Phys. Rev. Lett. **107**, 073602.
- Monin, A., and M. B. Voloshin, 2010, Phys. Rev. D **81**, 085014.
- Moniz, E. J., and D. H. Sharp, 1977, Phys. Rev. D **15**, 2850.
- Moore, C. I., A. Ting, S. J. McNaught, J. Qiu, H. R. Burris, and P. Sprangle, 1999, Phys. Rev. Lett. **82**, 1688.
- Mourou, G., 2010, Interview with Optik & Photonik **5**, 7.
- Mourou, G. A., T. Tajima, and S. V. Bulanov, 2006, Rev. Mod. Phys. **78**, 309.
- Müller, C., 2009, Phys. Lett. B **672**, 56.
- Müller, C., C. Deneke, and C. H. Keitel, 2008a, Phys. Rev. Lett. **101**, 060402.
- Müller, C., C. Deneke, M. Ruf, G. R. Mocken, K. Z. Hatsagortsyan, and C. H. Keitel, 2009a, Laser Phys. **19**, 791.
- Müller, C., K. Z. Hatsagortsyan, and C. H. Keitel, 2006, Phys. Rev. D **74**, 074017.
- Müller, C., K. Z. Hatsagortsyan, and C. H. Keitel, 2008b, Phys. Rev. A **78**, 033408.
- Müller, C., K. Z. Hatsagortsyan, and C. H. Keitel, 2008c, Phys. Lett. B **659**, 209.
- Müller, C., K. Z. Hatsagortsyan, M. Ruf, S. Müller, H. G. Hertzheim, M. C. Kohler, and C. H. Keitel, 2009b, Laser Phys. **19**, 1743.
- Müller, C., and C. H. Keitel, 2009, Nature Photon. **3**, 245.
- Müller, C., A. B. Voitkiv, and N. Grün, 2003a, Nucl. Instr. Meth. Phys. Res. B **205**, 306.
- Müller, C., A. B. Voitkiv, and N. Grün, 2003b, Phys. Rev. A **67**, 063407.

- Müller, C., A. B. Voitkiv, and N. Grün, 2003c, Phys. Rev. Lett. **91**, 223601.
- Müller, C., A. B. Voitkiv, and N. Grün, 2004, Phys. Rev. A **70**, 023412.
- Müller, C., A. B. Voitkiv, and B. Najjari, 2009, J. Phys. B **42**, 221001.
- Müller, S., and C. Müller, 2009, Phys. Rev. D **80**, 053014.
- Müller, T.-O., and C. Müller, 2011, Phys. Lett. B **696**, 201.
- Mulser, P., and D. Bauer, 2010, *High Power Laser-Matter Interaction* (Springer, Berlin).
- Mustafa, M. G., and B. Kämpfer, 2009, Phys. Rev. A **79**, 020103(R).
- Narozhny, N. B., S. S. Bulanov, V. D. Mur, and V. S. Popov, 2006, J. Exp. Theor. Phys. **102**, 9.
- Narozhny, N. B., and A. M. Fedotov, 2008, Phys. Rev. Lett. **100**, 219101.
- Narozhny, N. B., and M. S. Fofanov, 2000, J. Exp. Theor. Phys. **90**, 415.
- Naumova, N., T. Schlegel, V. T. Tikhonchuk, C. Labaune, I. V. Sokolov, and G. Mourou, 2009, Phys. Rev. Lett. **102**, 025002.
- Nedoreshta, V. N., S. P. Roshchupkin, and A. I. Voroshilo, 2009, Laser Phys. **19**, 531.
- Nerush, E. N., V. F. Bashmakov, and Kostyukov, 2011a, Phys. Plasmas **18**, 083107.
- Nerush, E. N., I. Yu. Kostyukov, A. M. Fedotov, N. B. Narozhny, N. V. Elkina, and H. Ruhl, 2011b, Phys. Rev. Lett. **106**, 035001.
- NIF (National Ignition Facility), 2011, URL <https://lasers.llnl.gov/about/nif/>.
- Nikishov, A. I., and V. I. Ritus, 1964a, Sov. Phys. JETP **19**, 1191.
- Nikishov, A. I., and V. I. Ritus, 1964b, Sov. Phys. JETP **19**, 529.
- NNDC (National Nuclear Data Center), 2011, URL <http://www.nndc.bnl.gov/>.
- Noble, A., J. Gratus, D. Burton, B. Ersfeld, M. R. Islam, Y. Kravets, G. Raj, and D. Jaroszynski, 2011, Proc. of SPIE **8079**, 80790L.
- OMEGA EP, 2011, URL http://www.1le.rochester.edu/omega_facility/omega_ep/index.php.
- Omori, T., T. Aoki, K. Dobashi, T. Hirose, Y. Kurihara, T. Okugi, I. Sakai, A. Tsunemi, J. Urakawa, M. Washio, and K. Yokoya, 2003, Nucl. Instr. Meth. Phys. Res. A **500**, 232.
- Palaniyappan, S., I. Ghebregziabher, A. D. DiChiara, J. MacDonald, and B. C. Walker, 2006, Phys. Rev. A **74**, 033403.
- Palaniyappan, S., R. Mitchell, R. Sauer, I. Ghebregziabher, S. L. White, M. F. Decamp, and B. C. Walker, 2008, Phys. Rev. Lett. **100**, 183001.
- Pálffy, A., 2008, J. Mod. Opt. **55**, 2603.
- Pálffy, A., 2010, Contemp. Phys. **51**, 471.
- Pálffy, A., J. Evers, and C. H. Keitel, 2007, Phys. Rev. Lett. **99**, 172502.
- Pálffy, A., J. Evers, and C. H. Keitel, 2008, Phys. Rev. C **77**, 044602.
- Paramonov, G. K., 2007, Chem. Phys. **338**, 329.
- Peccei, R. D., and H. R. Quinn, 1977, Phys. Rev. Lett. **38**, 1440.
- Perelomov, A. M., 1967, Sov. Phys. JETP **25**, 336.
- Peskin, M. E., and D. V. Schroeder, 1995, *An Introduction to Quantum Field Theory* (Addison-Wesley, Reading).
- PFS (Petawatt Field Synthesizer), 2011, URL <http://www.attoworld.de/Home/attoworld/High-fieldPhysics/ThePetawattFieldSynthesizer/index.html>.
- PHELIX (Petawatt High-Energy Laser for heavy Ion eXperiments), 2011, URL http://www.gsi.de/forschung/pp/phelix/index_e.html.
- Piskarskas, A., A. Stabinis, and A. Yankauskas, 1986, Sov. Phys. Usp. **29**, 869.
- Pogorelsky, I. V., I. Ben-Zvi, T. Hirose, S. Kashiwagi, V. Yakimenko, K. Kusche, P. Siddons, J. Skaritka, T. Kumita, A. Tsunemi, T. Omori, J. Urakawa, *et al.*, 2000, Phys. Rev. ST Accel. Beams **3**, 090702.
- Popmintchev, T., M.-C. Chen, A. Bahabad, M. Gerrity, P. Sidorenko, O. Cohen, I. P. Christov, M. M. Murnane, and H. C. Kapteyn, 2009, Proc. Natl. Acad. Sci. U.S.A. **106**, 10516.
- Popov, V., V. Mur, and B. Karnakov, 1997, JETP Letters **66**, 229.
- Popov, V. S., 1971, JETP Lett. **13**, 185.
- Popov, V. S., 1972, Sov. Phys. JETP **34**, 709.
- Popov, V. S., 2004, Phys. Usp. **47**, 855.
- Popov, V. S., B. M. Karnakov, V. D. Mur, and S. G. Pozdnyakov, 2006, J. Exp. Theor. Phys. **102**, 760.
- Postavaru, O., Z. Harman, and C. H. Keitel, 2011, Phys. Rev. Lett. **106**, 033001.
- Protopapas, M., C. H. Keitel, and P. L. Knight, 1997, Rep. Progr. Phys. **60**, 389.
- PVLAS (Polarizzazione del Vuoto con LASer), 2011, URL <http://w3.ts.infn.it/experiments/pvlas/>.
- Rabadán, R., A. Ringwald, and K. Sigurdson, 2006, Phys. Rev. Lett. **96**, 110407.
- Reiss, H. R., 1962, J. Math. Phys. **3**, 59.
- Reiss, H. R., 1971, Phys. Rev. Lett. **26**, 1072.
- Reiss, H. R., 1979, Phys. Rev. A **19**, 1140.
- Reiss, H. R., 1980, Phys. Rev. A **22**, 1786.
- Reiss, H. R., 1983, Phys. Rev. C **27**, 1199.
- Reiss, H. R., 1990a, Phys. Rev. A **42**, 1476.
- Reiss, H. R., 1990b, J. Opt. Soc. Am. B **7**, 574.
- Reiss, H. R., 2008, Phys. Rev. Lett. **101**, 043002.
- Reiss, H. R., 2009, Eur. Phys. J. D **55**, 365.
- Ringwald, A., 2001, Phys. Lett. B **510**, 107.
- Ritus, V. I., 1972, Ann. Phys. (N.Y.) **69**, 555.
- Ritus, V. I., 1985, J. Sov. Laser Res. **6**, 497.
- Rohrlich, F., 2007, *Classical Charged Particles* (World Scientific, Singapore).
- Rohrlich, F., 2008, Phys. Rev. E **77**, 046609.
- Roshchupkin, S. P., 2001, Phys. At. Nucl. **64**, 243.
- Ruf, M., G. R. Mocken, C. Müller, K. Z. Hatsagortsyan, and C. H. Keitel, 2009, Phys. Rev. Lett. **102**, 080402.
- SACLA (Spring-8 Angstrom Compact free electron LASer), 2011, URL <http://xfel.riken.jp/eng/>.
- Sakai, I., T. Aoki, K. Dobashi, M. Fukuda, A. Higurashi, T. Hirose, T. Iimura, Y. Kurihara, T. Okugi, T. Omori, J. Urakawa, M. Washio, *et al.*, 2003, Phys. Rev. ST Accel. Beams **6**, 091001.
- Salamin, Y. I., and F. H. M. Faisal, 1998, Phys. Rev. A **54**, 4383.
- Salamin, Y. I., Z. Harman, and C. H. Keitel, 2008, Phys. Rev. Lett. **100**, 155004.
- Salamin, Y. I., S. X. Hu, K. Z. Hatsagortsyan, and C. H. Keitel, 2006, Phys. Rep. **427**, 41.
- Sansone, G., E. Benedetti, F. Calegari, C. Vozzi, L. Avaldi, R. Flammini, L. Poletto, P. Villoresi, C. Altucci, R. Velotta, S. Stagira, S. De Silvestri, *et al.*, 2006, Science **314**, 443.
- Sarachik, E. S., and G. T. Schappert, 1970, Phys. Rev. D **1**,

- 2738.
- Schlegel, T., N. Naumova, V. T. Tikhonchuk, C. Labaune, I. V. Sokolov, and G. Mourou, 2009, *Phys. Plasmas* **16**, 083103.
- Schlenvoigt, H.-P., K. Haupt, A. Debus, F. Budde, O. Jäckel, S. Pfotenhauer, H. Schwoerer, E. Rohwer, J. G. Gallacher, E. Brunetti, R. P. Shanks, S. M. Wiggins, *et al.*, 2008, *Nature Phys.* **4**, 130.
- Schoenlein, R. W., W. P. Leemans, A. H. Chin, P. Volfbeyn, T. E. Glover, P. Balling, M. Zolotarev, K.-J. Kim, S. Chattopadhyay, and C. V. Shank, 1996, *Science* **274**, 236.
- Schroeder, C. B., E. Esarey, C. G. R. Geddes, C. Benedetti, and W. P. Leemans, 2010, *Phys. Rev. ST Accel. Beams* **13**, 101301.
- Schützhold, R., H. Gies, and G. V. Dunne, 2008, *Phys. Rev. Lett.* **101**, 130404.
- Schwinger, J., 1951, *Phys. Rev.* **82**, 664.
- Schwoerer, H., S. Pfotenhauer, O. Jäckel, K.-U. Amthor, B. Liesfeld, W. Ziegler, R. Sauerbrey, K. W. D. Ledingham, and T. Esirkepov, 2006, *Nature (London)* **439**, 445.
- Seipt, D., and B. Kämpfer, 2011a, *Phys. Rev. A* **83**, 022101.
- Seipt, D., and B. Kämpfer, 2011b, *Phys. Rev. ST Accel. Beams* **14**, 040704.
- Selstø, S., E. Lindroth, and J. Bengtsson, 2009, *Phys. Rev. A* **79**, 043418.
- Sengupta, N. D., 1949, *Bull. Math. Soc. (Calcutta)* **41**, 187.
- Shahbaz, A., T. J. Bürvenich, and C. Müller, 2010, *Phys. Rev. A* **82**, 013418.
- Shahbaz, A., C. Müller, T. J. Bürvenich, and C. H. Keitel, 2009, *Nucl. Phys. A* **821**, 106.
- Shahbaz, A., C. Müller, A. Staudt, T. J. Bürvenich, and C. H. Keitel, 2007, *Phys. Rev. Lett.* **98**, 263901.
- Shen, B., and J. Meyer-ter-Vehn, 2001, *Phys. Rev. E* **65**, 016405.
- Shen, C. S., 1970, *Phys. Rev. Lett.* **24**, 410.
- Shvyd'ko, Yu., S. Stoupin, V. Blank, and S. Terentyev, 2011, *Nature Photon.* **5**, 539.
- Sieczka, P., K. Krajewska, J. Z. Kaminski, P. Panek, and F. Ehlötzky, 2006, *Phys. Rev. A* **73**, 053409.
- Smeenck, C. T. L., L. Arissian, B. Zhou, A. Mysyrowicz, D. M. Villeneuve, A. Staudte, and P. B. Corkum, 2011, *Phys. Rev. Lett.* **106**, 193002.
- Smorenburg, P., L. Kamp, G. Geloni, and O. Luiten, 2010, *Laser Part. Beams* **28**, 553.
- Sokolov, I. V., N. M. Naumova, J. A. Nees, and G. A. Mourou, 2010a, *Phys. Rev. Lett.* **105**, 195005.
- Sokolov, I. V., N. M. Naumova, J. A. Nees, G. A. Mourou, and V. P. Yanovsky, 2009, *Phys. Plasmas* **16**, 093115.
- Sokolov, I. V., J. A. Nees, V. P. Yanovsky, N. M. Naumova, and G. A. Mourou, 2010b, *Phys. Rev. E* **81**, 036412.
- Spohn, H., 2000, *Europhys. Lett.* **50**, 287.
- SPRING8 (Super Photon Ring - 8 GeV), 2011, URL <http://www.spring8.or.jp/en/>.
- Strickland, D., and G. Mourou, 1985, *Opt. Commun.* **55**, 447.
- Sung, J. H., S. K. Lee, T. J. Yu, T. M. Jeong, and J. Lee, 2010, *Opt. Lett.* **35**, 3021.
- Tabak, M., J. Hammer, M. E. Glinsky, W. L. Kruer, S. C. Wilks, J. Woodworth, E. M. Campbell, M. D. Perry, and R. J. Mason, 1994, *Phys. Plasmas* **1**, 1626.
- Tajima, T., and J. M. Dawson, 1979, *Phys. Rev. Lett.* **43**, 267.
- Tajima, T., D. Habs, and G. A. Mourou, 2010, *Optik & Photonik* **5**, 24.
- Tamburini, M., T. V. Liseykina, F. Pegoraro, and A. Macchi, 2011, eprint arXiv:1108.2372.
- Tamburini, M., F. Pegoraro, A. Di Piazza, C. H. Keitel, and A. Macchi, 2010, *New J. Phys.* **12**, 123005.
- Taranukhin, V. D., 2000, *Laser Phys.* **10**, 330.
- Taranukhin, V. D., and N. Yu. Shubin, 2001, *Quantum Electronics* **31**, 179.
- Taranukhin, V. D., and N. Yu. Shubin, 2002, *J. Opt. Soc. Am. B* **19**, 1132.
- Teitelboim, C., 1971, *Phys. Rev. D* **4**, 345.
- Telnov, V., 1990, *Nucl. Instr. Meth. Phys. Res. A* **294**, 72.
- Teubner, U., and P. Gibbon, 2009, *Rev. Mod. Phys.* **81**, 445.
- Thoma, M. H., 2009a, *Rev. Mod. Phys.* **81**, 959.
- Thoma, M. H., 2009b, *Eur. Phys. J. D* **55**, 271.
- Ting, A., R. Fischer, A. Fisher, K. Evans, R. Burris, J. Krall, E. Esarey, and P. Sprangle, 1995, *J. Appl. Phys.* **78**, 575.
- Ting, A., R. Fischer, A. Fisher, C. Moore, B. Hafizi, R. Elton, K. Krushelnick, R. Burris, S. Jackel, K. Evans, J. Weaver, P. Sprangle, *et al.*, 1996, *Nucl. Instr. Meth. Phys. Res. A* **375**, ABS68.
- Tinsley, T. M., 2005, *Phys. Rev. D* **71**, 073010.
- Titov, A. I., B. Kämpfer, and H. Takabe, 2009, *Phys. Rev. ST Accel. Beams* **12**, 111301.
- Tommasini, D., and H. Michinel, 2010, *Phys. Rev. A* **82**, 011803.
- Toncian, T., M. Borghesi, J. Fuchs, E. d'Humières, P. Antici, P. Audebert, E. Brambrink, C. A. Cecchetti, A. Pipahl, L. Romagnani, and O. Willi, 2006, *Science* **312**, 410.
- TPL (Texas Petawatt Laser), 2011, URL <http://www.ph.utexas.edu/~utlasers/>.
- Tsai, Y. S., 1993, *Phys. Rev. D* **48**, 96.
- Tuchin, K., 2010, *Phys. Lett. B* **686**, 29.
- Varfolomeev, A. A., 1966, *Sov. Phys. JETP* **23**, 681.
- Verschl, M., and C. H. Keitel, 2007a, *J. Phys. B* **40**, F69.
- Verschl, M., and C. H. Keitel, 2007b, *Europhys. Lett.* **77**, 64004.
- Volkov, D. M., 1935, *Z. Phys.* **94**, 250.
- Vulcan, 2011, URL <http://www.clf.rl.ac.uk/Facilities/Vulcan/12248.aspx>.
- Vulcan 10PW, 2011, URL <http://www.clf.rl.ac.uk/New+Initiatives/The+Vulcan+10+Petawatt+Project/14684.aspx>.
- Wagner, R. E., M. R. Ware, Q. Su, and R. Grobe, 2010a, *Phys. Rev. A* **81**, 024101.
- Wagner, R. E., M. R. Ware, Q. Su, and R. Grobe, 2010b, *Phys. Rev. A* **81**, 052104.
- Walker, P., and G. Dracoulis, 1999, *Nature (London)* **399**, 35.
- Walser, M. W., D. J. Urbach, K. Z. Hatsagortsyan, S. X. Hu, and C. H. Keitel, 2002, *Phys. Rev. A* **65**, 043410.
- Wang, Z., C. Liu, Z. Shen, Q. Zhang, H. Teng, and Z. Wei, 2011, *Opt. Lett.* **36**, 3194.
- Weidenmüller, H. A., 2011, *Phys. Rev. Lett.* **106**, 122502.
- Weisskopf, V., 1936, *K. Dan. Vidensk. Selsk. Mat. Fys. Medd.* **14**, 1.
- Winterfeldt, C., C. Spielmann, and G. Gerber, 2008, *Rev. Mod. Phys.* **80**, 117.
- Woodward, P. M., 1947, *J. Inst. Electr. Eng.* **93**, 1554.
- Xiang, Y., Y. Niu, Y. Qi, R. Li, and S. Gong, 2010, *J. Mod. Opt.* **57**, 385.
- Yakovlev, V. P., 1965, *Sov. Phys. JETP* **22**, 223.
- Yamakawa, K., Y. Akahane, Y. Fukuda, M. Aoyama, N. Inoue, and H. Ueda, 2003, *Phys. Rev. A* **68**, 065403.
- Yamakawa, K., Y. Akahane, Y. Fukuda, M. Aoyama, N. Inoue, H. Ueda, and T. Utsumi, 2004, *Phys. Rev. Lett.* **92**,

- 123001.
- Yanovsky, V., V. Chvykov, G. Kalinchenko, P. Rousseau, T. Planchon, T. Matsuoka, A. Maksimchuk, J. Nees, G. Cheriaux, G. Mourou, and K. Krushelnick, 2008, *Opt. Express* **16**, 2109.
- Zakowicz, S., 2005, *J. Math. Phys.* **46**, 032304.
- Zeldovich, Ya. B., and R. A. Sunyaev, 1969, *Astrophys. Space Sci.* **4**, 301.
- Zhang, P., Y. Song, and Z. Zhang, 2008, *Phys. Rev. A* **78**, 013811.
- Zhi, M. C., and A. V. Sokolov, 2009, *Phys. Rev. A* **80**, 023415.
- Zhidkov, A., J. Koga, A. Sasaki, and M. Uesaka, 2002, *Phys. Rev. Lett.* **88**, 185002.
- Zon, B. A., 1999, *J. Exp. Theor. Phys.* **89**, 219.
- Zon, B. A., 2000, *J. Exp. Theor. Phys.* **91**, 899.